

ICESat-2 Algorithm Theoretical Basis Document for the Atmosphere, Part I: Level 2 and 3 Data Products

Steve Palm

Yeukui Yang

Ute Herzfeld

Version 7.5

June 16, 2018

Contents

Release Notes	4
1 Introduction and Background	8
2 Corrections to the Raw Atmospheric Profiles.....	14
2.1 Dead Time Correction	14
2.2 Correction for Raw Profile Shifting	19
2.3 Transmit Echo Pulse	19
3 L2A Product: Normalized Relative Backscatter (ATL04)	21
3.1 L2A Required Inputs.....	21
3.2 L2A Outputs	22
3.3 NRB Computation	25
3.3.1 Molecular Backscatter Computation	26
3.3.1.1 Molecular Transmission	29
3.3.2 Molecular Scattering Folding Correction	30
3.3.2.1 Error Analysis of Molecular Contribution	32
3.3.3 Ozone Transmission Computation.....	32
3.3.4 Background Computation	33
3.3.4.1 Theoretical Background	38
3.3.5 Surface Signal	38
3.3.6 Vertical Height Adjustment.....	39
3.3.7 Calculation of the Calibration Coefficient.....	41
3.3.7.1 Theory	41
3.3.7.2 Calibration Algorithm using the Atmosphere	42
3.3.7.3 Calibration Algorithm using Surface Reflectance	44
3.3.7.4 Calibration Error and Confidence	46
4 Level 3 Product (ATL09)	47
4.1 L3 Required Inputs	47
4.2 L3 Outputs.....	47
4.3 Calibrated, Attenuated Backscatter Profiles.....	52
4.4 Layer Heights and Flags from Backscatter Profiles	53
4.4.1 Layer Integrated Attenuated Backscatter.....	54
4.4.2 Cloud Folding Flag	55

4.5 Blowing Snow	55
4.5.1 Blowing Snow Layer Height.....	55
4.5.2 Blowing Snow Layer Optical Depth	57
4.5.3 Blowing Snow Layer Confidence	58
4.5.4 Blowing Snow Probability	59
4.6 Apparent Surface Reflectance (ASR).....	60
4.6.1 Cloud Detection using ASR.....	62
4.6.2 ASR Cloud Detection Algorithm Implementation	66
4.6.2.1 Initial Clear Sky ASR Climatology.....	66
4.6.2.2 Final Clear Sky ASR Determination	68
4.6.2.3 Cloud Detection Using Apparent Surface Reflectance	71
4.7 Ocean (or Open Water) Surface Reflectivity.....	73
4.8 Total Column Optical Depth Using ASR.....	75
The Column_OD_ASR_QF will be computed using the NOAA flag and the IGBP flag.....	76
5.0 Consolidated Cloud Flag.....	76
6.0 Quality Assessment.....	77
6.1 Calibration.....	77
6.2 Background	78
6.3 Surface Signal.....	78
6.4 Calibrated Attenuated Backscatter	78
6.5 Layer Heights.....	78
6.6 Apparent Surface Reflectance	78
6.7 Ocean Surface Reflectance	78
6.8 Total Column Optical Depth.....	78
6.9 Multiple Scattering Warning Flag	78
7 Product Quality Parameters.....	79
Appendix A.....	79
Appendix B.....	82
References	83

Release Notes

For version 7.5, **dated June 16, 2018** changed the calibration solar angle limit from zenith to elevation (section 3.3.7.2) and in Table 3.6. Changed the wording of the TEP removal in section 2.3. Modified equation 4.7 (apparent surface reflectance) by replacing the energy received with the number of photons received and removed equation 4.8 and associated text as it is no longer necessary. Re-made figure 4.6.1 using new modified equation 4.7. Modified the molecular scattering folding equation (eqn. 3.15) to replace the number of photons transmitted with laser energy. Added section 3.3.4.1 the computation of the theoretical background (equation 3.25). Added a new parameter (*backg_theoret*) to the ATL09 product defined in section 3.3.4.1. All relevant changes in red.

Prior Version Updates:

For version 7.4, **dated April 10, 2018**, all changes in red font. We have modified the apparent surface reflectance equation 4.7 by replacing T_{opt} with S_{ret} which is defined as the system receiver response and comes from ATL03.

The deadtime equation 2.1 had an error. Please replace with new equation 2.1.

The equation to compute molecular folding (equation 3.15) was altered. The product of the detector quantum efficiency (Q_e) and the receiver optical transmission (T_{opt}) was replaced with S_{ret} .

Section 2.3 was modified to correct the equations for removal of the Transmit Echo Pulse (TEP) from the atmospheric profiles.

In section 4.4, some clarification wording was added to explain the parameter *msw_flag*.

Added section 6.9, multiple scattering warning flag plot.

For **version 7.3, dated November 15, 2017**, all changes in red font. We have added a paragraph to section 2.1 – Dead Time Correction – which introduces a control parameter “*dtime_select*” which is used to determine which dead time factor to use in the processing.

Added some wording to section 2.1 –Dead Time Correction for clarification.

Changed equation 2.1 to now define just the dead time correction factor and added equation 2.1a to define how the dead time correction factor is applied.

Added “*dtime_select*” parameter to Table 3.5

Deleted two sentences from the first paragraph of section 3.3.5 to avoid confusion.

Added discussion of how to apply dead time correction to section 3.3.5

Added a paragraph describing added parameters to the ATL09 product in Section 4.2. These include `density_pass2` and renaming old “density” to `density_pass1`. Updated Table 4.1 in that section to reflect this change.

Added parameter `Surface_Bin` to ATL09 output in Table 4.1. This parameter is stored on ATL04 and should simply be passed to ATL09.

Fixed Table 4.2 description of “`Surface_Signal_Source`” to be consistent with text.

Rewrote section 4.5 – Blowing Snow. Added Table 4.3 on page 55.

In Section 4.6.2.1, updated the input GOME data set for surface reflectance from a 1x1 degree to the new 0.25x0.25 degree data set. Also changed the value of R_{snow} to 0.8 from 0.6.

For version 7.2, **dated July 28, 2017**, note all changes in red font.

Updated section 2.1 – dead time correction.

Added `Surface_Signal_Source` (Table 4.2) control parameter to define the source of the surface signal in computation of Apparent Surface Reflectivity. Paragraph describing this is in section 4.6, page 56.

Modified surface signal computation – step 4 – in section 3.3.5, page 37.

Added ATL09 parameter `Surface_Signal_Source` to Tables 4.1 and 4.2. This is a constant read in from an ancillary file that tells whether to use the surface signal from ATL03 or that from ATL04 to compute apparent surface reflectance.

Changed section 4.4 to specify a maximum of 10 cloud layers (was 6).

Added definition of `layer_attr` flag to section 4.4.

Added clarification to section 4.5 – Blowing Snow.

Added new section 5.0 – Consolidated Cloud Flag. Old sections 5 and 6 become new sections 6 and 7. Added new parameter `layer_flag` to ATL09 (Table 4.1).

Outstanding issues: The TEP correction must be implemented and tested. The quality assurance parameters (Section 6) have not yet been added to the products.

For Version 7.1 **dated March 28, 2017**, changes and additions to the prior version (Version 7.0, dated October 20, 2016) have been entered in red font. The main changes are:

Added Section 2 – Corrections to the Raw Atmospheric Profiles. This section addresses dead time correction, vertical shifting of profiles and the transmit echo pulse (TEP) correction. Prior

version dead time correction was in section 2.3.5.1. This version dead time correction procedure has not changed from the prior version and is complete except for identifying the laboratory-produced detector efficiency table. Discussion of vertical shifting (section 2.2) and the TEP (section 2.3) are new to this version.

In Table 3.1 – List of ATL04 product parameters – added parameter *Backg_Method3* which is the background computed from the 200 Hz onboard background. This is defined in section 3.3.4 on page 32. Also added in Table 3.1 is the ATL04 parameter *mol_backs_folded*. Though the procedure to compute this parameter was in the prior ATBD version, it was not in the ATL04 product parameter list.

Added further explanation of the application of the dead time correction factor in Section 3.3.5

In Table 4.1 – List of ATL09 Parameters – added parameter *Backg_Select* (from ATL04) and parameter *Bsnow_Prob* which is defined in section 4.5.1

For Version V7.0, dated **October 22, 2016**, changes and additions to the prior version (Version 6.0, dated November 3, 2015) have been entered in **red font**. The main changes are:

Replaced section 2 with new section entitled “Correction to the Raw Atmospheric Profiles”. The previous ATBD version section 2 becomes section 3, section 3 becomes 4, etc.

Added more complete discussion of dead time correction in section 2.1 including Figure 2.2.

Section 2.3: Added discussion of the removal of the Transmit Pulse Echo (TPE) from the atmospheric profiles

Secant theta added to equation 3.12

Added more MET parameters to ATL04 and ATL09 output

Added two dead time correction parameters (Dtime_Fac1 and Dtime_Fac2) to ATL04 and ATL09

Added ATL03 background and surface signal parameters to ATL04 and ATL09

Added folded molecular profile to ATL09 product (Equation 3.19a)

Added some pseudo code to vertical alignment section (section 3.3.6)

Discussion added to section 3.3.4 on the use of the onboard 50 shot background

Multiple scattering warning flag (Msw_flag) added to ATL09 product

Section 4.4 discussion of cloud flags added

Changed the ATLAS receiver transmission from 0.30 to 0.49 in Table 1.1

Energy of strong beams now 120 μ J in Table 1.1

Added discussion of calibration in Section 4.3

Added Cal_Default ANC parameter to Table 4.2

Added section 4.4.2 and equation 4.5a for the computation of a new ATL09 parameter called Cloud_fold_flag

Added section 5.0 – Quality Assessment

Added section 6.0 – Product Quality Parameters

Added Appendix B – Geopotential height to geometric height conversion

The main changes for version V6.0, dated **November 3, 2015** from the prior version (V5.0 dated June, 2015) are:

Section 2.1, new required input to ATL04 (ATL03)

Added section 2.3.2.1

Updated section 2.3.5.1 – Dead time correction

Revised section 3.5 and added Table 3.4

Revised section 3.6.2 – ASR Cloud detection algorithm implementation

Updated Tables 2.7 and 3.1

Version V5.0 was the first to split the ATBD into two parts. Part I addresses L2A (ATL04) and all of L3A (GLA09) except for layer detection which is handled exclusively in a separate document: ICESat-2 Algorithm Theoretical Basis Document for the Atmosphere, Part II: Detection of Atmospheric Layers and Surface Using a Density Dimension Algorithm, V5.0 dated **4 June 2015**.

The main differences to this document (Part I) compared to the prior version (V4.0 dated 1 November, 2014) are listed below:

- 1) Addition of section 2.3.2 – Molecular Scattering Folding Correction. This attempts to remove the molecular scattering folded from above from the measured signal.
- 2) Modified background computation detailed in Method 2.
- 3) Added section 2.3.6.3 – Calibration Algorithm using Surface Reflectance
- 4) Corrected errors and added clarification to the ozone transmission calculation.
- 5) Fixed Equation 2.7
- 6) Changed equation 2.10 to be consistent with CALIPSO ATBD
- 7) Updated Table 3.1
- 8) Put code for vertically interpolating pressure into Appendix A

1 Introduction and Background

Scheduled for launch in 2017, the ICESat-2 satellite will carry only one instrument – ATLAS (Advanced Topographic Laser Altimeter System) which utilizes a high repetition rate (10 KHz) 532 nm laser and photon counting detectors for high resolution altimetry measurements. It will use a diffractive optical element (DOE) to produce 6 individual laser beams simultaneously emitted from the satellite. Three of the beams will have nominal energies of about 30 μJ (weak beams) and the other 3 will have energies roughly 4 times the weak beams (strong beams). The altimetry measurements will utilize all 6 laser beams while the atmospheric measurements will only use the 3 strong beams. Each footprint of the strong beams will be separated by about 3 km on the ground (across track) as shown in Figure 1.1.

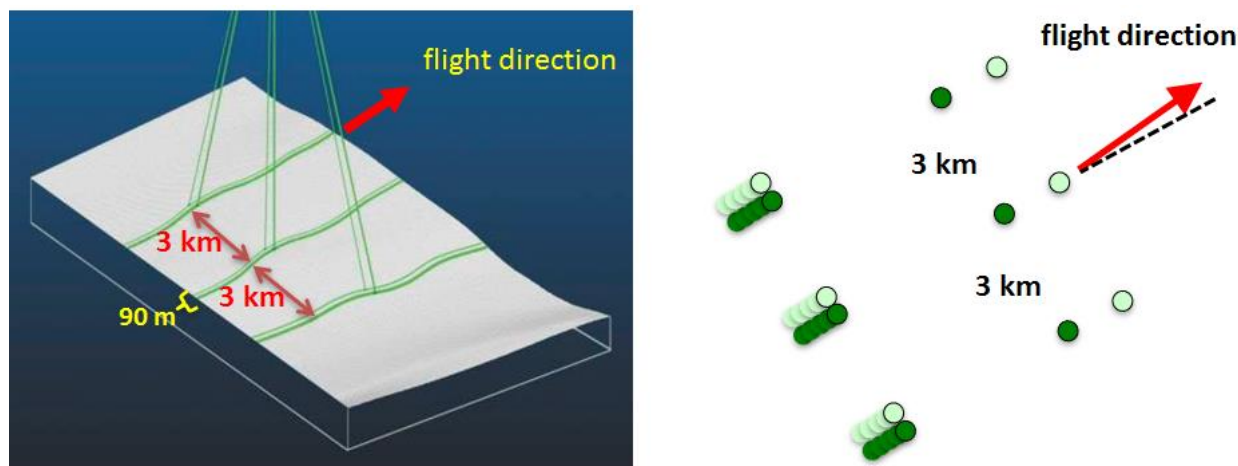


Figure 1.1 ICESat-2 laser beams and surface tracks. The satellite is yawed by 2 degrees such that the weak beams trail the strong beams and vice versa depending on spacecraft orientation which is determined by solar beta angle. Separation of strong and weak beam tracks is 90 m on the ground. Beam pairs are separated by 3 km.

The ICESat-2 atmospheric profiles will consist of 30 m bins in a 14 km long column. Nominally the top of the column will be 13.75 km (above the local value of the onboard Digital Elevation Model (DEM)) and the bottom -0.250 km. For the atmosphere, the 3 strong beams (approximately 120 μJ at 532 nm) will be downlinked after summing 400 shots, resulting in three 25 Hz profiles (280m along track resolution). Thus, each summed, 25 Hz profile is equivalent to roughly 48 mJ of energy, which is about twice the level of GLAS 532 L2A measurements. However, GLAS used geiger mode Single Photon Counting Module (SPCM) detectors which have a very low dark count rate and high quantum efficiency (60%). ATLAS will use Photo Multiplier Tube (PMT) detectors which are inherently noisier (with a factor of 10 to 100 more dark count rate compared to SPCMs) and less efficient. At present, the best estimate of dark count rate for the ATLAS detectors is between 10 and 50 KHz. The exact nighttime performance of the atmospheric channel will depend on the magnitude of the dark count rate. This is

illustrated in Figure 1.2 which compares the expected nighttime performance of ATLAS for two different values of the detector dark count rate.

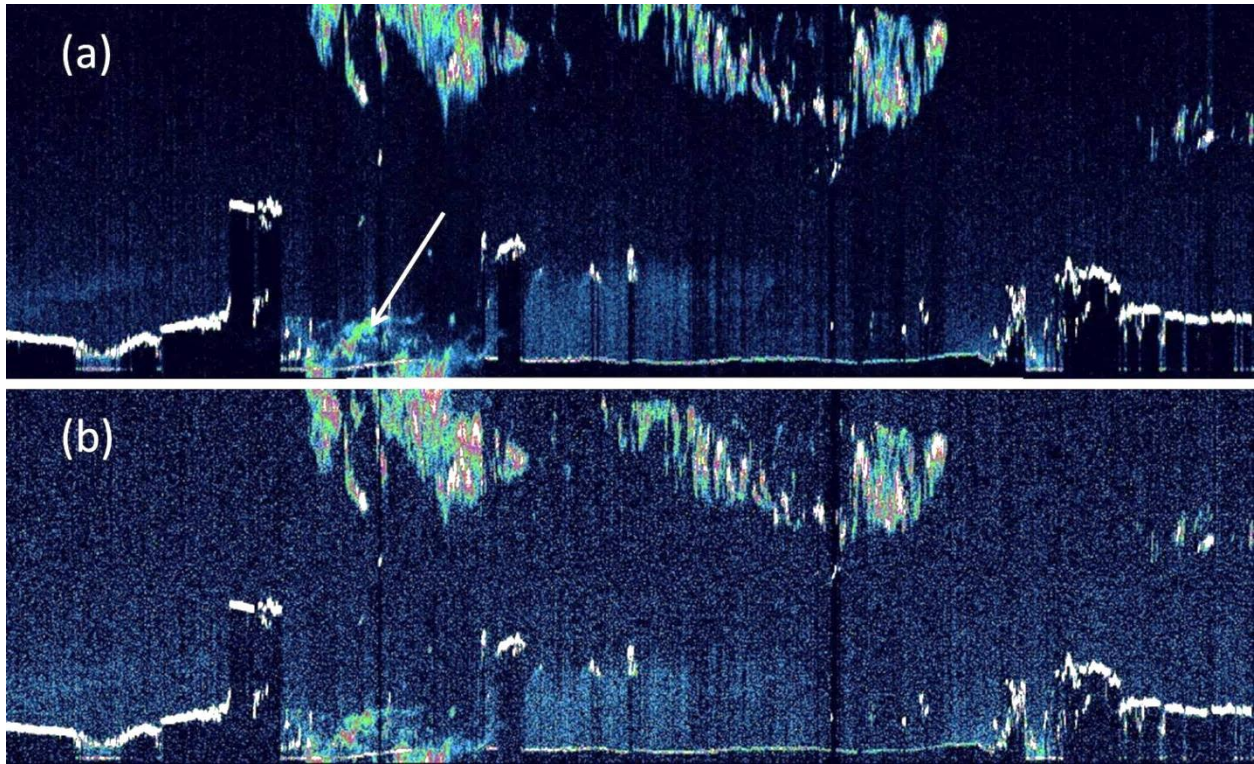


Figure 1.2. Full resolution (25 Hz, 400 shot sum) simulation of the nighttime performance of the ATLAS atmospheric channels (3 strong beams). The top panel (a) is for a detector dark count rate of 10 KHz and the bottom panel (b) is 5 times that number. The actual on-orbit detector dark count rate will likely lie somewhere in between these extremes. The scattering at the position of the arrow in (a) is from a cloud above 15 km (refer to aliasing discussion below).

Figure 1.2 shows simulated nighttime ATLAS data at full resolution (25 Hz or 400 shot sum). The top panel is for a dark count rate of 10 KHz, while in the bottom panel the dark count rate is five times that (50 KHz). Laboratory measurements to characterize the ATLAS instrument indicate initial dark count rate to be about 10 KHz. However this value will increase over time on orbit. As can be seen, the nighttime performance of ATLAS is expected to be very good, with both thin cloud and aerosol easily detected even for the higher dark count rate.

For daytime, the magnitude of the detector dark count does not matter as much since the performance will be determined by the solar background which, on average, will be between 1 and 5 MHz (about 100 times the detector dark count rate). Daytime ATLAS data will be noisier than the GLAS L2A data because when summing signals over some fixed time interval the solar noise in a lidar system scales with the laser repetition rate (GLAS was 40 Hz; ATLAS is 10KHz). This degradation in daytime signal to noise (compared to GLAS) is likely to be a factor of 100 or more. Thus, during the day thin cloud and aerosol will be detectable only after a large

amount of averaging, if at all. Model results like those shown in Figure 1.3 indicate that in order to detect thin cloud and aerosol during daytime would require averaging at least 100,000 lidar pulses (10 seconds or about 70 km horizontal resolution).

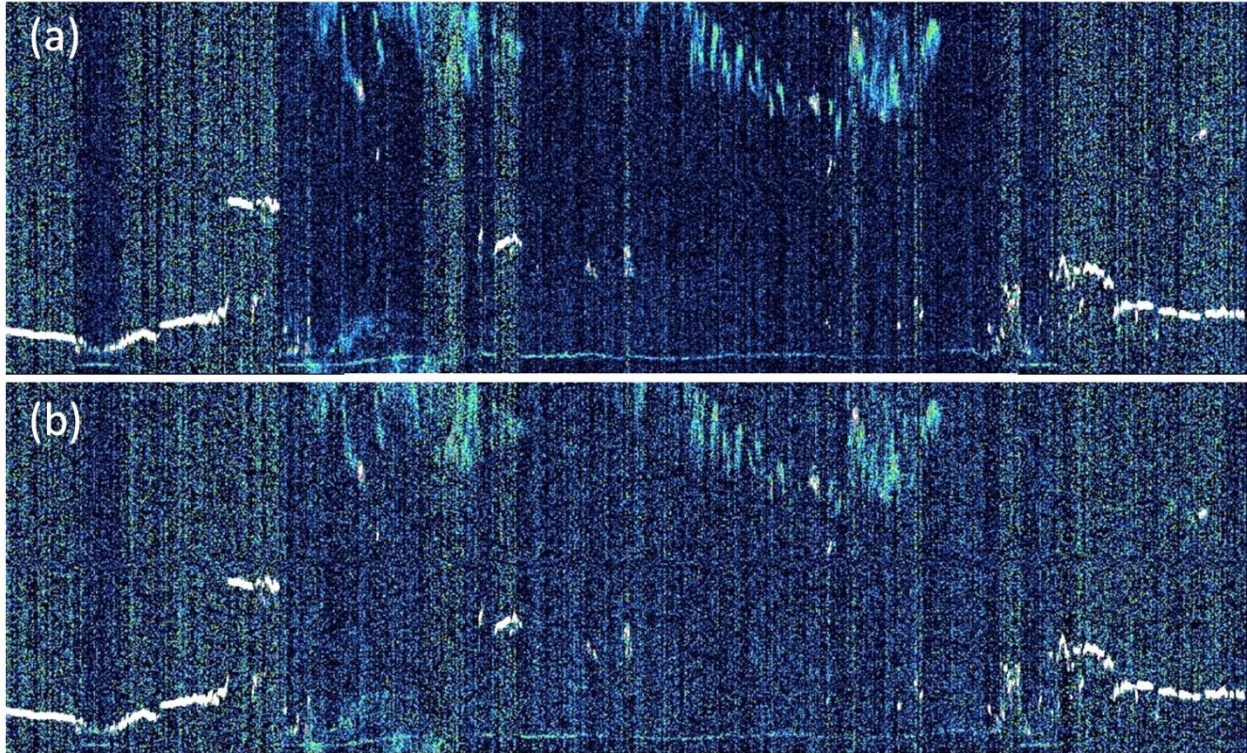


Figure 1.3. Simulation of the ATLAS atmospheric channel (1 beam) based on GLAS 532 nm data. Shown is the sum of 400 shots (full ATLAS resolution for the atmosphere) for daytime over a surface albedo of 0.10 (a), and daytime over a surface with albedo 0.30 (b).

Table 1.1 Pertinent ATLAS instrument parameters and their values at present.

ATLAS Instrument Parameter	Current (pre-lab measured) Value
Laser Repetition Rate	10 KHz
Laser Energy (strong beams)	120 μ J
Telescope Effective Area	0.43 m ²
Telescope FOV	83 μ r
Detector Quantum Efficiency	0.15
Detector Dead Time	3 ns
Detector Dark Count Rate	10-100 KHz
Bandpass Filter Width	30 pm
Nominal Receiver Optics Throughput	0.49
Nominal Orbit Height	495 km
Laser/Telescope FOV Spot Size (on ground)	14 m/41 m

While the daytime background presents a big problem for ATLAS, there are other problems that are even more formidable. To acquire high resolution altimetry measurements, ATLAS is using a high repetition rate laser (10 KHz). Each laser pulse will be separated by only 30 km in the vertical. Thus, when a pulse (pulse 1) strikes the ground, the laser pulse right after it (pulse 2) is at 30 km altitude. When the ground return from pulse 1 reaches 15 km altitude (on its way back to the satellite), laser pulse 2 is at 15 km also (but travelling downward). The atmospheric return from pulse 2 (from 15 km altitude) will travel back to the receiver at the same time as the ground return from pulse 1. Thus, if there were a cloud at 15 km, its scattering signature would appear at the position of the ground return. Clouds at 16 km altitude will appear at 1 km above the ground, etc. This effect will be termed “pulse aliasing” or “folding” in future references within this document. To put it in a more general way, the atmospheric scattering that will be recorded by the instrument at height H is the sum of the scattering at height H, H+15, H-15, H+30, H-30, H+45, H-45 etc., where the numbers are in km. Even in the tropics, 99.9% of clouds are below 18 km. Thus, there will be a range in the downlinked profiles from -0.25 km to about 3 km that can potentially contain cloud scattering from 14.75 to 18 km. Above 3 km, this effect should be minimal (with exception of the highest of clouds in the tropics and Polar Stratospheric Clouds). Pulse aliasing can be seen in the simulated data of Figure 1.1a at the position of the arrow. The scattering shown there is actually from the top of the cloud above 15 km. Above 3 km to the top of the profile (nominally 13.75 km), we should have no ambiguity in the scattering signatures, since there is usually only molecular scattering above 18 km (of course this does not apply to Polar Stratospheric Clouds that typically occur in the altitude range 12-25 km over the polar region in winter, or stratospheric aerosol).

Even though ATLAS can theoretically capture 15 km of data, the instrument will only download 14 km of data. Unfortunately the ATLAS instrument will require a hardware reset between shots that will effectively create a blind spot in the top 1 km of the profile (nominally 14-15 km). In this region no information is returned. Thus, if a cloud exists in this region we will never know it except for the case where it is optically thick and has the effect of attenuating the laser beam such that no other cloud or surface return is seen below it.

These “characteristics” produce severe problems for lidar data processing. First, there is nowhere in the profile where one can calculate the solar background. Normally, this is done using the signal either very high up (> 100 km as in the case of GLAS) or below the ground. However, we have no signal either very high up or below ground, since for instance, the scattering in the roughly 500 m of the profile below ground will be equal to the sum of the scattering at 14.5 – 15.0 km, 29.5 – 30.0 km, etc. So even if there were no particulate scattering at 14.5-15 km, the signal below ground will still have the molecular return in the 15 to 14.5 km altitude range. This can be modeled and subtracted from the computed background when there are no clouds. If clouds are present (in the 15 to 14.5 km altitude range) then there would be no way to recover the background from the 0.50 km segment of data below ground. Yet another problem caused by the high repetition rate laser pertains to calibration. With a normal (lower repetition rate)

atmospheric lidar, calibration is performed using the molecular return from a known, clear region of the atmosphere normally in the low to mid stratosphere (25-35 km). For instance for GLAS, we used the 28 to 24 km altitude range for calibration. CALIPSO uses the 36-39 km region. ATLAS will not have access to this region used by GLAS (or more correctly, it will be folded into the scattering between 6 and 9 km altitude). Calibration also requires long stretches (100's of km) of data devoid of particulate scatterers. For ICESat-2, the only place that might offer the necessary conditions for calibration is over the poles during darkness or very low sun angle where there is a high probability that no clouds will exist between 13.5 and 11-12 km. Darkness or at least twilight is required because the signal from molecular scattering (i.e. the calibration target) is so small, that it would be buried in the solar background noise for daytime data. However, in the polar regions in winter, polar stratospheric clouds may exist and will contaminate the calibration if not recognized and removed from the calibration procedure.

The unique characteristics of ICESat-2 atmospheric data discussed above represent unprecedented difficulties in producing level 2 and 3 atmospheric products. It should be stressed, however, that ATLAS is not intended to be an atmospheric lidar. ICESat-2 is not an atmospheric mission. Any atmospheric information that can be obtained is a bonus to the project, but its quality will undoubtedly be less than ideal for atmospheric science. The main intent of the atmospheric channel is the detection of clouds, blowing snow and fog that will adversely affect the altimetry measurements. The mission objective (for the atmospheric data) is to produce a cloud/no cloud flag and to loosely characterize the likely intensity of multiple scattering of the pulse due to clouds, fog and blowing snow. This information is highly valuable to the altimetry analysis. This objective can be met without accurate calibration of the data because we have designed a layer finding algorithm that does not require calibrated data to find clouds and blowing snow. Thus in summary, it will be challenging to produce an atmospheric product but the main objective of aiding the altimetry data analysis is attainable. We will, however, have to come up with creative ways to get around the above cited problems if we are to have a useful atmospheric product.

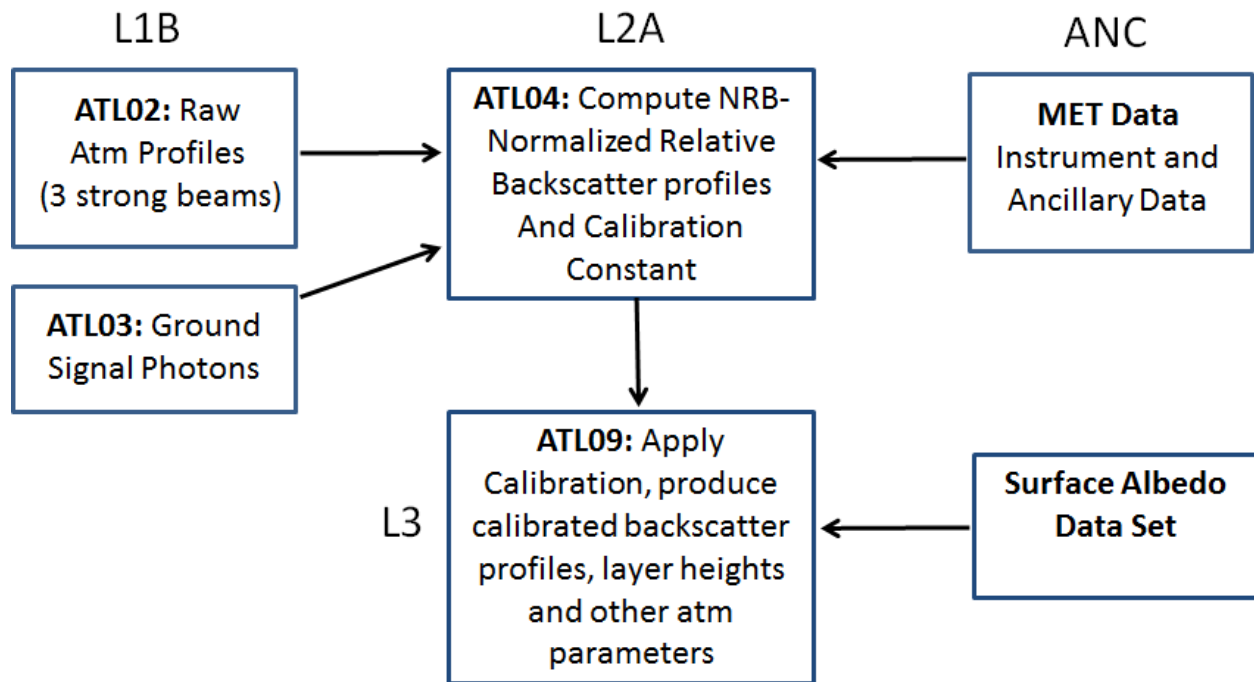


Figure 1.4. Overview of processing steps from the raw atmosphere profiles (ATL02) to the L3 atmosphere product (ATL09).

2 Corrections to the Raw Atmospheric Profiles

There are a number of corrections that need to be applied to the raw atmospheric profiles before they are processed to produce the level 2 products. These include removal of the transmit echo pulse (TEP), dead time correction and compensation for shifting between major frames. These issues are discussed below. Before we address those issues, we should note that the 3 strong beams which make up the atmosphere profiles will be named by convention atmospheric profile 1, profile 2 and profile 3. These three profiles correspond to ATLAS beam 1, 2 and 5. In the initial spacecraft orientation, ATLAS beam 1 is to the left of the nadir ground track, ATLAS beam 2 is along the nadir track and beam 5 is to the right. The spacecraft flies in two orientations, depending on the solar beta angle. The spacecraft rotates 180 degrees from one orientation to the other. Thus, sometimes beam 1 is on the left side of the ground track and sometimes on the right. Likewise with beam 5. ATLAS beam 2 is always in the center regardless of the spacecraft orientation. There will be a parameter called `sc_orient` that will tell the user which orientation the spacecraft is in. When `sc_orient = 1` (spacecraft facing forward), ATLAS beam 1 will be to the right of the nadir ground track and will map to atmospheric profile 3. When `sc_orient = 0`, (spacecraft facing backward), ATLAS beam 1 is on the left side of the nadir ground track and will map to atmospheric profile 1. For both spacecraft orientations, ATLAS beam 2 will map to atmospheric profile 2.

2.1 Dead Time Correction

Unlike the SPCM detectors of the GLAS 532 nm channel, the ATLAS detectors will have much shorter dead times (about a factor of 10 less). In addition, the low laser pulse energy of ATLAS (about a factor of 200 less than GLAS) means that detector dead time will not be important for atmospheric signals, as even dense clouds will not produce more than 3 or 4 photons per 30 m bin per shot. However, this does not apply to surface signals that can produce 10 to 20 photons per shot and, for some surfaces, may arrive in just a few nanoseconds. Dead time correction of surface signals is thus very important. Figure 2.1 shows a model of the ATLAS detector efficiency (labeled lines) as a function of the received return pulse strength (y axis) and width (x axis).

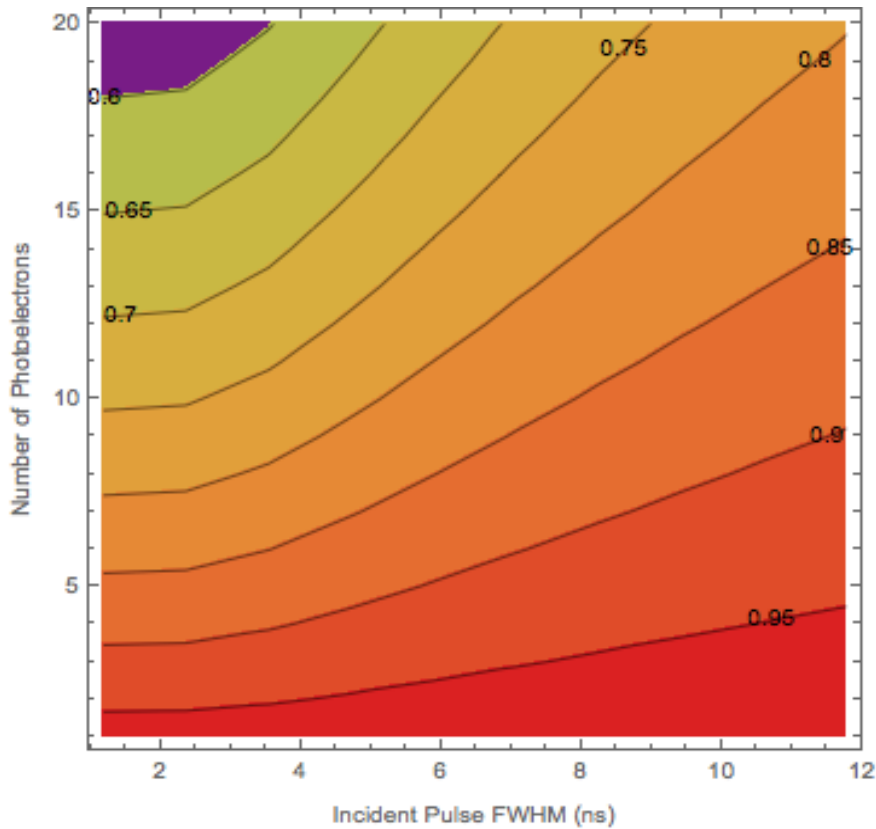


Figure 2.1 A model of effective radiometric efficiency as a function of actual (incident) return strength (photoelectrons per shot) and actual surface return pulse width (in nanoseconds).

As can be seen from the plot, the stronger and shorter the return pulse, the less efficient the detector is at capturing all the photons. This loss is due to the dead time effect. The figure also shows that in order to correct for this effect, we have to know both the return signal strength and the width of the return pulse. The latter is problematic as it is not recorded by the instrument but can be obtained by the aggregation of many shots. Tables which relate the dead time correction factor to the ground signal strength and width have been produced as part of the calibrations done on ATLAS in the laboratory (CAL 34). The table y axis contains the number of photons received for a single shot and the x axis is the width of the pulse in nanoseconds. There are 6 tables in all, one for each value of detector dead time ranging from 2.9 ns to 3.4 ns. There are 6 of these tables which are for specific detector dead times:

- CAL_34_DT29_2017172.csv
- CAL_34_DT30_2017172.csv
- CAL_34_DT31_2017172.csv
- CAL_34_DT32_2017172.csv
- CAL_34_DT33_2017172.csv

Where “DT29” means dead time 2.9 ns, “DT30” means dead time 3.0 ns, etc. Thus, we must have a procedure to choose which CAL 34 table to use.

The dead time for each of the three strong beam atmospheric profiles are computed by the average of each of their detectors 1-16 dead times. The dead times for each of these 16 detectors are contained in CAL 42 tables which depend on temperature. The correct CAL 42 table will be identified in the current granule ANC39 ancillary file. We need to average the 16 deadtimes contained in the CAL 42 file to identify which CAL 34 table to use for the dead time correction. We will use the CAL 34 table with the deadtime closest to the averaged value. Once the appropriate CAL 34 table has been identified, it is then used to obtain the dead time correction factor by the procedure shown in Figure 2.2 below. This procedure uses parameters from ATL03 to define the surface signal strength (*sig_count_hi*, *sig_count_med* and *sig_count_low*). These parameters are read in by ATL04 and represent the surface signal photon count summed over 400 shots reported by confidence level (high, medium and low). Also from ATL03 are the parameters *sig_h_sdev_hi*, *sig_h_sdev_med* and *sig_h_sdev_low* which are the standard deviation of the height of all signal (surface) photons for the 400 shot interval. Figure 2.2 below shows the logic we propose to use for computing the dead time correction using the ATL03 parameters and the radiometric table (CAL 34) discussed above. All six of these parameters in addition to *sig_h_mean_hi*, *sig_h_mean_med* and *sig_h_mean_low* are to be stored on the ATL04 product (see Table 3.1).

We propose to sum *sig_count_hi* and *sig_count_med* and divide by 400 to obtain the signal strength value in photons per shot (y axis on Figure 2.1). To compute the signal width, if *sig_count_hi* is greater than 200, we will use *sig_h_sdev_hi* multiplied by a factor (Dead_Time_Sfac, nominally 1.5) to represent the signal width and convert to nanoseconds (divide by half the speed of light). If *sig_h_sdev_hi* is invalid, then set *Dtime_fac1* to invalid.

If *sig_count_hi* is less than or equal to 200 and *sig_count_med* is not invalid, we compute the sum of *sig_count_hi* and *sig_count_med*. If this sum is less than or equal to 200, we set the dead time correction factor to 1.0. If this sum is greater than 200, then we compute the signal width by summing *sig_h_sdev_hi* and *sig_h_sdev_med*, multiplying by Dead_Time_Sfac and dividing by the speed of light. If *sig_h_sdev_med* is invalid, then only use *sig_h_sdev_hi* multiplied by Dead_Time_Sfac divided by half the speed of light to compute the signal width. If *sig_h_sdev_hi* is invalid, then set *Dtime_fac1* to invalid. The resulting signal width and signal strength are used to index into the laboratory-produced detector efficiency table to obtain the dead time correction factor (*Dtime_Fac1*). Note that the dead time correction factor obtained from CAL 34 will be a number ≥ 1.0 . To correct the *Surface_signal* parameter for dead time, it should be multiplied by *Dtime_fac1*.

NOTE: If the above data needed to compute $Dtime_Fac1$ are not available, then its value should be set to invalid. See section 3.3.5 on how to obtain $Surface_signal$.

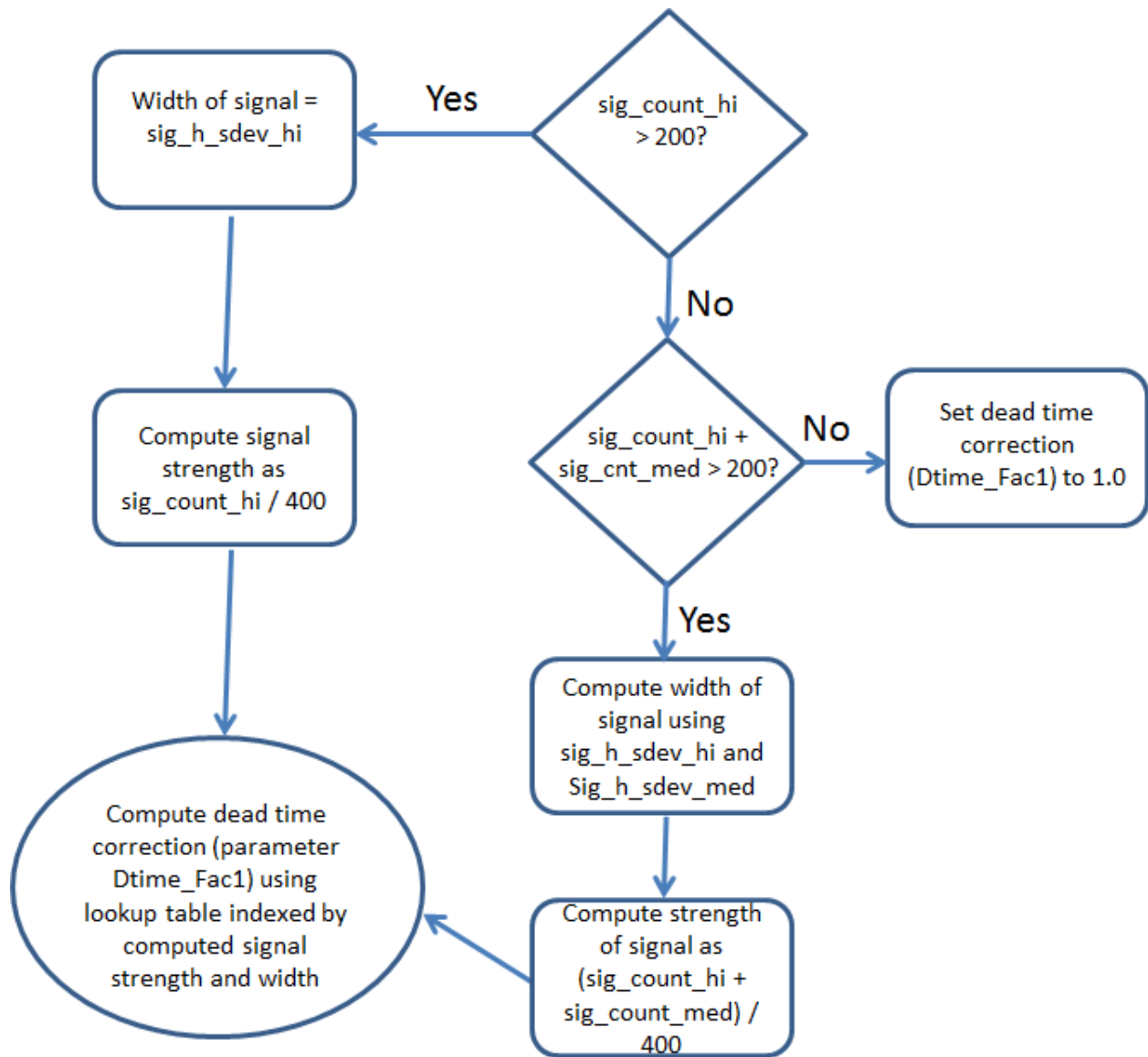


Figure 2.2. Flow diagram for computing the dead time correction factor using ATL03 measured surface signal photon count and standard deviation.

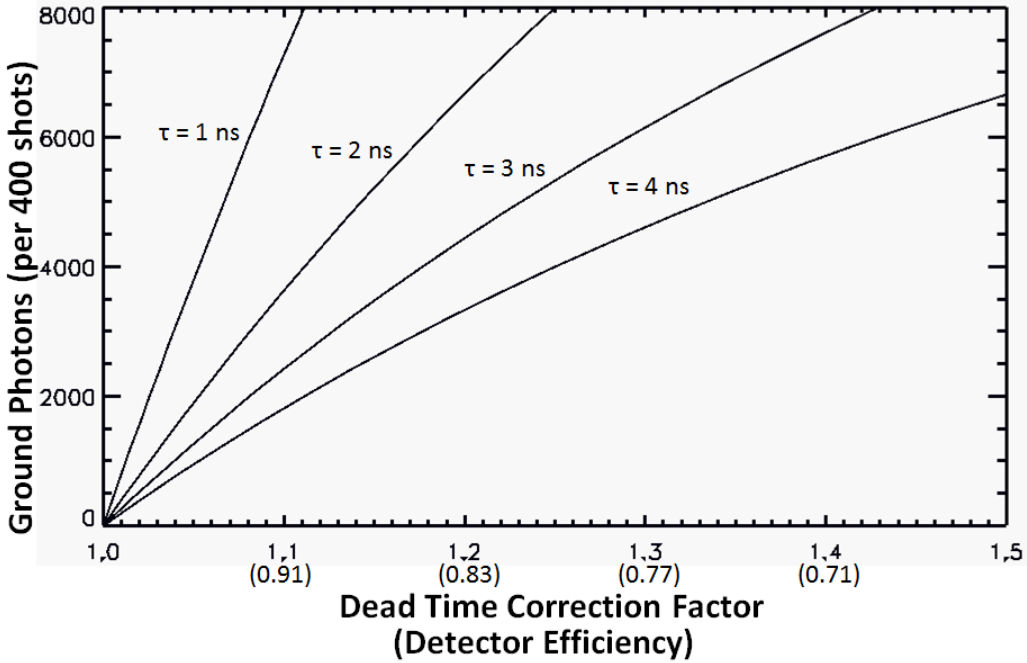


Figure 2.3. Detector dead time correction factor and efficiency as computed from equation 2.1 as a function of received photons (400 shot sum) within a 30 m bin for different values of detector dead time (τ).

The dead time correction can also be computed analytically. This method does not include the effects of pulse width and is thus not as accurate as the above method.

$$D_c = \frac{1.0}{1.0 - \frac{\tau P_m}{80.0 \times 10^{-6}}} \quad (2.1)$$

$$P_c = D_c P_m \quad (2.1a)$$

Where D_c is the dead time correction factor (*Dtime_fac2*), P_m is the measured photon count (surface signal, per bin per 400 shots), τ is the detector dead time ($\sim 3.0 \times 10^{-9}$ s), and P_c is the dead time corrected signal. The exact value of τ to use can be calculated from the appropriate CAL42 table by averaging the dead time for all 16 strong spot detectors. The atmosphere bins are 30 m which is equivalent to 0.20 microseconds, so the dead time must be scaled to this time interval. To do so we divide the detector dead time by the bin length (in time – 0.20×10^{-6} s) multiplied by the number of shots summed (400). The latter accounts for the fact that the ATLAS atmosphere data are sums of 400 shots. Figure 2.3 shows the result of equation 2.1. Referring to Figure 2.1, the effect of roughness is to broaden the return pulse, which decreases the effect of dead time. It is as if increasing surface roughness decreases the dead time of the detector (see the 4 curves in Figure 2.3). This value (D_c from equation 2.1) should be written to

ATL04 as parameter *Dtime_Fac2* in addition to *Dtime_Fac1*. P_m in equation 2.1 is in fact the surface signal (parameter *Surface_Sig*) as determined in section 3.3.5. Thus to calculate *dtime_fac2*, one must first have the magnitude of the surface signal in photons per bin. See section 3.3.5 for the method to compute the surface signal (parameter *Surface_Sig*).

~~Note that if no surface signal was found, then *Dtime_Fac1* and *Dtime_Fac2* should be set to invalid.~~

Equation 2.1 defines *dtime_fac2*. It is a number between 1.0 and 2.0. Usually about 1.1 – 1.5. The surface signal only (*Surface_Sig*) is multiplied by that factor to dead time correct the surface signal. No need to apply this to atmospheric bins. Equation 2.1 is an approximation to the method used to compute *dtime_fac1*. We want to define a control parameter that specifies which dead time factor to use. Call this "dtime_select". If 1, then use *dtime_fac1*, if 2 then use *dtime_fac2*. Default value of 1. The code should use what "dtime_select" specifies, but if it is asking for *dtime_fac1* and for some reason, it cannot be calculated, it should be smart enough to default to *dtime_fac2*. *Dtime_fac2* can always be calculated as long as there is a surface signal. *Dtime_select* should be on both ATL04 and ATL09.

2.2 Correction for Raw Profile Shifting

The raw atmosphere profiles are constructed from two sets of 200 shot summed profiles onboard the satellite. The top bin of all 200 shots of each sum will begin at the same height above the WGS84 ellipsoid. It is possible that the height of the top bin of the next 200 shot sum is different than that of the previous 200 shot sum. In this case, when the flight software sums the two 200 shot sums together to produce the 400 shot sum that is downlinked, the shifting can result in some bins of the 400 shot profile containing only the sum of 200 shots. The flight software removes the bins at the top of the profile with only a 200 shot sum and the bins with only a 200 shot sum at the bottom of the profile will be retained. To determine how many bins at the end of the profile do not overlap (and, hence, contain the original 200 shot values), the flight software computes the parameter *atm_shift_amount* that is stored on the ATL02 product. For those bins (with only a 200 shot sum) the ATL04 processing is to double the photon counts in the lower bins therein to make them consistent with the rest of the 400 shot sum profile. The bins to be doubled are simply the last "*atm_shift_amount*" bins of each 25 Hz profile. This correction is required for each of the 3 profiles. Note: There is a slight difference in the start of the range window, to the order of about 40 ns. This currently is not corrected for in the L2A processing.

2.3 Transmit Echo Pulse

The ATLAS beams 1 and 2 will have within them the transmit echo pulse (TEP). The position of the TEP can be calculated and should reside within 1 or 2 atmospheric bins (30 m wide) for each 400 shot (summed) profile. We will need to calculate the location of this bin and set its value to the average of the bin above and below. The algorithm to compute the location of the TEP within the atmospheric profile is given below. This correction must be made to ATLAS beams 1 and 2 (atmospheric profiles 1 and 2). ATLAS beam 5 (atmospheric profile 3) will not contain the TEP. This correction should be the first thing done before any other ATL04 processing.

To compute the TEP location within the atmospheric profile, we need the range from spacecraft to the top of the atmospheric profile in nanoseconds. Call this value R. Then the time of flight (TOF) of the TEP center position (in nanoseconds) is:

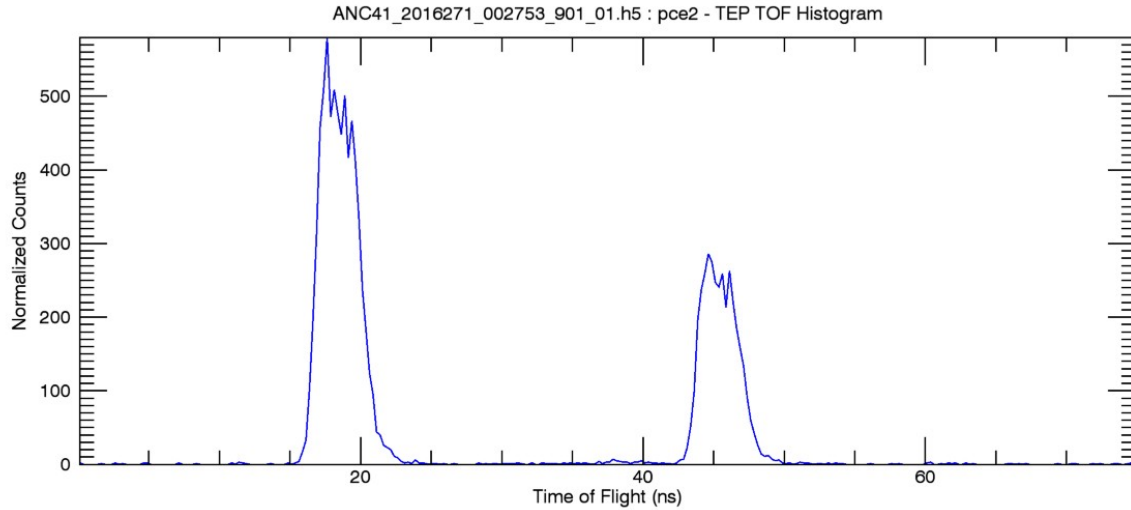


Figure 2.4 The Transmit Echo Pulse (TEP) shape and magnitude as a function of time from laser fire. The smaller second pulse (past 40 ns) is the TEP echo.

$$T = \text{INT}(R/\text{prf_inv}+1)*\text{prf_inv}+\text{TEPstart}+0.5*\text{TEPwidth} \quad (2.2)$$

Where TEPstart is a parameter that varies by picoseconds but can be considered constant for our purposes. TEPstart is a parameter on ATL03 (/ancillary_data/tep/tep_range_prim) and should be put on ANC39 and used in equation 2.2. The nominal value of TEPstart is 15 ns. TEPwidth will also be a constant and will equal the time between the beginning of the TEP and the end of the TEP echo as seen in Figure 2.4. Thus, the nominal value for TEPwidth is 40 ns. Prf_inv is the time in seconds between laser pulses (= 1.0e-4s). The bin of the atmospheric profile that contains the TEP is then:

$$\text{TEP_bin} = (T-R)/\text{ATMbinwidth} \quad (2.2a)$$

Where ATMbinwidth is the atmospheric bin width in seconds (= 200 e-9s). This bin and the bins immediately above and below it (as a margin of safety) must be replaced by the adjacent atmospheric bins as:

$$\text{ATM_bins}(\text{TEP_bin}-1) = \text{ATM_bins}(\text{TEP_bin}-2)$$

$$\text{ATM_bins}(\text{TEP_bin}+1) = \text{ATM_bins}(\text{TEP_bin}+2)$$

$$\text{ATM_bins}(\text{TEP_bin}) = (\text{ATM_bins}(\text{TEP_bin}-1) + \text{ATM_bins}(\text{TEP_bin}+1))/2$$

Where ATM bins represents the atmospheric profile.

3 L2A Product: Normalized Relative Backscatter (ATL04)

The atmosphere L2A product will be called ATL04 and will consist of what is termed Normalized Relative Backscatter (NRB) profiles and calculated 532 nm calibration coefficients (plus other ancillary/supporting data parameters). The NRB profiles are created from the profiles of raw photon counts (supplied from ATL02 – parameter /atlas/pcex/atmosphere_sw/atm_bins) by subtracting the background, multiplying by the square of the range from the satellite to the return height and normalizing by the laser energy. It was recognized by the reviewer of this document that since scattering within a bin originates from multiple altitudes, there is no unique range that can be applied to the bin. We now recognize this and have devised a method which will help alleviate this effect. In section 3.3.2 we develop a method to remove the molecular scattering from adjacent laser pulses from the recorded profile. We recognize that this method cannot remove particulate scattering that has been folded down into the profile, but it is the best that can be done.

The calibration coefficient (C) is derived from the NRB profiles (and knowledge of the temperature and pressure of the atmosphere) and is used to compute calibrated, attenuated backscatter profiles (which will be on the ATL09 product, not on ATL04). We do not know how variable C will be or how it will change with time. Normally, the factors that cause C to change are 1) boresite misalignment, 2) detector changes in responsivity, 3) changes in laser characteristics not accounted for by laser energy monitor data, and 4) overall changes in either or both the transmit and receive (optics) system throughput. Past experience with GLAS and CALIPSO indicates that calibration changes are mainly related to temperature change effects on the boresite as the satellite travels from sunlight to darkness and vice versa. However, since ATLAS will have an active continuous boresite alignment process, this may not be the case for ICESat-2. A thorough discussion of the calibration coefficient and how it is calculated is presented in section 3.3.7. There is also the possibility of using the transmit echo, which will be recorded onboard periodically, to monitor changes in the receiver optics transmission and detector quantum efficiency. These two parameters are part of what determines the value of C for lidar systems (see Equation 3.26).

For the computation of latitude and longitude (of the laser footprint on the surface), the range from the satellite to the topmost bin of the atmosphere profile will suffice for surface (laser) spot location determination. The top of the profile will be the determined height above the WGS84 ELLIPSOID for this geolocation.

3.1 L2A Required Inputs

Raw strong beam atmosphere profiles (ATL02 parameter atm_bins)

ATL03: Ground signal photon magnitude and width

Laboratory data relating signal magnitude and width to detector efficiency (see Figure 2.1).

Meteorological data: wind, temperature, pressure, relative humidity and others (GMAO)

Ozone concentration (mixing ratio), source GMAO

DEM at 1x1 km resolution (GMTED2010 or as defined in ATL03 ATBD)

Surface Type (IGBP)
 Solar azimuth and zenith angle
 Range from Spacecraft to start of atmosphere profile (ATL02 parameter atm_rw_start)
 Spacecraft altitude (wrt the WGS84 ellipsoid)
 Pointing angles for each beam
 Laser energy for each of the 3 strong beams, time, lat/lon
 Onboard 50 shot background (ATL02)
 200 shot sum shift amount - ATL02 parameter atm_shift_amount

The raw atmosphere profiles are the sum of 400 shots from the 3 strong beams and are assumed to come from ATL02 no with dead time correction applied.. The meteorological data should be the initial analysis fields (or a short term forecast less than 12 hour) from a global weather prediction model such as GEOS-5 (from GMAO) or the GFS or NAM models (from NCEP). The ozone concentration is included in the GMAO files.

3.2 L2A Outputs

- Normalized Relative Backscatter (NRB) profiles for each of the 3 strong beams at 25 Hz.
- Background at 25 Hz (includes Bin_{max1} , Bin_{max2} , S_{m1} , S_{m2} , S_{std} and p_{b1} and S_{tot} , P_{mtot} and p_{b2} – see section 3.3.2 below for definitions)
- Molecular backscatter profile from 20 to 0 km at 0.1 Hz, 30 m vertical resolution.
- Calibration coefficients with time and location tags
- Molecular Backscatter Average used to compute C (calibration coefficient)
- Signal average used to compute C
- Pressure, temperature from 30 to 0 km at 0.1 Hz, 30 m vertical resolution.
- Range from spacecraft to start of atm profile
- Pointing angles for each beam
- Laser energy, time, lat/lon
- Solar zenith and azimuth angle, DEM, surface type
- Surface (2 m) wind velocity and temperature
- Wind velocity and temperature at 10 m height
- Onboard 50 shot background
- MET data defined in Table 3.1

Table 3.1. ATL04 Product Parameters

Parameter	Datatype	Units	Rate	Description
Time	float	seconds	25 Hz	
Latitude	double	degrees	25 Hz	Based on range to local DEM
Longitude	double	degrees	25 Hz	
prof_dist_x	float	m	25 Hz	Along track distance from start of segment
prof_dist_y	float	m	25 Hz	Across track distance from reference pair track
Bckgrd_counts	Integer	photons	200 Hz	Onboard 50 shot background counts
Bckgrd_counts_reduced	Integer	photons	200 Hz	Onboard 50 shot background counts minus signal photons
Bckgrd_rate	Float	Photons/s	200 Hz	50 shot background rate in per second (signal)

				photons removed)
Bckgrd_hist_top	Float	m	200 Hz	50 shot background integration window top ht
Bckgrd_int_height	Float	m	200 Hz	50 shot background integration window width
Bckgrd_int_height_reduced	Float	m	200 Hz	bckgrd_int_height – signal photon height range
Sig_count_hi	Integer	photons	25 Hz	Ground signal photons for a 400 shot sum, high confidence
Sig_count_med	Integer	photons	25 Hz	Ground signal photons for a 400 shot sum, med confidence
Sig_count_low	Integer	photons	25 Hz	Ground signal photons for a 400 shot sum, low confidence
Sig_h_mean_hi	Float		25 Hz	Mean height of surface wrt EGM2008 ellipsoid, high confidence
Sig_h_mean_med	Float		25 Hz	Mean height of surface wrt EGM2008 ellipsoid, medium confidence
Sig_h_mean_low	Float		25 Hz	Mean height of surface wrt EGM2008 ellipsoid, low confidence
Sig_h_sdev_hi	Float		25 Hz	Standard deviation of surface height, high confidence
Sig_h_sdev_med	Float		25 Hz	Standard deviation of surface height, medium confidence
Sig_h_sdev_low	Float		25 Hz	Standard deviation of surface height, low confidence
NRB_Prof	Float(700,3)	Photons km ² /Joule	25 Hz	3 strong beams from 20 to -1 km (based on local DEM value) with vertical resolution of 30 m
NRB_Top_Bin	Integer(3)	NA	25 Hz	The starting (top) bin number within the -1 to 20 km frame where data begins
NRB_Bot_Bin	Integer(3)	NA	25 Hz	The ending (bottom) bin number within the -1 to 20 km frame where data ends
Backg_Max_Bin1	Float(3)	NA	25 Hz	Background method 1 maximum bin (Bin_{max1} defined in section 3.3.4)
Backg_Max_Bin2	Float(3)	NA	25 Hz	Background method 1 maximum bin 2 (Bin_{max2} defined in section 3.3.4)
Backg_Signal_Max1	Float(3)	photons/bin	25 Hz	Background signal max 1 (S_{m1} defined in section 3.3.4)
Backg_Signal_Max2	Float(3)	photons/bin	25 Hz	Background signal max 2 (S_{m2} defined in section 3.3.4)
Backg_Std_Dev1	Float(3)	photons/bin	25 Hz	Background standard deviation from method 1 (S_{std1} defined in section 3.3.4)
Backg_Method1	Float(3)	photons/bin	25 Hz	Background from method 1 (p_{b1} defined in section 3.3.4)
Backg_Std_Dev2	Float(3)	photons/bin	25 Hz	Background standard deviation from method 12 (S_{std2} defined in section 3.3.4)
Backg_Mean2	Float(3)	photons/bin	25 Hz	Signal mean from method 2 (S_{bar} defined in section 3.3.4)
Backg_Method2	Float(3)	photons/bin	25 Hz	Background from method 2 (p_{b2} defined in section 3.3.4)
Backg_Method3	Float(3)	photons/bin	25 Hz	Background from method 3 (defined in section 3.3.4)
Backg_Select	Integer	NA	1/granule	The background method used in calculation of NRB
Cal_N	Integer	NA	1/granule	Number of calibration points for this granule
Cal_C	Float(3,Cal_N)	NA	Cal_N/orbit	Calculated calibration coefficients (one per beam, eqn 3.27)

Cal_Con	Integer(3,Cal_N)	NA	Cal_N/ orbit	Calibration Confidence
Cal_Start_Time	float(Cal_N)	UTC	Cal_N/ orbit	Start Times of calibration calculation
Cal_End_Time	float(Cal_N)	UTC	Cal_N/ orbit	End Times of calibration calculation
Cal_Start_Latitude	float(Cal_N)	degrees	Cal_N/ orbit	Start Latitude of calibrations
Cal_Stop_Latitude	float(Cal_N)	degrees	Cal_N/ orbit	Stop Latitude of calibrations
Cal_Start_Longitude	float(Cal_N)	degrees	Cal_N/ orbit	Start Longitude of calibrations
Cal_Stop_Longitude	float(Cal_N)	degrees	Cal_N/ orbit	Stop Longitude of calibrations
Cal_Molec	float(Cal_N)	m ⁻¹ sr ⁻¹	Cal_N/ orbit	Molecular Backscatter value used to compute Cal_C
Cal_NRB	float(Cal_N)	NA	Cal_N/ orbit	NRB value used to compute Cal_C
Cal_C_Trans	float(Cal_N)	NA	Cal_N/ orbit	The total transmission used to compute Cal_C
Cal_Ozone_Trans	float(Cal_N)	NA	Cal_N/ orbit	Ozone transmission term used to compute C
MET_Temp	Float(700)	K	1 Hz	Temperature profiles from 30 to 0 km
MET_Pres	Float(700)	Pa	1 Hz	Pressure profiles from 30 to 0 km
MET_Latitude	Float	deg	1 Hz	Latitude of MET data
MET_Longitude	Float	deg	1 Hz	Longitude of MET data
MET_PS	Float	Pa	1 Hz	Surface Pressure
MET_U2M	Float	ms ⁻¹	1 Hz	Eastward component of wind at 2m height
MET_U10M	Float	ms ⁻¹	1 Hz	Eastward component of wind at 10m height
MET_U50M	Float	ms ⁻¹	1 Hz	Eastward component of wind at 50m height
MET_V2M	Float	ms ⁻¹	1 Hz	Northward component of wind at 2m height
MET_V10M	Float	ms ⁻¹	1 Hz	Northward component of wind at 10m height
MET_V50M	Float	ms ⁻¹	1 Hz	Northward component of wind at 50m height
MET_T2M	Float	K	1Hz	Temperature at 2 m height
MET_T10M	Float	K	1Hz	Temperature at 10 m height
MET_QV2M	Float	Kg/Kg	1 Hz	Specific humidity at 2 m height
MET_QV10M	Float	Kg/Kg	1 Hz	Specific humidity at 10 m height
MET_TS	Float	K	1 Hz	Surface (skin) temperature
MET_TROPPB	Float	Pa	1 Hz	Blended tropopause pressure
MET_TROPT	Float	K	1 Hz	Tropopause temperature
MET_TQL	Float	Kg/m ²	1 Hz	Total column cloud liquid water
MET_TQI	Float	Kg/m ²	1 Hz	Total column cloud ice
MET_CLDPRS	Float	Pa	1 Hz	Cloud top Pressure
Molec_Backscatter	Float(700)	m ⁻¹ sr ⁻¹	1 Hz	Molecular backscatter profile, 30 m resolution, -1 to 20 km
Moec_Trans	Float(700)		1 Hz	Molecular transmission profile, 30 m resolution, -1 to 20 km
Ozone_Trans	Float(700)		1 Hz	Ozone transmission profile, 30 m resolution, -1 to 20 km
Mol_Backs_folded	Float(700)	m ⁻¹ sr ⁻¹	1 Hz	Folded molecular backscatter profile (equation 3.17)
Dtime_select		NA		Control parameter for determining which method to use to compute the dead time correction factor

Dtime_Fac2	Float(3)	NA	25 Hz	Dead time correction factor for surface signal computed from equation 2.1
Dtime_Fac1	Float(3)	NA	25 Hz	Dead time correction factor for surface signal computed from radiometric lookup table
Surface_Sig	Float(3)	Photons	25 Hz	Surface signal from the 3 strong beams
Surface_Bin	Integer(3)	NA	25 Hz	Bin number of surface return
Surface_Height	Float(3)	m	25 Hz	Surface height (from signal) for each beam
Range_S	float	km	25 Hz	Range from spacecraft to top of profile
ATLAS_Altitude	Float	m	25 Hz	Altitude of Spacecraft wrt the WGS84 ellipsoid
ATLAS_PA	float	degrees	25 Hz	Pointing angle of spacecraft
Laser_Energy	Float(3)	Joules	10 Hz	Laser energy of each beam
Solar_Zenith	float	degrees	1 Hz	Solar Zenith Angle
Solar_Azimuth	float	degrees	1 Hz	Solar Azimuth Angle
Dem_h	float	km	25 Hz	DEM value from a 1 kmx1km
Surf_type_igbp	integer	NA	25 Hz	IGBP Surface Type

Note: Data Product quality parameters not listed

3.3 NRB Computation

The first step in the lidar data processing is to compute what we call normalized relative backscatter (NRB) from the raw level 0 data. In this step, three corrections to the data are made: 1) Laser energy normalization, 2) range square correction and 3) background subtraction. The lidar equation is:

$$S(z) = \frac{CE\beta(z)T^2(z)}{r^2} + p_b + p_d \quad (3.1)$$

In the above, r is the range from the spacecraft to the height z , $S(z)$ is the measured raw signal (photons) at height z , C is the lidar system calibration coefficient, E the laser energy, $\beta(z)$ the 180° backscatter coefficient at height z , $T(z)$ the one way atmospheric transmission from the spacecraft to height z , p_b the solar background and p_d the detector dark count rate. The NRB (computed for each of the 3 strong beams) is then:

$$NRB(z) = (S(z) - p_b - p_d)r^2/E = C\beta(z)T^2(z) \quad (3.2)$$

For ICESat-2, the most difficult thing in the above is the solar background (p_b) computation as both E and r are well known. In practice we will lump p_b and p_d together and their sum will be called simply ‘background’. At night, with no moon (and no effect from city lights), the background will simply be the dark count rate (p_d), while during the day the background will be a sum of p_b and p_d . The NRB will constitute an L2A product (Parameter *NRB_Prof* on ATL04). ICESat-2 is using PMT detectors with very short dead times (3 ns). The count rates associated with atmospheric scattering and solar background will not require dead time correction (unlike the SPCMs used in GLAS), however, dead time is important for the ground return. The ground return signal (in photon counts) will be computed in ATL04 and carried forward to ATL09 where it is used to compute Apparent Surface Reflectance (ASR) which is a level 3 product (ATL09) and is discussed in section 4.

Prior to computing the NRB, the raw photon count profiles ($S(z)$) need to be corrected for the folding of molecular scattering from above 15 km into the recorded profile. This correction is discussed in section 3.3.2, after we discuss how to compute molecular backscatter below.

3.3.1 Molecular Backscatter Computation

A fundamental parameter that will be used in a number of places in this document is the molecular backscatter coefficient (β_m). Molecular backscatter is a function of atmospheric density which is computed from the ancillary MET data. We will compute β_m from 60 km altitude to the ground once per second along the orbit track. Though only 20 km will be stored on the ATL04 product, we need to compute the molecular backscatter up to 60 km to correct the raw signal for molecular scattering folded into the profile from above (see section 3.3.2). Also on the product will be the latitude and longitude of the molecular backscatter profile (ATL04 parameters *MET_Latitude* and *MET_Longitude*).

The MET data (as obtained from the GMAO ancillary data) are reported at standard pressure levels which include temperature, relative humidity and the geopotential height at that pressure level. The geopotential height is very close to the geometric height (above mean sea level) and only varies by a few percent due to gravitational variation (mostly) as a function of latitude. Please see Appendix B for how to convert from geopotential height to geometric height. The pressure ($P(z)$), temperature ($T(z)$) and relative humidity ($RH(z)$) are calculated for the bins (heights) between the standard pressure levels. The temperature and relative humidity can be linearly interpolated (to 30 m vertical resolution) from the model pressure levels. The pressure cannot be (linearly) interpolated and must be computed using the hypsometric formula (Byers, 1974):

$$z_2 - z_1 = \frac{R\bar{T}}{g} \ln(P(z_1)/P(z_2)) \quad (3.3)$$

In equation 3.3, let us set

$$\frac{R\bar{T}}{g} = \psi$$

Where \bar{T} is the average temperature of the layer between z_1 and z_2 , g the gravitational constant and R the ideal gas constant for dry air (see Table 3.2). Now we re-write equation 3.3 as:

$$\psi = \frac{(z_{m2} - z_{m1})}{\ln(P(z_{m1})/P(z_{m2}))} \quad (3.4)$$

Here, z_{m1} and z_{m2} are the heights of the model temperature and pressure data and $z_{m2} > z_{m1}$. The top model height will ideally be greater than 60.0 km as we are computing the pressure (and following that, the molecular backscatter) to 60 km altitude.

Then, for all z between z_{m1} and z_{m2} we compute the pressure at lidar bin resolution ($\Delta z=30$ m here) as:

$$P(b_i) = P(b_{i-1}) \exp \left[\frac{(\Delta z)}{\psi} \right] \quad (3.5)$$

Where b_i denotes the lidar bin number. Here we are computing the pressure at 30 m increments starting at the lowest model level (highest pressure) and working upward in height. Thus Δz will always be 30 m (in this case).

An example program, written in IDL is shown in Appendix A. This program is used with radiosonde data as a demonstration, but it can just as well be used with model data such as GEOS-5. Note that this code will produce profiles of pressure, temperature and molecular backscatter from the ground upward (bin 0 at the ground). In the ATL04 product we want bin 0 to be at the top of the profile. Also, relative humidity is not included in the code, but if available in the model data, it can be linearly interpolated as is done for the temperature. The moisture effect on the calculation of molecular backscatter is negligible except for possibly within the boundary layer.

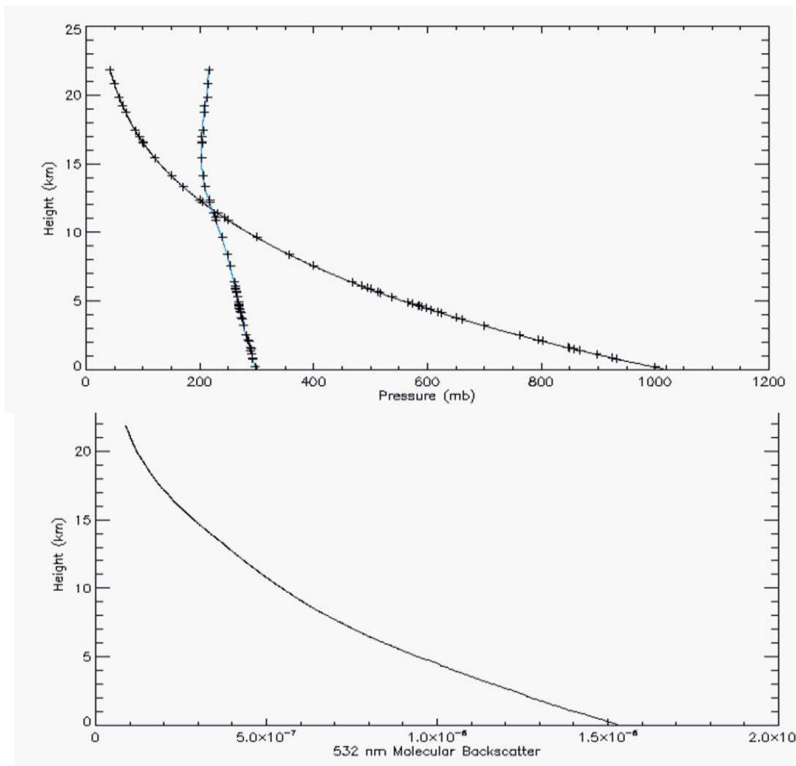


Figure 3.1 Output from the code in Appendix A to interpolate pressure and temperature (blue line, °K) from observation levels to 30 m lidar bin resolution (top). Molecular backscatter calculated from the resulting temperature and pressure profiles using equations 3.6 and 3.10 (virtual temperature was not used here).

The output of the code in the Appendix is shown above in Figure 3.1 above. The ‘+’ signs indicate the radiosonde data for both the pressure (black line) and the temperature (blue line).

From the calculated temperature, relative humidity and pressure profiles, the molecular number density ($N(z)$) is calculated from the ideal gas law as:

$$N(z) = P(z) / (kT_v(z)) \quad (3.6)$$

where $N(z)$ is in units of molecules per cubic centimeter, k is the Boltzmann constant for dry air in units of ergs per degree per molecule ($k=1.3806488 \times 10^{-16}$ ergs per degree Kelvin), P is the atmospheric pressure in units of ergs per cm^2 (or millibars times 10^3), and T_v is the virtual temperature in degrees Kelvin. This equation is very similar to the equation to compute atmospheric density ($\rho(z)$), which is the same as (3.6) except that the Boltzmann constant is replaced by the ideal gas constant for dry air (R), which has a value of $287.058 \text{ m}^2 \text{ s}^{-2} \text{ }^\circ\text{K}^{-1}$. Note that we will be computing atmospheric density for the computation of ozone transmission, in equation 3.21. The effect of moisture on atmospheric density is included through the use of the virtual temperature in equation 3.6, but these effects are generally negligible above the lower troposphere. T_v is computed from the relative humidity (obtained from the MET data) by first converting it to water vapor mixing ratio. To accomplish this, we need to first compute the saturation vapor pressure (e_s) which is a function of the atmospheric temperature (T in Kelvin)) as:

$$e_s = 0.6112 e^{(17.67(T-273.16))/(T-29.66)} \quad (3.7)$$

and from that compute the saturation mixing ratio (q_s):

$$q_s = 0.622 e_s / (P / 10.0) \quad (3.8)$$

where P is the atmospheric pressure in millibars. The relative humidity is simply the actual atmospheric water vapor mixing ratio divided by the saturation mixing ratio times 100. Thus, the actual atmospheric water vapor mixing ratio is given by

$$q = r q_s / 100.0$$

where r is the relative humidity. And finally, the formula to compute the virtual temperature (T_v) is:

$$T_v = \frac{T}{1.0 - 3q/5} \quad (3.9)$$

Following She (2001) and the CALIPSO ATBD, from the atmospheric molecular number profile, the molecular backscatter coefficient ($\beta_m(z, \lambda)$) in units of $\text{m}^{-1} \text{sr}^{-1}$ is then:

$$\beta_m(z, \lambda) = 5.1909 N(z) (550.0 / \lambda)^4 10^{-26} \quad (3.10)$$

where λ is the wavelength in nanometers (532 in our case). The molecular backscatter profile (parameter *Mol_Backscatter*) will be computed up to 20 km altitude and will be on the ATL04 product at 1 Hz. Also on the product at that rate will be the temperature and pressure profiles (parameters *MET_Temp* and *MET_Pres*) at 30 m vertical resolution.

Table 3.2 Constants Used in this Section

Constant	Value
Boltzman (k)	$1.3806488 \times 10^{-16}$ ergs per degree Kelvin
Ideal Gas Constant (R)	$287.058 \text{ m}^2 \text{ s}^{-2} \text{ }^\circ\text{K}^{-1}$
Gravitational constant at sea level (g)	9.80171 ms^{-2}

3.3.1.1 Molecular Transmission

To calculate the molecular transmission, $T_m(z)$, we first compute the molecular extinction profile ($\sigma_m(z)$), by multiplying the molecular backscatter cross section by the molecular extinction to backscatter ratio, which is known theoretically to be $8\pi K_f/3$.

$$\sigma_m(z) = 8\pi K_f \beta_m(z) / 3 \quad (3.11)$$

Where K_f is known as the King factor (Bodhaine et al., 1999) which has a value of 1.0401. The molecular optical thickness from the top of the profile (z_{top} , here we are using 60 km for z_{top}) to height z is equal to the integral of the molecular extinction profile as shown in equation 2.12

$$\tau_m(z) = \text{Sec}(\theta) \int_{z_{top}}^z \sigma_m(z) dz \quad (3.12)$$

Where θ is the off nadir pointing angle. Finally, the two-way molecular transmission ($T_m^2(z)$) between z_{top} and any height z is:

$$T_m^2(z) = e^{-2\tau_m(z)} \quad (3.13)$$

The attenuated molecular backscatter is defined as:

$$\beta_m(z) T_m^2(z) T_o^2(z) \quad (3.14)$$

Where $T_o^2(z)$ is the ozone transmission from the top of the atmosphere to height z (see equation 3.23 and 3.24 in section 3.3.3).

3.3.2 Molecular Scattering Folding Correction

As discussed in sections above, the raw photon data captured by ATLAS at height z (where z is ≤ 14 km) will have contributions from atmospheric scattering at height $z+15$ km, $z+30$ km, $z+45$ km, etc. It is important to remove as much of this as possible. There will be particulate and molecular scattering contributions, but we will have no knowledge of the former. The best that can be done is to model and remove the latter. The molecular contribution to the received photon count can be computed from equation 3.15:

$$P_m(z) = \frac{E}{r^2} \beta_m(z) \Delta z A_t T_m^2(z) T_o^2(z) S_{ret} N_a R(z) \alpha \quad (3.15)$$

In equation 3.15, α is used to adjust the computed photon count in case equation 3.15 is obviously producing too many or too few photons. Nominally α will have a value of 1.0 and will be adjusted using actual data during the checkout phase of the mission shortly after launch. The other terms used in equation 3.15 above are:

E – The laser energy in Joules

r – The range from the satellite to the height z (in m).

$\beta_m(z)$ – the molecular backscatter cross section at height z ($\text{m}^{-1} \text{sr}^{-1}$). See section 3.3.1 and equation 3.10.

Δz – the bin size in meters (30 m)

A_t – Area of telescope (m, effective)

$T_m(z)$ – Molecular atmospheric transmission from top of atmosphere to height z (Eqn 3.13).

$T_o(z)$ – Ozone transmission: top of atmosphere to height z (See section 3.3.3).

S_{ret} – Receiver return sensitivity (photons/J) from ATL02 via ATL03

N_a – Number of shots summed (nominally 400)

$R(z)$ – aerosol scattering ratio

Note that Equation 3.15 will have to be computed for each of the 3 strong laser beams if the emitted laser energy is much different for each beam. Equation 3.15 is used to compute a profile of molecular scattering contribution from 60 km to 0 km ($P_m(z)$). From that profile, the molecular scattering contribution (folded from above) to the measured ATLAS photon profile is computed as:

$$P'_m(z) = P_m(z+15) + P_m(z+30) + P_m(z+45) \quad (3.16)$$

For z between -1 and 20 km. Note that we must compute this quantity up to 20 km since the raw profile is being captured 13.5 km above the value of the DEM at the satellite location, and there will be times (which occur over elevated terrain) when we need the values between 13.5 km and 20 km. We do not need to go higher than 20 km since, that portion of the profile (if it exists) will be eliminated as part of the vertical alignment process (see section 3.3.6). Note also the height in third term in 3.16 will go above 60 km for $z > 15$ km. This is above the top height of the MET data (60 km). The values of $P_m(z)$ for $z > 60$ should be set to $P_m(60)$.

Then the corrected raw photon count profile is:

$$S'(z) = S(z) - P'_m(z) \quad (3.17)$$

Where $S(z)$ is the raw photon count profile measured by ATLAS. Note that this process leaves the molecular scattering of the original profile ($S(z)$) intact. It only removes the molecular scattering folded down from above. Also note that the quantity subtracted from the right side of Equation 3.17 ($P'_m(z)$) will be a fractional value. The raw photon count ($S(z)$) is an integer value and at times will be zero. Thus, the result ($S'(z)$) will at times be negative.

The NRB corrected for the molecular folding can now be computed as:

$$NRB'(z) = (S'(z) - p_b - p_d)r^2/E = C\beta(z)T^2(z) \quad (3.18)$$

Since we may not know all the instrument parameters accurately, or they may drift somewhat with time, a scale factor (α) is used in equation 3.15. If we knew all instrument parameters perfectly, the value of α would be 1. In practice it will not be unity. One way to find the value of α is to compute the average of the top 1 km of the raw (photon count) profile over the polar region (in darkness) and compare it with the average of that computed from equation 3.15 for the same vertical range. Over the poles, with no cloud or aerosol above 12.5 km, the average of the raw photon count between 12.5 and 13.5 km from the profile should match that computed from equation 3.15. Adjustment to α can then be made so that the ratio of the result of equation 3.15 to the 1 km profile top average is unity. The main problem with this method for determining α is knowing for sure that there is no cloud or aerosol scattering above 12.5 km. $R(z)$, the aerosol scattering ratio can be obtained from either GMAO model output or based on a climatological value computed from CALIPSO data as a function of latitude, height and season. $R(z) = 1.0 + \beta_a(z)/\beta_m(z)$ where $\beta_a(z)$ is the aerosol scattering coefficient at height z . Initially we will use $R(z) = \text{constant} = 1.02$.

In order to compute Equation 3.16, the molecular backscatter profile must be computed up to 60 km. Above 60 km (or the top height of the MET data) the molecular backscatter can be set to the value at 60 km (or the top height of the MET data). Here we define the folded molecular backscatter profile as:

$$\beta'(z) = \beta(z) + \beta(z+15) + \beta(z+30) + \beta(z+45) \quad (3.19)$$

The folded molecular backscatter profile from $z=-1$ km to $z=20$ km (700 30 m bins) will be on the ATL04 and ATL09 products (parameter *Mol_Backs_folded*). For z below ground level, $\beta'(z)$ can be set to the lowest (in height) valid value.

3.3.2.1 Error Analysis of Molecular Contribution

The uncertainty related to the calculation of molecular contribution to the signal (equation 3.15) can be estimated as:

$$\left(\frac{\Delta P_m}{P_m}\right)^2 = \left(\frac{\Delta \beta_m}{\beta_m}\right)^2 + \left(\frac{\Delta A_t}{A_t}\right)^2 + \left(\frac{\Delta T_m}{T_m}\right)^2 + \left(\frac{\Delta T_o}{T_o}\right)^2 + \left(\frac{\Delta Q_e}{Q_e}\right)^2 + \left(\frac{\Delta T_s}{T_s}\right)^2 \quad 3.20$$

Values of the above equation will be included in the next version of this ATBD.

3.3.3 Ozone Transmission Computation

The first step in computing the ozone transmission is to calculate an atmospheric density profile following the methods presented in section 3.3.1 above. Equation 3.6 computes the molecular number density ($N(z)$). Replacing the Boltzmann constant (k) with the ideal gas constant for dry air (R) in equation 3.6, yields the atmospheric density:

$$\rho(z) = \frac{P(z)}{RT(z)} = \frac{k}{R} N(z) \quad (3.21)$$

The ozone transmission, $T_o^2(z_c)$, is calculated using ozone mass mixing ratios obtained from the GMAO meteorological data set which contains ozone mass mixing ratios. This, like other MET parameters are given at specific pressure levels. They are first linearly interpolated to 30 m bins as temperature was in section 3.3.1 forming a profile from 60 km to the ground ($r_o(z)$). The ozone mass mixing ratio profile is then converted to column density per kilometer (atm-cm/km), $\epsilon_o(z)$, using the following equation

$$\epsilon_o(z) = \frac{r_o(z)\rho(z)}{2.14148 \times 10^{-5}} \quad (3.22)$$

where z is the altitude in km, and $\rho(z)$ is the atmospheric density at z and calculated from equation 3.21.

The next step is to calculate the ozone transmission term. $T_o^2(\lambda)$ is calculated using the following equation:

$$T_o^2(\lambda, z) = \exp\left[-2c_o(\lambda)\int_H^z \epsilon_o(z') dz'\right] \quad (3.23)$$

where $c_o(\lambda)$ is the Chappius ozone absorption coefficient in cm^{-1} . The ozone absorption coefficient is obtained at the correct wavelength from a table compiled in Iqbal [1984] using data from Vigroux [1953]. $c_o(\lambda)$ is 0.065 cm^{-1} at 532 nm. H is nominally 60 km.

The ozone transmission to the top of the calibration zone (z_c) is then corrected for the off-nadir angle of the laser beam (θ - different for each of the 3 strong beams):

$$T_o^2(\lambda, z_c) = T_o^2(\lambda, z_c)^{\sec(\theta)} \quad (3.24)$$

Where λ is 532 nm. The calculated ozone transmission (down to the top of the calibration zone – nominally 13.5 km) will be on the ATL04 product (parameter *Cal_Ozone_Trans*). A nominal value for the ozone transmission at the 13 km altitude is about 0.97.

3.3.4 Background Computation

As discussed in the introduction, the background computation would normally be done using the data below the ground. However, both molecular and cloud scattering may exist within this region from pulse aliasing (due to the 10 KHz laser rep rate). Hence, an alternative approach for background computation must be devised. There really is no way to do it accurately, unless one could remove all atmospheric scattering from the profile (which is essentially impossible). Here we present two separate methods for background computation using the atmospheric profiles. At present we feel both should be implemented and the results stored on the product. The background to be used in the computation of NRB (Equation 3.2) will be selected by the ancillary input parameter “Backg_Select” (see Table 3.5) which will also be stored on both the ATL04 and ATL09 products. The basis for this approach is as follows: Since there is no place in the atmospheric profile where we are guaranteed of no contribution from atmospheric particulate scattering, the best that can be done is to locate and remove any cloud layers in the data and look for a minimum in the cloud-cleared profile. The minimum may be associated with a particulate-free area of the profile but at a minimum, will still contain molecular scattering. However, we can model and remove molecular scattering leaving only background. The steps can be summarized as:

- 1) Locate and remove any cloud scattering within the $S'(z)$ profile
- 2) Search the profile for an extended (vertically) minimum of the signal. This is the part of the profile that is most likely to contain only molecular scattering. In totally clear conditions, this will normally be the top portion of the profile.
- 3) Compute the molecular scattering photon count contribution to the signal.
- 4) Compute the mean of the profile in the region of minimum signal. Subtract from this the molecular photon contribution. The result is the background.

Of course this assumes the mean was constructed from a totally ‘clean’ area of the profile, devoid of cloud or aerosol scattering. We can never be totally sure of this and it will many times introduce error into the background computation. In addition, attenuation from layers above 14 km cannot be computed. If such attenuation is present, then the result of step 4) could be negative as it will contain less molecular scattering than was removed to form the $S'(z)$ profile in equation 3.18. In such cases we would set the background to 0.0.

The procedure to accomplish this is as follows:

For each 400 shot sum ($S'(z)$ corrected photon count data) and for each of the 3 strong beams, from the top of the profile (bin 0) to the bottom (bin 466) do the following:

- 1) Find the bin ($\text{Bin}_{\text{max}1}$) with the maximum value (S_{m1}) in the $S'(z)$ profile
- 2) Set to -1 the maximum bin and two bins before and ten bins after the maximum bin (13 bins total).
- 3) Repeat steps 1) and 2) to obtain maximum bin ($\text{Bin}_{\text{max}2}$) and value (S_{m2}).
- 4) Compute the standard deviation of the non-negative bins of the profile. Call this $S_{\text{std}1}$
- 5) Divide the profile into 'Backg_Nseg' (nominal value of 5) number of segments and compute the mean of each segment, using only non-negative values in the sum. If more than 50% of the bins in that segment are negative, throw that segment away.
- 6) Find the minimum mean of the computed means. Call this Seg_{min} .
- 7) Compute the molecular scattering contribution (photons) within Seg_{min} using equation 3.15. Call this M_p . Note that equation 3.15 is used to compute the molecular contribution of each bin within Seg_{min} and then summed over all bins to obtain M_p
- 8) Compute background as $p_{b1} = (\text{Seg}_{\text{min}} - M_p) * \text{Back_F1}$
- 9) If p_{b1} is negative, set p_{b1} to Seg_{min} . If it is still negative, set p_{b1} to 0.0.

Back_F1 is a scaling factor with nominal value of 1.0 (see Table 3.5). It will be used to adjust the computed background if it is seen to be continuously too high or low. Steps 1-3 above are designed to remove clouds and or the ground return. The values $\text{Bin}_{\text{max}1}$, $\text{Bin}_{\text{max}2}$, S_{m1} , S_{m2} , $S_{\text{std}1}$ and p_{b1} should be on the ATL04 output product as defined in Table 3.1. These correspond to the ATL04 output parameters *Backg_Max_Bin1*, *Backg_Max_Bin2*, *Backg_Signal_Max1*, *Backg_Signal_Max2*, *Backg_Std_Dev1* and *Backg_Method1*, respectively.

The following is a second method. It only differs in the way clouds are removed from the profile. Note that this method also uses the modified raw profile ($S'(z)$) as defined by equation 3.18.

- 1) Compute the mean and standard deviation of the $S'(z)$ profile. Call this S_{bar} and $S_{\text{std}2}$, respectively.
- 2) Set all bins that are greater than $S_{\text{bar}} + S_{\text{std}2} * \text{Back_F2}$ to -1. Where Back_F2 is an adjustable, read-in constant (see Table 3.5).
- 3) Set all bins below 3 km to -1 in the profile. To eliminate overlap region with highest probability of cloud contributions
- 4) Compute (using equation 3.15) and subtract from the profile the molecular photon contribution for each bin.
- 5) Compute the average of the bins in the profile that are greater than -1.0. This is the background (p_{b2}).
- 6) If p_{b2} is negative, set to 0.0.

The values of S_{std2} , S_{bar} and p_{b2} should be stored on the ATL04 product. These values correspond to the product variables (in Table 3.1) *Backg_Std_Dev2*, *Backg_Mean2* and *Backg_Method2*.

A third alternative for background (ATL04 parameter *Backg_Method3*) is the use of the onboard 50 shot background rate parameter originating from ATL03. This parameter (*bckgrd_rate* – see the ATL03 ATBD for details) has units of photons per second and must be converted to units of per atmospheric bin which is 30 m or 1/5 of a microsecond (0.20×10^{-6} s). Since there are 8 of these 50 shot values per the 400 shots that comprise each atmospheric profile, we average the 8 values and multiply by 400 to obtain a value consistent with the 400 shots summed to produce the atmospheric profile.

$$Backg_Method3 = bckgrd_rate * 0.20 \times 10^{-6} * 400.0$$

Where *bckgrd_rate* is actually the average of the 8 ATL03 *bckgrd_rate* values. Also stored on ATL04 should be the ATL03 parameters *Bckgrd_counts_reduced*, *Bckgrd_int_height*, *Bckgrd_rate*, and *Bckgrd_int_height_reduced*.

The parameter *Backg_Select* will be read in from an ancillary file and will control which background is used in equation 3.2 to compute the NRB. *Backg_Select* = 1 will use background method 1. *Backg_Select*=2 will use background method 2 and *Backg_Select*=3 will use background method 3. *Backg_Select* will be on both the ATL04 and ATL09 products.

One thing to mention and think about with regard to background computation is that for nighttime data, it may be better to simply set the background to the value of the detector dark count rate. This could be implemented based on the value of the solar zenith angle. For zenith angles greater than about 95 degrees, it can be assumed nighttime. However, until we get real data it is unknown whether we want to implement this approach.

It may very well turn out that we will not be able to reliably calculate the background during daytime due to the fact that no portion of the profile is devoid of atmospheric scattering. However, at present, results from applying this algorithm to simulated ATLAS data suggest that method 1 works fairly well (see below). At night, the background computation could introduce error from cloud or aerosol scattering. In practice, for nighttime data, it may be better not to calculate the background by the above methods, but instead use the lab-measured value of the detector dark counts for the nighttime background value. However, we will not know this until we can analyze actual ATLAS data.

The background algorithm (method 1) has been coded and tested using simulated ATLAS data (produced from GLAS data). Folding of clouds and molecular scattering has been included in these simulations. The results of the background computation are shown in Figure 3.2. The algorithm output is plotted versus the actual background used in the model to produce the simulated data. It is apparent that the algorithm cannot reproduce exactly the model background, but it does a reasonable job. This can be seen in Figure 3.3. The top panel represents the ATLAS simulated data with the actual (model) background subtracted. The bottom panel is again the ATLAS simulated data, but the background subtracted was computed using the method 1

algorithm. Comparison of the two images suggests the background algorithm introduces some additional noise into the data, but that its magnitude is not large.

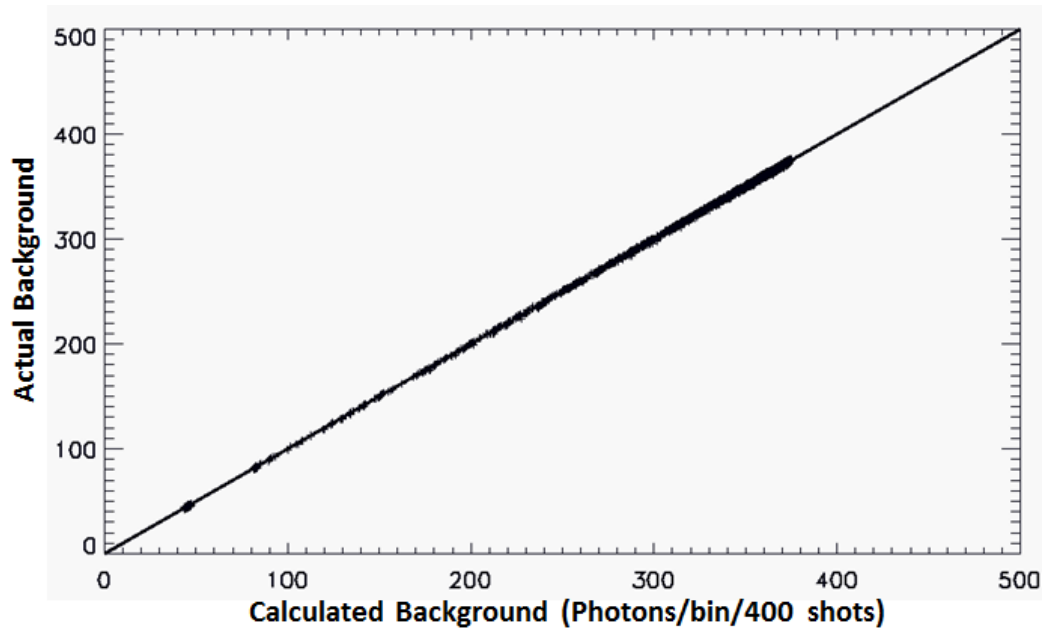


Figure 3.2 The actual (model) background versus the calculated background using the method 1 algorithm.

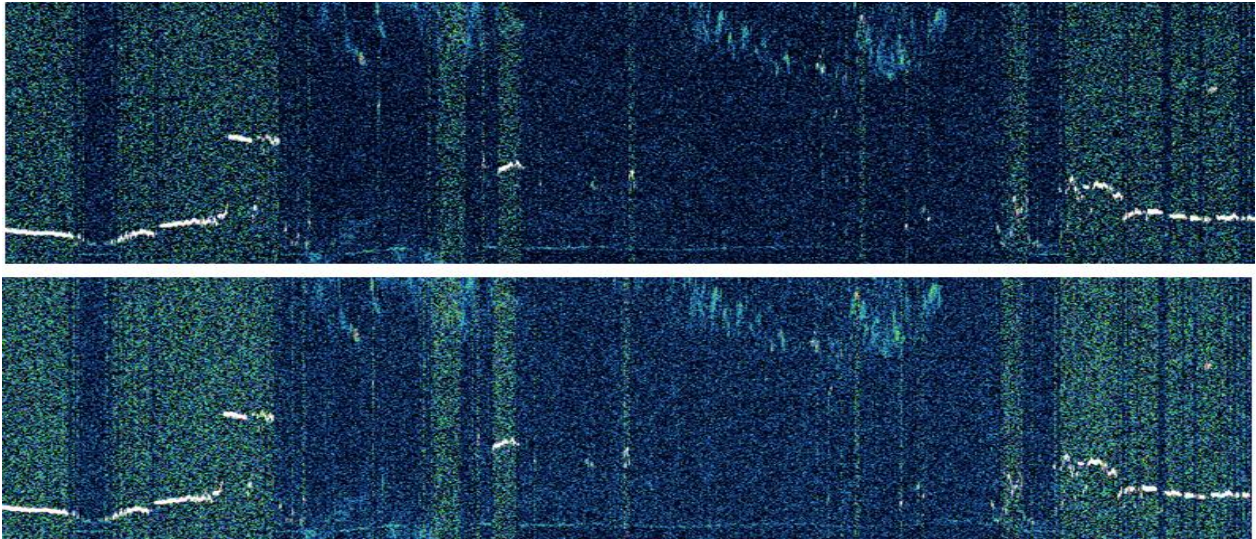


Figure 3.3. Top panel: The simulated ATLAS data with the actual (modeled) background subtracted. Bottom panel: Same data but with background subtracted computed using algorithm method 1.

Table 3.3. Background related parameters on the ATL04 product

Symbol used in background discussion	Suggested ATL04 Product Variable Name
Bin_{max1}	Backg_Max_Bin1
Bin_{max2}	Backg_Max_Bin2
S_{m1}	Backg_Signal_Max1
S_{m2}	Backg_Signal_Max2
S_{std1}	Backg_Std_Dev1
p_{b1}	Backg_Method1
S_{std2}	Backg_Std_Dev2
S_{bar}	Backg_Mean2
p_{b2}	Backg_Method2

Table 3.4. Ancillary constants used in this section. Note that some of the ATLAS instrument parameter values may change slightly by launch.

Constant	Value
Speed of light (c)	$2.9979 \times 10^8 \text{ ms}^{-1}$
Planck constant (h)	$6.6256 \times 10^{-34} \text{ Js}$
Bin size (Δz)	30 m
Effective collection area of telescope (A_t)	0.502655 m^2
Detector quantum efficiency (Q_e)	0.15
Transmission of receiver optics (T_s)	0.34
Number of laser shots summed (N_a)	400
King Factor	1.0401

Table 3.5 Adjustable parameters used in this section.

Constant/Adjustable Parameter	Use/Meaning	Nominal Value
Backg_F1	Scaling factor in Method 1 background computation	1.0
Backg_F2	Scaling factor in Method 2 background computation	2.5
α	Scaling factor for photons due to molecular scattering (Eqn 2.11)	1.0
Backg_Nseg	The number of segments to use for method 1 background computation	5

Backg_Select	Background method to use in computation of NRB	1
Dtime_Select	Defines which dead time correction factor to use (dtime_fac1 or dtime_fac2)	1

3.3.4.1 Theoretical Background

The solar background measured by ATLAS in clear sky is a function of the surface reflectivity, solar angle, atmospheric transmission and instrument parameters like the telescope field of view, filter width and telescope size. We want to compute the expected or theoretical background as it might provide useful for cloud detection during the day. This new parameter (for version 7.5) will be called *backg_theoret* and must be calculated by and stored on ATL09, since its computation relies on an estimate of the surface reflectivity. Surface reflectivity (*aclr_true*) is computed and stored on ATL09 – see section xx. ATL04 does not have access to *aclr_true*. The equation below gives the ATLAS theoretical background for a clear atmosphere and assuming a Lambertian surface reflectance (following Ismail and Browell, 1989).

$$B_t = \frac{B_{ret} \cos(S_a) S_i R_s T_{fov}^2 T_a F_w A_{tran}^{(1+Sec(S_a))/2}}{4} \quad (3.25)$$

Where:

B_t = ATLAS theoretical background in photons/second

S_a = Solar zenith angle (degrees)

S_i = Solar irradiance at top of atmosphere at 532 nm (1.84d0 W/(m²*nm))

R_s = Reflectivity of the surface (use ATL09 parameter *aclr_true*)

T_{fov} = Telescope field of view (radians)

T_a = Telescope area (m²)

F_w = Interference filter width (nm)

A_{tran} = Two-way atmospheric transmission (0.81)

B_{ret} = Overall receiver sensitivity to background light (photons/J) (from ATL03)

The parameter *backg_theoret* is then set to $B_t * 0.2e-6$ to get it in terms of photons per 30 m bin.

Note that in equation 3.25 we are using the ATL09 parameter *aclr_true* for the surface reflectivity term (R_s). In the computation of *aclr_true*, we have already taken into account the two-way atmospheric transmission at 532 nm. We thus must multiply the result of equation 3.25 by 1.0/0.81.

3.3.5 Surface Signal

The surface signal is intended to be all of the photons reflected from the surface. There are two ways to obtain the surface signal. The first is by searching the atmospheric profile as described

below and the second is by using the surface signal photons that are detected via the ATL03 algorithm (see section 2.1 for a discussion of these ATL03 parameters). Here we outline the procedure to locate the surface signal from the atmospheric profiles.

The data used for the search should be the raw atmospheric profile (photon counts) with the background subtracted. The algorithm will search in a narrow window about 1000 m wide for the maximum signal return using the raw photon count data. The search will start at the bottom of the profile and proceed upwards. Note that the bottom of the profile will be nominally 500 m below the ground as determined by the onboard DEM and data system software. The bin with the maximum signal plus the bin preceding and after is then the surface signal (in photons). A simple algorithm follows:

- 1) Find the maximum return starting 1 bin before the end of the profile (nominally 500 m below the ground) and continuing for 32 bins (about 1 km). The search proceeding upwards. Call the maximum bin number B_{\max}
- 2) Compare the signal value ($S(B_{\max})$) with the ground threshold ($Ground_Thresh$). $Ground_Thresh$ is in terms of photons/bin per 400 shots and will have the nominal value of 200 (see Table 3.7).
- 3) If $S(B_{\max})$ is $< Ground_Thresh$ then no ground return. Set ground signal ($Surface_Sig$) to zero and set $Surface_Height$ to invalid. Also set the surface bin number to invalid (parameter $surf_bin$).
- 4) If $S(B_{\max})$ is $\geq Ground_Thresh$, then compute $Surface_Height$ and set $Surface_Sig$ to $S(B_{\max})$
- 5) Apply dead time correction to $Surface_Sig$. The new parameter “ $dtime_select$ ” will define which dead time correction factor to use. If $dtime_select=1$, then use $dtime_fac1$. If $dtime_fac1$ is not available, then use $dtime_fac2$. If $dtime_select=2$, then use $dtime_fac2$. Note: this is only required if the atmosphere profiles from ATL02 have not been dead time corrected.

B_{\max} (ATL04 parameter $Surface_Bin$) and the ground signal ($Surface_Sig$) will be on the product.

The computation of $dtime_fac1$ and $dtime_fac2$ was presented in section 2.1. The dead time correction factor is a number greater than one. The surface signal is corrected for dead time by multiplying it by the dead time factor.

3.3.6 Vertical Height Adjustment

The raw atmosphere profiles will be captured based on the value of the DEM at the sub-satellite point. They will extend from about 500 m below the DEM value to roughly 13.5 km above (14 km total). The height of the top bin can shift from one 25 Hz profile to the next as it follows the DEM (but more likely at a slower rate). Before horizontal averages of the data can be made (needed for section 3.3.7 - calibration), they must be put in a constant height reference frame

(vertical height adjustment). The profiles will be placed into a constant reference frame with respect to the WGS84 ellipsoid (or mean sea level). The resulting 25 Hz profiles (and the subsequent NRB that will be stored on the ATL04 product – parameter *NRB_Prof* in Table 3.1) will cover the vertical range from -1 km to 20 km altitude and consist of 700 bins. Thus, over the oceans and low terrain, the data above about 13.5 km will be set to an invalid value, as will the data below about -500 m. When we are over elevated terrain, some of the bins above 13.5 km will then be populated. For instance over the high plateau of Antarctica, surface height (with respect to the WGS84 ellipsoid) can approach 4 km. In this case, the -1 to 20 km profile would have invalid values between -1 and about 3.5 km, data between 3.5 km and 17.5 km, and invalids between 17.5 and 20 km. As part of the vertical alignment algorithm, the bin number (starting from 1 at the top – call this parameter *NRB_Top_Bin*) of the first valid data bin (within the 20 to -1 km data frame) will be stored on the product for each profile. The last valid data bin is then *NRB_Top_Bin* + 466. It is acknowledged that when DEM values are greater than 6 km, data will be cut off at the top. Horizontal averages using the same bin number will then be at the same altitude. However, care must be taken to avoid invalid data bins when summing or averaging.

Since the pointing angles of the 3 strong beams will be on the order of 0.3 – 0.5 degrees with respect to nadir, vertical shifting of the bins will be negligible. However, at times ICESat-2 will off point to no more than 5 degrees for (altimetry) calibration scans. Even in these cases, the change in vertical size of the bin is only 12 cm which amounts to a 44 m change in the overall vertical extent of the profile. The pointing angle will be considered in the algorithm to place the data in the constant height reference frame. The best way to describe such an algorithm is by the (IDL) code segment below:

```
Nbins_atlas = 467      ; Number of bins in the raw (level 0) ATLAS data.
Nbins_frame = 700    ; Number of bins in constant reference frame (20 to -1 km wrt WGS84
ellipsoid)
Frame = fltarr(Nbins_frame)
Frame(*) = 9999.      ; Set all bins in Frame to invalid value
ATLAS_profile = fltarr(Nbins_atlas)
Frame_top = 20.0
Bin_size = 0.030
ATLAS_altitude = 495.0    ; Height of satellite in km wrt WGS84 ellipsoid (supplied to this
algorithm)
Range_to_data_start      ; The range from satellite to the top of the atm profile (ATL02?)
Height_top_bin = ATLAS_altitude - Range_to_data_start    ; This can range from 13.5 to over
; 20 km depending on DEM value

Pointing_angle = y      ; This is the pointing angle off nadir of spacecraft from ATL02?
Frame_ht = Height_top_bin
Bin_size_angle = Bin_size * cos(Pointing_angle)

i1 = 0
If (Frame_ht gt Frame_top) then begin
```

```

    i1 = fix((Frame_ht - Frame_top) / Bin_size_angle)
    Frame_ht = Frame_top
endif

For i=i1,Nbins_ATLAS-1 do begin
    Frame_bin = fix((Frame_top - Frame_ht) / Bin_size)
    If (Frame_bin ge Nbins_frame) then Frame_bin = Nbins_frame - 1
    Frame(Frame_bin) = ATLAS_profile(i)
    Frame_ht = Frame_ht - Bin_size_angle
Endfor

```

Note that it is possible for this process to skip a bin in the frame leaving the bin undefined. After the above is executed it is recommended to add the following code that interrogates all bins in the vertically aligned frame:

```

do i = va_first_bin, va_last_bin
    if (atm_va_bins(i) == INVALID_R4B) then
        if (i-1 >= va_first_bin .and. atm_va_bins(i-1) /= INVALID_R4B) then
            atm_va_bins(i) = atm_va_bins(i-1)
        else if (i+1 <= va_last_bin .and. atm_va_bins(i+1) /= INVALID_R4B) then
            atm_va_bins(i) = atm_va_bins(i+1)
        endif
    endif
endif
enddo

```

3.3.7 Calculation of the Calibration Coefficient

3.3.7.1 Theory

The following discussion is not required for the coded algorithm. It is merely meant as an introduction to the meaning and use of the lidar calibration coefficient. The lidar calibration coefficient relates the power received by the detector to a physical quantity – the volume backscatter cross section. The theoretical or instrument lidar calibration coefficient (C_t) is mainly a function of the transmission of the system optics (transmitting and receiving), detector efficiency, geometric considerations, and the degree of alignment between the receiver field of view and the laser spot (boresite alignment). The following equation gives the theoretical derivation of the lidar calibration coefficient.

$$C_t = FA_t T_s Q_e \lambda \Delta z / (hc) \quad (3.26)$$

Where A_t is the telescope area, c the speed of light, h the Planck constant, T_s the receiver system transmission, Q_e the quantum efficiency (or responsivity) of the detector, Δz is the bin size, λ the laser wavelength and F is the boresite factor. If the system is perfectly boresited, $F=1$. As the

receiver field of view becomes misaligned with the laser footprint (some of the laser energy is outside of the telescope FOV), F becomes less than 1. In practice, it is mainly thermally driven changes in boresite that cause changes in C_t . However, changes in detector responsivity, and system transmission are also common causes for variation in C_t . Because these factors can and do change with time in the typical lidar system, and these changes cannot easily be monitored, calibration of the lidar signal is usually performed continuously by comparing the measured signal to a reference target. The atmosphere itself can act as a reference target so long as it is devoid of particulate scatterers (or the magnitude of particulate loading is known) and the density of the atmosphere is sufficiently well known. For instance, in the lower and mid stratosphere, in the absence of large volcanic eruptions, the air is typically very clean. The scattering there consists only of molecular or Rayleigh scattering which depends on only the pressure and temperature of the atmosphere. We can very accurately calculate the molecular backscatter cross section (i.e. the target) in near real-time from NCEP (National Center for Environmental Prediction) or GMAO (Goddard Modeling and Assimilation Office) meteorological analyses or short range forecasts of temperature, pressure and moisture fields.

3.3.7.2 Calibration Algorithm using the Atmosphere

NOTE: In the discussion below, the algorithm adjustable parameters are in blue font and are assumed read in by the SIPS code from an ancillary file. These are summarized in Table 3.7 below.

GLAS successfully used the 26 to 30 km region of the stratosphere for calibration of its 532 nm channel. CALIPSO uses an even higher region for its calibration. Unfortunately, this portion of the atmosphere will not be available in ATLAS data. We will be forced to calibrate in the region 13.5-11 km. This severely limits where we can perform the calibration, since clouds typically occur up to 18 km height in the tropics and subtropics. However, for latitudes poleward of 60 – 65 degrees, clouds are generally confined below 10 – 11 km. The exception to this occurs in late winter when Polar Stratospheric Clouds often form in the stratosphere (most frequently over Antarctica). Thus, while this region offers the best hope for calibration, the data will have to be carefully screened to avoid the inclusion of cloud signal into the calibration procedure. This will be accomplished by setting a TBD threshold – call this **Cal_Cloud_Thresh** - on the value of the integrated signal between 11 and 13.5 km.

Due to the very weak molecular signal, we will most likely not be able to calibrate during daylight conditions. For each orbit we will use the data poleward of 60 degrees (exact latitude will be an adjustable algorithm parameter – call this **Cal_Latitude_Bound**) that have low background (determined by solar Zenith angle). The bins between 11 and 13.5 km will be interrogated and those that pass a threshold test to eliminate clouds (value will be adjustable – **Cal_Cloud_Thresh**) will be summed (horizontally and vertically). The result will be the calibration target. The length of time the data will be summed within the calibration zone will likely be at least 4-5 minutes. This summing length will be an adjustable algorithm parameter – call this **Cal_Integ_Time**. While this sum is being computed, concurrently the average molecular

backscatter for the same vertical window and horizontal distance will be computed from the ancillary meteorological (MET) data. The computation of the calibration coefficient then is:

$$C = \overline{NRB'(z_c)} / [\overline{(\beta_m(z_c))} T^2(z_c) R(z_c)] \quad (3.27)$$

Where $\overline{NRB'(z_c)}$ and $\overline{(\beta_m(z_c))}$

are the horizontally and vertically integrated normalized lidar signal (corrected for molecular folding – equation 3.19) and molecular backscatter through the 2.5 km thick calibration layer (11-13.5 km), respectively. These are known as product parameters *NRB_C* and *Molec_C*, respectively. Note that the molecular backscatter at z_c is simply from that height, since in the computation of NRB we have removed the folded molecular scattering.

The length of the horizontal average will vary according to the solar background conditions and the presence of cloud above 11 km altitude. In general we want to make this horizontal averaging length long enough to gather sufficient signal, but not too long so as to include varying atmospheric conditions along the horizontal averaging path. The exact averaging length is TBD and will be an algorithm parameter ([Cal_Integ_Time](#)), initially set to 300 seconds (roughly 20 degrees of latitude). We will attempt to do this at least twice while the spacecraft is poleward of 60 degrees. In equation 3.27, the *R* factor is known as the aerosol scattering ratio. This also appears in equation 3.15. In a totally clean atmosphere devoid of cloud or aerosol is equal to 1.0. In practice it is always greater than 1.0 due to the presence of aerosol (except possibly in the mid stratosphere, 30-40 km altitude – an area we do not have access to). We will assume a value of *R* based on climatology. We hope to use data from the CALIPSO mission to help determine a nominal value. This will generally be between 1.01 and 1.20 and is an algorithm parameter – call this [Cal_Scat_Ratio](#). Closer to launch, we will analyze CALIPSO 532 nm data in the polar region to calculate a representative value to use which can vary seasonally.

The computation of $\overline{NRB'(z_c)}$ in equation 3.22 will proceed for each of the 3 strong beams by summing the NRB in the altitude range 11 to 13.5 km. Thus, there will be a calibration coefficient for each of the 3 strong beams. If this 2.5 km sum is greater than [Cal_Cloud_Thresh](#), then that sum will not be included in the calculation of $\overline{NRB'(z_c)}$. In addition, summing will only occur for those profiles that are obtained with the solar **elevation** angle **less than** than [Cal_Solar_Angle_Limit](#) degrees (nominally **0.0** degrees). The sum will then be normalized by the total number of bins summed.

The molecular backscatter used in equation 3.27, will be computed once per second and computed for each 30 m bin in the calibration zone(s). One molecular backscatter value is then computed for the layer(s) by averaging the bins within the calibration zone(s). The final average molecular backscatter is then computed from the sum of these layer averages for the duration of the calibration time ([Cal_Integ_Time](#) - nominally 300 seconds). The latitude, longitude and time

of the start of the calibration (*Cal_Start_Latitude*, *Cal_Start_Longitude* and *Cal_Start_Time*) will be stored on the ATL04 product. The same average molecular backscatter value will be used for each of the 3 beams.

In equation 3.27, $T^2(z_c)$ represents the two-way path transmission from the top of the atmosphere to the calibration height and is composed of Rayleigh, particulate and ozone components as: $T^2(z_c) = T_m^2(z_c)T_p^2(z_c)T_o^2(z_c)$. $T_p^2(z_c)$, the particulate transmission term, will not be known exactly and must be estimated from climatology. The expected value of $T_p^2(z_c)$ will range between 0.90 and 1.0 and will be an algorithm adjustable parameter – call this **Cal_Atm_Trans**. The molecular transmission term $T_m^2(z_c)$ is computed from the molecular backscatter as from equations 3.10, 3.11, 3.12 and 3.13 in section 3.3.1. T_m^2 has a value of about 0.81 at sea level but will be closer to 0.90 at the 13 km height. A representative value of the ozone transmission term would be about 0.97 at 532 nm.

The procedure to calculate the ozone transmission, $T_o^2(z_c)$, is given in section 3.3.3.

3.3.7.3 Calibration Algorithm using Surface Reflectance

Note: this section is not to be implemented in the SIPS processing code. After launch, this technique will be investigated using actual ATLAS data. If it is deemed a viable approach to calibration, it may be incorporated into SIPS processing at a later date.

The calibration coefficient can in theory be calculated from the surface return if certain conditions are met. Both the surface reflectivity and the atmospheric transmission to the surface must be well known. The interior of East Antarctica provides one of the best places where both of these conditions can be met. Over the ice sheet, the surface reflectivity is well known and fairly constant (to within about 5%). Additionally, the atmosphere is very dry and usually cloud and aerosol free which enables a good estimate of the atmospheric transmission. Another possibility is over the ocean where the surface reflectivity can be estimated from the surface wind speed (see section 4.7). However, over the ocean, it is much more difficult to characterize the atmospheric transmission and it is much more variable than over East Antarctica. Over the ocean, careful cloud and aerosol clearing would have to be done. This will be possible at night, but during the day it will be more difficult. However, over the ocean in daylight, clouds can easily be recognized over the dark ocean surface through their effect on the background. If cloud clearing can be done sufficiently well, then using the ocean surface return for calibration should be possible. In this section we present an algorithm for computing the system calibration coefficient using the surface return.

Repeating equation (2.1), the lidar equation can be written as:

$$S(z) = \frac{CE\beta(z)T^2(z)}{r^2} + P_b + P_d \quad (3.28)$$

Where $S(z)$ is the measured signal or photon count at height z , C is the system calibration coefficient, E is the laser pulse energy, $\beta(z)$ is the atmospheric backscatter coefficient at height z , and $T^2(z)$ the atmospheric transmission from the top of the atmosphere to height z , p_b is the solar background and p_d the detector dark count.

Following equation 2.15, the received number of photons can also be written as:

$$S(z) = \frac{P_e}{r^2} \beta(z) \Delta z A_t T^2(z) Q_e T_{opt} + p_b + p_d \quad (3.29)$$

Where P_e is the number of photons transmitted in the laser pulse. From equations 2.28 and 2.29 we can solve for C :

$$C = \frac{\lambda \Delta z A_t Q_e T_{opt}}{hc} \quad (3.30)$$

Since $P_e = E\lambda/hc$ where E is the laser pulse energy. The apparent surface reflectance (ASR) which is defined in greater detail in section 4.6 is:

$$\rho_{app} = \frac{\pi E_{rec} r^2 D_c}{EA_t T_{opt} Q_e} = \frac{\pi P_{rec} hcr^2}{\lambda EA_t T_{opt} Q_e} \quad (3.31)$$

Since the energy received from the surface return is $E_{rec} = \frac{P_{rec} hc}{\lambda}$ where P_{rec} is the number of photons received from the surface.

Substituting equation 2.29 into the right hand side of 2.31 yields:

$$\rho_{app} = \frac{\pi P_{rec} r^2 \Delta z}{CE} \quad (3.32)$$

Now, the measured apparent surface reflectance is simply the actual surface reflectance (R_s) times the two-way atmospheric transmission between the satellite and the ground (T_{atm}^2):

$$\rho_{app} = R_s T_{atm}^2 \quad (3.33)$$

Substituting 2.32 into 2.33 and solving for C gives:

$$C = \frac{\pi P_{rec} r^2 \Delta z}{ET_{atm}^2 R_s} \quad (3.34)$$

Thus, to compute the system calibration coefficient using ground returns, we must know the true surface reflectance (R_s), the number of photons received from the surface (P_{rec}), the emitted laser

energy (E_{emit}), and the two-way atmospheric transmission between the satellite and the ground (T_{atm}^2). If we assume we can compute R_s over the ocean to within 5% (see section 4.7), one approach is to use equation 2.34 over large stretches of the ocean to create a scatter plot of C using 25 Hz data. For an assumed value of T_{atm}^2 the highest values of C will occur for the cleanest atmosphere. Averaging the top 10% or so of these values computed with T_{atm}^2 equal to the molecular value times ozone transmission may give reliable measurement of C. Alternatively, using data over the East Antarctic plateau, one can assume a surface reflectance value of 0.95 and an atmospheric transmission computed from molecular and ozone.

Table 3.6 Constants Used in this Section

Constant	Value
Ideal gas constant (R)	287.058 m ² s ⁻² °K ⁻¹
Gravity at sea level (g)	9.80171ms ⁻²

Table 3.7. Algorithm adjustable parameters read in and used in this section.

Constant/Adjustable Parameter	Use/Meaning	Nominal Value
Ground_Thresh	Threshold for Ground detection (photons/bin)	200
Cal_Cloud_Thresh	Threshold for excluding data in calibration zone.	TBD
Cal_Latitude_Bound	The latitude boundary for calibration calculation	60 (N&S)
Cal_Integ_Time	Calibration integration time	300 sec
Cal_Scat_Ratio	Calibration Zone (13 to 11 km) aerosol scattering ratio	1.05
Cal_Atm_Trans	Particulate transmission from top of atmosphere to the calibration height (13 km)	0.95
Cal_Solar_Angle_Limit	Maximum solar elevation angle for calibration calculation	0.0

3.3.7.4 Calibration Error and Confidence

Because of the various limitations of the ICESat-2 atmospheric data and the fact that we likely will be able to compute only a few calibration points per orbit, the error and even confidence in calibration will be difficult to establish. We could estimate the error in calibration by computing the standard deviation of the calibration points over a given polar region or orbit, but we don't expect to have enough calibration points to make this plausible. Even if we could do this, we will not have calibration points outside of the polar regions and thus will not know if the system remains well calibrated there. A possible way to check on calibration outside of the polar regions would be to construct averages of cloud free (down to say 4-5 km altitude) calibrated, attenuated backscatter profiles and fit a line to this average profile. The absolute value of the difference between this line and the attenuated molecular backscatter profile summed (bin by bin) over the

length of the profile could be used as a measure of calibration error. Most likely, this would only work over the nighttime hemisphere and would have to be done in the level 3ATL09 process.

For ATL04, we recommend a 3 scale system: 1 – little confidence, 2 – medium confidence, and 3 – high confidence. These levels will be based on the standard deviation of the computed calibration coefficient within a given orbit. The output parameter name for this is *Cal_Con* (in Table 3.1). The exact values of standard deviation to define the confidence levels will be determined in a later ATBD release. A more rigorous evaluation of calibration error is deferred to the next ATBD release.

4 Level 3 Product (ATL09)

The atmosphere L3 product will be called ATL09 and will contain the calibrated, attenuated backscatter profiles and all other atmospheric parameters that can be obtained from the data. This will include cloud layer height, layer integrated attenuated backscatter and a host of other parameters discussed below. Note that the layer heights are discussed in a separate document: "ICESat-2 Algorithm Theoretical Basis Document for the Atmosphere, Part II: Detection of Atmospheric Layers and Surface Using a Density Dimension Algorithm". The output parameters listed in Table 4.1 with an asterisk are those that are described in Part II.

4.1 L3 Required Inputs

ATL04 of current granule and previous granule
 NOAA Global Multi-sensor Snow/Ice Cover Map:
http://www.star.nesdis.noaa.gov/smcd/emb/snow/HTML/multisensor_global_snow_ice.html
 Surface Albedo data set (global, 1x1 degree) by month – produced by science team (see section 4.6.2)

4.2 L3 Outputs

Currently, on ATL09 exists the “/profilex/high_rate/density” parameter which is dimensioned at (700,3). This parameter is described in the Atmosphere ATBD, part II and is a partial output of the Density Dimension Algorithm (DDA). The DDA can run in 2 modes: the first mode just creates one density field and the 2nd mode creates two density fields. The first density field is used to bring out the optically thick clouds and in the second density run, the data are aggregated with a larger kernel, to show the tenuous cloud layers and the aerosols. Over time, testing has determined that we will most likely be running the DDA in the “two density” mode. Because of this we request that the current “density” parameter be renamed to “density_pass1” and that a second parameter called “density_pass2” (also dimensioned at 700,3) be added to the product. If the DDA is ever run in the 1 density mode, then this parameter is populated with invalids.

Table 4.1. ATL09 Output Parameters

Parameter	Datatype	Units	Rate	Description	Source
Time	Float	seconds	25 Hz		
Latitude	Double	degrees	25 Hz	Based on range to local DEM	
Longitude	Double	degrees	25 Hz		

prof_dist_x	float	m	25 Hz	Along track distance from start of segment	ATL04
prof_dist_y	float	m	25 Hz	Across track distance from reference pair track	ATL04
CAB_Prof	Float(700,3)	NA	25 Hz	Calibrated Attenuated Backscatter 3 strong beams from 20 to -1 km with vertical resolution of 30 m (eqn 3.4)	Computed
Mol_Att_Backscatter	Float(700)	m ⁻¹ sr ⁻¹	1 Hz	Molecular Backscatter Profile 20 to -1 km (eqn 3.10)	ATL04
Mol_Backs_folded	Float(700)	m ⁻¹ sr ⁻¹	1 Hz	Folded molecular backscatter profile (equation 3.17)	ATL04
MET_Temp	Float(700)	K	1 Hz	Temperature profiles from 20 to -1 km	Computed
MET_Pres	Float(700)	Pa	1 Hz	Pressure profiles from 20 to -1 km	ATL04
MET_Latitude	Float	deg	1 Hz	Latitude of MET observation	ATL04
MET_Longitude	Float	deg	1 Hz	Longitude of MET observation	ATL04
MET_PS	Float	Pa	1 Hz	Surface Pressure	ATL04
MET_U2M	Float	ms ⁻¹	1 Hz	Eastward component of wind at 2m height	ATL04
MET_U10M	Float	ms ⁻¹	1 Hz	Eastward component of wind at 10m height	ATL04
MET_U50M	Float	ms ⁻¹	1 Hz	Eastward component of wind at 50m height	ATL04
MET_V2M	Float	ms ⁻¹	1 Hz	Northward component of wind at 2m height	ATL04
MET_V10M	Float	ms ⁻¹	1 Hz	Northward component of wind at 10m height	ATL04
MET_V50M	Float	ms ⁻¹	1 Hz	Northward component of wind at 50m height	ATL04
MET_T2M	Float	K	1Hz	Temperature at 2 m height	ATL04
MET_T10M	Float	K	1Hz	Temperature at 10 m height	ATL04
MET_QV2M	Float	Kg/Kg	1 Hz	Specific humidity at 2 m height	ATL04
MET_QV10M	Float	Kg/Kg	1 Hz	Specific humidity at 10 m height	ATL04
MET_TS	Float	K	1 Hz	Surface (skin) temperature	ATL04
MET_TROPPB	Float	Pa	1 Hz	Blended tropopause pressure	ATL04
MET_TROPT	Float	K	1 Hz	Tropopause temperature	ATL04
MET_TQL	Float	Kg/m ²	1 Hz	Total column cloud liquid water	ATL04
MET_TQI	Float	Kg/m ²	1 Hz	Total column cloud ice	ATL04
MET_CLDPRS	Float	Pa	1 Hz	Cloud top Pressure	ATL04
Backg_C	Float(3)	Photons per bin	25 Hz	Background used in computation of NRB (for each beam)	ATL04
Backg_Select	Integer	NA	1/granule	The background method used in calculation of NRB	ATL04
Backg_theoret	Float	Photons/bin	25 Hz	The theoretical background	Computed
Cal_C	Float(3)	NA	1 Hz	Calibration Coefficient (for each beam at 1 Hz)	Computed

Cal_Con	Integer(3)	NA	1/Orbit	Confidence in calibration	ATL04
Cal_Error	Float(3)		1/Orbit	Error in calibration	ATL04
Layer_flag		NA	25 Hz	Consolidated cloud flag	Computed
Layer_Top*	Float(10,3)	km	25 Hz	Height of top of detected layers (max 10)	Computed
Layer_Bot*	Float(10,3)	km	25 Hz	Height of bottom of detected layers (max 10)	Computed
Layer_Attr	Byte(10,3)	NA	25 Hz	Layer attribute flag for each layer	Computed
Layer_Conf	Integer(10,3)	NA	25 Hz	Layer confidence flag for each layer	Computed
Cloud_Flag_Atm	Integer(3)	NA	25 Hz	Cloud flag from backscatter profile	Computed
Msw_Flag	Byte(3)	NA	25 Hz	Multiple Scattering warning flag	Computed
Cloud_Fold_Flag	Byte(3)	NA	25 Hz	Cloud Folding Flag	Computed
Layer_IB	Float(10,3)	NA	25 Hz	Layer integrated backscatter	Computed
Column_OD_ASR	Float(3)	NA	25 Hz	Optical depth of atmosphere column from apparent surface reflectance	Computed
Column_OD_ASR_QF	Integer(3)	NA	25 Hz	Optical depth from ASR quality flag	Computed
Density_pass1*	Float(700,3)	NA	25 Hz	Density profile from the first density run to locate thick clouds	Computed
Density_pass2*	Float(700,3)	NA	25 Hz	Density profile from the second density run to locate thin clouds	Computed
Layer_Dens*	Float(6,3)	NA	25 Hz	Integrated Layer Density	Computed
Surface_H_Dens*	Float(3)	m	25 Hz	Surface height from density	Computed
Bsnow_H_Dens*	Float(3)	m	25 Hz	Blowing snow layer height from density	Computed
Bsnow_Dens*	Float(3)	NA	25 Hz	Blowing snow layer integrated density	Computed
Ocean_Surf_Reflec	Float	NA	25 Hz	Ocean Surface Reflectance from Eqn 4.9	Computed
Apparent_Surf_Reflec	Float(3)	NA	25 Hz	Apparent Surface Reflectance from Eqn 4.7	Computed
Surface_Signal_Source	Byte	NA		Source of surface signal used to compute ASR	ANC
Surf_Refl_True	Float	NA	25 Hz	The value of ACLR _{tru} from section 4.6.2.2	Computed
Cloud_Flag_ASR	Integer(3)	NA	25 Hz	Cloud probability from ASR (Table 4.5)	Computed
Bsnow_H	Float(3)	m	25,1 Hz	Blowing snow layer top height	Computed
Bsnow_OD	Float(3)	NA	25,1 Hz	Blowing snow layer optical depth	Computed
Bsnow_Con	Integer(3)	NA	25,1 Hz	Blowing snow confidence	Computed
Bsnow_PSC	Byte(3)	NA	25,1 Hz	Blowing Snow PSC flag	Computed
Bsnow_Prob	Float	NA	1 Hz	The probability of blowing snow occurrence based on MET data (Eqn 4.6a)	Computed
Surface_H	Float(3)	m	25 Hz	Surface height from	ATL04

				backscatter profile	
Surface_Sig	Float(3)	Photons	25 Hz	Surface signal	ATL04
Surface_Bin	Integer(3)	NA	25 Hz	Bin number of profile associated with the surface signal	ATL04
Surf_type_igbp	integer	NA	25 Hz	IGBP Surface Type	ATL04
Dtime_select		NA		Control parameter for determining which method to use to compute the dead time correction factor	ATL04
Dtime_Fac2	Float(3)	NA	25 Hz	Dead time correction factor for surface signal computed from equation 2.25	ATL04
Dtime_Fac1	Float(3)	NA	25 Hz	Dead time correction factor for surface signal computed from radiometric lookup table	ATL04
ACLR_True	Float	NA	25 Hz	Clear sky initial ASR based on GOME climatology or Cox-Munk model: see Fig 3.6	Computed
USE_ATLAS	Integer	NA		Flag to control the computation of ACLR_True parameter: see pages 52-53	ANC
Msw_flag	Integer(3)	NA	1 Hz	Multiple scattering warning flag	Computed
Range_S	Float	km	25 Hz	Range from spacecraft to top of profile	ATL04
ATLAS_PA	Float	degrees	25 Hz	Pointing angle of spacecraft	ATL04
Laser_E	Float	Joules	10 Hz	Laser energy	ATL04
Solar_ZA	Float	degrees	1 Hz	Solar Zenith Angle	ATL04
Solar_AZ	Float	degrees	1 Hz	Solar Azimuth Angle	ATL04
Dem_h	Float	km	25 Hz	DEM value from a 1 kmx1km	ATL04
Surf_T	Integer	NA	1 Hz	IGBP Surface Type	ATL04
Snow_Ice	Integer	NA	1 HZ	NOAA snow-ice flag	ANC
Bckgrd_counts	Integer	Photons	200 Hz	Onboard 50 shot background	ATL03
Bckgrd_counts_reduced	Integer	photons	200 Hz	Onboard 50 shot background minus signal photons	ATL04
Bckgrd_rate	Float	Photons/s	200 Hz	50 shot background rate in per second (signal photons removed)	ATL04
Bckgrd_hist_top	Float	m	200 Hz	50 shot background integration window top height	ATL04
Bckgrd_int_height	Float	m	200 Hz	50 shot background integration window width	ATL04
Bckgrd_int_height_reduced	Float	m	200 Hz	bckgrd_int_height – signal photon height range	ATL04
Sig_count_hi	Integer(3)	photons	25 Hz	Ground signal photons for a 400 shot sum, high confidence	ATL04
Sig_count_med	Integer(3)	photons	25 Hz	Ground signal photons for a 400 shot sum, med confidence	ATL04
Sig_count_low	Integer(3)	photons		Ground signal photons for a 400 shot sum, low confidence	ATL04

Sig_h_mean_hi	Float(3)	m	25 Hz	Mean height of surface wrt EGM2008 ellipsoid, high confidence	ATL04
Sig_h_mean_med	Float(3)	m	25 Hz	Mean height of surface wrt EGM2008 ellipsoid, medium confidence	ATL04
Sig_h_mean_low	Float(3)	m	25 Hz	Mean height of surface wrt EGM2008 ellipsoid, low confidence	ATL04
Sig_h_sdev_hi	Float(3)	m	25 Hz	Standard deviation of high confidence surface signal photons	ATL04
Sig_h_sdev_med	Float(3)		25 Hz	Standard deviation of medium confidence surface signal photons	ATL04
Sig_h_sdev_low	Float(3)		25 Hz	Standard deviation of low confidence surface signal photons	ATL04

***Described in ATBD Part II. Note Data product quality parameters not listed.**

Table 4.2. Algorithm adjustable parameters read in and used by the ATL09 algorithm.

Constant/Adjustable Parameter	Use/Meaning	Nominal Value
BS_Thres_wind	Surface wind speed minimum in order for blowing snow to exist	5.0
BS_Thresh_Scale	Scaling factor for computing the blowing snow threshold (molecular*BS_Thresh_Scale)	20.0
BS_Top_Scale	Scale factor to obtain top of layer threshold (BS_Top_Scale*	0.20
BS_Extinc_Backs	The assumed blowing extinction to backscatter ratio	20.0
Cal_Cloud_Thresh	Threshold for excluding data in calibration zone.	TBD
Cal_Latitude_Bound	The latitude boundary for calibration calculation	60 (N&S)
Cal_Back_Max	The background level above which calibration will not be calculated (summed)	0.60 MHz

Cal_Integ_Time	Calibration integration time	300 sec
Cal_Scat_Ratio	Calibration Zone (13 to 11 km) aerosol scattering ratio	1.05
Cal_Atm_Trans	Particulate transmission from top of atmosphere to the calibration height (13 km)	0.95
Cal_Solar_Angle_Limit	Minimum solar zenith angle for calibration calculation	90.0
Use_ATLAS	0/1 flag to tell cloud detection using apparent surface reflectance algorithm to use ATLAS data	0
Cal_Default	Calibration constant default value if it cannot be calculated from the data	TBD
Surface_Signal_Source	1/2 flag to tell ASR algorithm which surface signal to use. 1 = from ATL04; 2 = from ATL03	0

4.3 Calibrated, Attenuated Backscatter Profiles

The ATL04 processing has generated the normalized relative backscatter profiles as:

$$NRB'(z) = (S'(z) - p_b - p_d)r^2 / E = C\beta(z)T^2(z) \quad 4.1$$

Where $S'(z)$ is the raw photon count profile corrected for molecular folding. The calibrated, attenuated backscatter profiles are obtained by simply dividing the NRB profiles by the calibration coefficient (C) which was computed in ATL04:

$$\beta(z)T^2(z) = (\beta_p(z) + \beta_m(z))T_p^2(z)T_m^2(z) = NRB'(z) / C \quad 4.2$$

The calibration coefficient is computed only over the polar regions and stored in ATL04, most likely producing only 3-4 calibration values per orbit. The ATL09 process will need to have access to the ATL04 product for the current granule and also the ATL04 product for the previous and next granules. This is because the calibration values used in ATL09 must have a smooth transition from granule to granule. To accomplish this, we will use the last calibration point from the prior ATL04 granule, all calibration points from the current ATL04 granule and the first calibration point from the next granule. To obtain a calibration value at any time t within a

granule, a linear piece-wise interpolation between calibration points will be used. If the prior and or next ATL04 granules are missing, then the first (last) record of the current granule will be before (after) the first (last) calibration point. In this case, a linear least squares fit to the calibration points in the current granule will be used to assign a calibration value to time t within the granule:

$$C(t) = a + bt \tag{4.3}$$

Where t spans the entire current granule time. If there are no calibration points for the current granule, but there are calibration values for the prior and next granules, then a linear fit is made between the last calibration value of the prior granule and the first calibration point of the next granule. If there are no calibration points for the current granule and just one of the prior or next granules contain calibration values, then use the average of that granule's values as the current granule calibration. If there are no calibration points for any of the three granules (current, prior or next), then the calibration value will default to a TBD value – *Cal_Default* parameter in Table 4.2.

The calibrated attenuated backscatter computation is then a function of time:

$$\beta(z,t)T^2(z,t) = NRB'(z,t) / C(t) \tag{4.4}$$

The calculated calibration coefficient should be calculated at a time resolution of 1 second and is also on the ATL09 product at that resolution (parameter *Cal_C*).

4.4 Layer Heights and Flags from Backscatter Profiles

The detection of layer heights will be performed on each of the 3 strong beams using the Density Dimension Algorithm (DDA) that is detailed in Part II of the Atmospheric ATBD. Please refer to that document for information pertaining to the algorithm. Here we define the parameters associated with the layers retrieved by the DDA and related flags.

There will be a maximum of ten layer heights (top and bottom) stored on the product for each of the 3 strong beams – parameters *layer_top* and *layer_bot*. Associated with these will be a layer confidence flag (parameter *layer_conf*) and a layer attribute flag (parameter *layer_attr*). The confidence flag is calculated by averaging the calibrated backscatter within a layer and dividing it by the average molecular backscatter for the same vertical range. The integer value of this calculation will constitute the confidence flag (a value from 0 to approximately 1000). If this ratio is less than unity, it will be set to 0. The higher the number, the greater the confidence.

The layer attribute flag is intended to discriminate between cloud and aerosol. If the layer top is above 6 km, then the layer is cloud (*layer_attr* = 1). If the layer top is at or below 6 km and the layer confidence is less than 10, then the layer is aerosol (*layer_attr* = 2). If the layer top is less than 6 km, and the layer confidence is greater than or equal to 20, then the layer is cloud

(*layer_attr* = 1). If the layer top is less than 6 km and the layer confidence is greater than or equal to 10 and less than or equal to 20, then the layer type is unknown (*layer_attr* = 3).

Also included on the product is a cloud flag which can be used to determine whether or not a layer was detected for a given profile (ATL09 product parameter *Cloud_Flag_Atm*). The *Cloud_Flag_Atm* flag is set to a positive number corresponding to the number of layers found. This flag should be used for nighttime (solar zenith angle > 90.0) data as solar background will make the detection of clouds very difficult and prone to false positives. For daytime data it is best to use the ATL09 product parameter *Cloud_Flag_ASR* which is based on Apparent Surface Reflectance (please see section 4.6.2 and Table 4.5 for further information on this flag).

Atmospheric layers such as clouds and blowing snow can cause multiple scattering which will increase photon path length and make a surface appear to be lower than it actually is. The magnitude of multiple scattering is related to the height and optical depth of the scattering layer. The lower and denser the layer, the greater the multiple scattering. Hence, thick blowing snow or fog layers (which touch the ground) are of greatest concern. In theory it is possible to calculate the magnitude of photon delay if the height, thickness, optical depth and particle size are known. Unfortunately, we will not be able to measure these parameters from the ATLAS data itself accurately enough to compute a delay. Instead we use the height, thickness and estimated optical depth of the layer to produce a multiple scattering warning flag. Note that these parameters are derived from the atmospheric backscatter profiles and are only viable for nighttime data.

The multiple scattering warning flag (ATL09 parameter *msw_flag*) has values from -1 to 5 where zero means no multiple scattering and 5 the greatest. If no layers were detected, then *msw_flag* = 0. If blowing snow is detected and its estimated optical depth is greater than or equal to 0.5, then *msw_flag* = 5. If the blowing snow optical depth is less than 0.5, then *msw_flag* = 4. If no blowing snow is detected but there are cloud or aerosol layers detected, the *msw_flag* assumes values of 1 to 3 based on the height of the bottom of the lowest layer: < 1 km, *msw_flag* = 3; 1-3 km, *msw_flag* = 2; > 3km, *msw_flag* = 1. **If no cloud layers are detected, then the value of *msw_flag* is set to zero.** A value of -1 indicates that the signal to noise of the data was too low to reliably ascertain the presence of cloud or blowing snow. We expect values of -1 to occur only during daylight. **The algorithm to determine when this condition is present is TBD.**

4.4.1 Layer Integrated Attenuated Backscatter

While it is highly desirable to compute the optical depth of the cloud and aerosol layers that are detected by the layer finding algorithm (discussed in Part II of the ATBD – a separate document), because of the various limitations of the atmospheric channel, this may prove to be impossible. The main problem is that we need to know the total attenuation of the signal from the top of the atmosphere down to the top of the layer. In many (most) cases we will not know this. There may be cases where the atmosphere is totally clear down to the first layer at say 13 km, but we can never be sure of that. Remember, we are totally blind in the 14-15 km region and the scattering above that is folded down into the lower few km of the atmosphere. In essence we are

screwed. Possibly, over the polar regions, optical depth retrieval would be possible, but until we get actual ATLAS data we do not feel it is worth pursuing here. Instead we will compute and store on the ATL09 product the layer integrated total (particulate plus molecular) attenuated backscatter, which is related to optical depth. The integrated backscatter is thus defined as

$$\gamma' = \int_{z_{top}}^{z_{bot}} (\beta_p(z) + \beta_m(z)) T_p^2(z) T_m^2(z) dz \quad (4.5)$$

Where z_{top} is the top of the layer and z_{bot} the bottom. At this point we recognize that $\beta_p(z)$ can have particulate scattering from $z+15$ km (as will $\beta_m(z)$, but it will be small). However, above 4 km, this should in general not be the case. When layers occur below 4 km, we cannot guarantee that the particulate scattering is actually from that height. In these cases, a quality flag will be set to indicate this. There will be an integrated backscatter value for each layer detected (maximum of 6). Note that the integrand in equation 3.5 is simply the calibrated, attenuated backscatter as in equation 3.2.

4.4.2 Cloud Folding Flag

Clouds above 15 km will be folded down into the lower portion of the 14 km atmospheric profile. It is very beneficial to know when this is a possibility. Here we define the new parameter *Cloud_fold_flag* to be included on ATL09. This parameter is based on the GEOS-5 parameter CLDPRS or cloud top pressure, which is the pressure of the highest cloud layer in the current model grid box. We convert that pressure to a height and if it is greater than 15 km, the *Cloud_fold_flag* is set to 1. Otherwise it is 0. Rewriting Equation 2.3, we have:

$$z_2 = \frac{RT}{g} \ln(P(z_1)/P(z_2)) + z_1 \quad (4.5a)$$

Where $P(Z_2)$ is the GEOS-5 parameter CLDPRS (cloud top pressure) and Z_2 is the geometric height of that pressure level. $P(Z_1)$ will be set to the surface pressure defined by GEOS-5 parameter PS and Z_1 will be the current surface height retrieved from the DEM. The average temperature of the layer (\bar{T} in °K) can be computed as the average of the temperature of all GEOS-5 layers between PS and CLDPRS, inclusive.

4.5 Blowing Snow

4.5.1 Blowing Snow Layer Height

The blowing snow module will output 3 parameters stored on ATL09 (see Table 4.1): high rate and low rate *Bsnow_H*, *Bsnow_OD*, *Bsnow_Con*, and *Bsnow_PSC* which are blowing snow height (height above the surface of the top of the blowing snow layer), optical depth of the layer, blowing snow confidence flag and blowing snow PSC flag, respectively. The blowing snow detection algorithm will be invoked over any surface determined to be snow, ice sheet or sea ice. This determination is made by reading in the NOAA daily snow/ice cover map (see section

4.6.2.2 and Figure 4.6.8). If the orbit is not over snow, ice sheet or sea ice, then both the high rate and low rate *Bsnow H*, *Bsnow_OD* and *Bsnow_Con* should be set to invalid.

If over the appropriate surface type, the algorithm must first check to see whether the surface was detected. This can be done by checking the ATL04 high rate parameter “Surface_Bin”. If Surface_Bin is not invalid, then the surface has been detected. If the surface has been detected and the 10 m wind speed is greater than BS_Thresh_Wind (nominally 5 m s⁻¹ see Table 4.2), then the blowing snow detection algorithm is invoked. If the surface is not detected then **set *Bsnow H* and *Bsnow_OD* to invalid and *Bsnow_Con* to -3**. If the surface is detected, but the wind speed is less than BS_Thresh_Wind then **set *Bsnow H* and *Bsnow_OD* to invalid and *Bsnow_Con* to -2**

If the 10 m wind speed is greater than BS_Thresh_Wind and the surface was detected, the algorithm interrogates the lidar return bins (calibrated, attenuated backscatter) directly above the ground for an elevated backscatter signal indicative of a scattering layer in contact with the ground. If the backscatter signal in the bin immediately above the ground (Surface_Bin-1) exceeds the blowing snow threshold (about 2.5x10⁻⁵ m⁻¹ sr⁻¹), then a low-level, wind-induced “scattering layer” is assumed to be present. The blowing snow threshold is constructed from a scaling factor times the magnitude of 532 nm attenuated molecular (Rayleigh) scattering at the surface height of the current retrieval location. The scaling factor (BS_Thresh_Scale) has a value of 20.0 and was determined by an iterative approach of adjustment and review of retrieval results until they were satisfactory. The resulting threshold must be great enough to insure minimal false positive detections while small enough to retain adequate sensitivity.

If the bin immediately above the ground (Surface_Bin-1) has a backscatter value less than the blowing snow threshold, then no blowing snow is found. In this case **set *Bsnow H* and *Bsnow_OD* to invalid and *Bsnow_Con* to -1**. If Surface_Bin-1 does have a scattering value greater than or equal to the blowing snow threshold, then the algorithm interrogates the bins above (Surface_Bin-2, Surface_Bin-3, etc., moving upward) until the backscatter within the bin is less than the blowing snow threshold times a scale factor (BS_Top_Scale) that is nominally 0.20. Call this bin T. The top of the blowing snow layer is then the bin immediately below bin T (i.e. bin T+1). The search for the top will not exceed 500 m above the ground as the likelihood of a blowing snow layer deeper than this is very small. If the search upward has reached 500 m, but no top of the layer was found, then **set *Bsnow H* and *Bsnow_OD* to invalid and *Bsnow_Con* to 0**.

Once the top of the layer has been found (at bin T), the height of the blowing snow layer (parameter *Bsnow_H*) is then defined as (T – Surface_Bin) * 30.0, where T is the layer top bin and Surface_Bin is the ground bin. *Bsnow_OD* and *Bsnow_Con* are then defined following the discussion in sections 4.5.2 and 4.5.3, respectively.

Note that this algorithm will be applied to the full resolution atmospheric profiles (to produce the *high_rate* blowing snow height) and to profiles that are averaged to 1 second to produce a *low_rate* blowing snow height parameter. In the case of the *low_rate* blowing snow height, the location of the ground bin should be determined as the highest bin of the valid surface bins that make up that second of data. If there are less than 10 valid surface bins for this second, then set the *low_rate Bsnow H and Bsnow_OD to invalid and Bsnow_Con to -3*. If there are ≥ 10 valid surface bins for this second, but the wind speed is less than *BS_Thresh_Wind* then set *Bsnow H and Bsnow_OD to invalid and Bsnow_Con to -2*. If blowing snow is not detected, set *Bsnow H and Bsnow_OD to invalid and Bsnow_Con to -1*. If the top of the layer cannot be found, then set *Bsnow H and Bsnow_OD to invalid and Bsnow_Con to 0*.

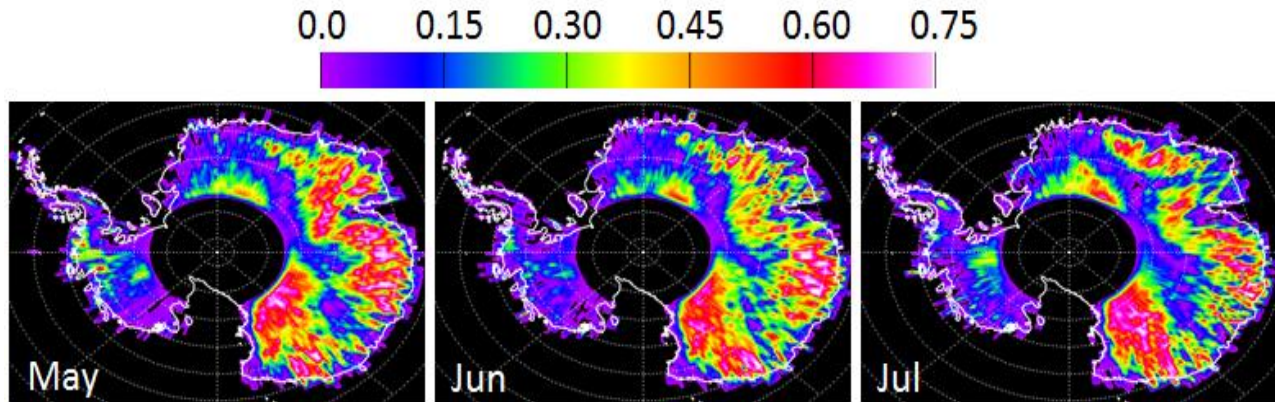


Figure 4.5.1 Blowing snow frequency over Antarctica for May-July, 2009 as derived from analysis of CALIPSO data.

Table 4.3

Value of <i>Bsnow_con</i>	Meaning
invalid	Orbit not over land ice, snow or sea ice
-3	Surface not detected
-2	Surface detected, but the 10 m wind speed is less than <i>BS_Thresh_Wind</i>
-1	Blowing snow was searched for, but not found
0	Blowing snow layer top not found
> 0	Blowing snow was found. See Section 4.5.3 for the computation of the value of <i>Bsnow_con</i>

4.5.2 Blowing Snow Layer Optical Depth

The optical depth of the layer is then computed using an assumed extinction to backscatter ratio. (*BS_Extinc_Backs*) with a nominal value of 20 sr (see Table 4.2). To compute the blowing

snow layer optical depth (τ_{bs}), we sum the calibrated attenuated backscatter within the blowing snow layer and multiply by the product of the bin size and the extinction to backscatter ratio (S):

$$\tau_{bs} = B_s S \sum_{z=z1}^{z2} \beta(z) \quad (4.6)$$

Where $z1$ is the top bin of the layer (bin T) and $z2$ the bottom bin (bin G-1), B_s is the bin size in meters (30), and $\beta(z)$ is the calibrated attenuated backscatter.

The extinction to backscatter ratio of blowing snow is not known and is a subject of current research by the author. Algorithm details and further example of retrievals can be found in Palm et al., 2011.

The output of the blowing snow detection algorithm has been extensively checked for consistency and quality by generating and reviewing hundreds of images of the detected blowing snow layers using both ICESat-1 and CALIPSO data. A limitation of the lidar technique is that the blowing snow layer has to be at least 30 m thick in order for enough backscatter signal to be collected in the bin immediately above the ground. This means that shallow blowing snow layers, which may be frequent, will probably not be detected. Further, blowing snow cannot be detected beneath thick or highly attenuating layers (tropospheric or polar stratospheric clouds with optical depth $>$ about 2.5-3.0), since detection of a ground return is required. The latter limitation implies that most of the blowing snow associated with winter storms (cyclones) will go undetected. These limitations will certainly result in lower blowing snow frequencies than actually exist. Furthermore, the magnitude of the discrepancy will depend on the cloud cover frequency of a given region. For instance, along the coast of Antarctica where blowing snow frequency is known to be high, it is also cloudier than more inland regions.

We also recognize that scattering from the region 15 km above the surface that is folded into the near-surface scattering can produce a false positive detection. This would only happen in the presence of polar stratospheric clouds that occur most frequently in late winter and early spring in high latitudes. We have a flag on the ATL09 produce (*Bsnow_PSC*) which indicates the potential of PSCs to affect the blowing snow retrieval. The flag will be a function of month and hemisphere. And be applied only poleward of 60 north and south. If the blowing snow retrieval is outside of these latitudes, set this flag to zero regardless of month. Please see Table 4.5.

4.5.3 Blowing Snow Layer Confidence

When blowing snow has been detected, the blowing snow confidence flag will be constructed from a combination of the signal strength within the layer and the wind speed. We will compute the average scattering ratio (attenuated total backscatter divided by the attenuated molecular) within the layer multiplied by the surface wind speed:

$$\chi = \frac{\bar{\beta}}{\beta_m} U_s$$

Where U_s is the surface (10 m) wind speed. Table 4.4 shows the value of the blowing snow confidence flag as a function of χ . Note: the proposed limits may (will) change after launch.

Table 4.4. Blowing snow confidence flag

χ	Value	Confidence
< 5	1	None-little
5 - 10	2	Weak
>10 - 15	3	Moderate
>15 - 20	4	Moderate-high
>20 - 25	5	High
>25	6	Very high

Table 4.5. Blowing Snow PSC interference flag for latitudes poleward of 60 N/S

Month	Southern Hemisphere	Northern Hemisphere
Jan	0	2
Feb	0	3
Mar	0	2
Apr	0	1
May	0	0
Jun	1	0
Jul	2	0
Aug	3	0
Sep	2	0
Oct	1	0
Nov	0	0
Dec	0	1

4.5.4 Blowing Snow Probability

Essery et al., 1999 present a method to predict the probability of the occurrence of blowing snow based on the 2m temperature (T , degrees Celsius), 10 meter wind speed (u_{10} m/s) and the age of the snow (A). We would like to include the results of this calculation in the ATL09 product. The blowing snow probability (ATL09 parameter $Bsnow_Prob$) is defined as:

$$P(u_{10}) = \left[1 + \exp \left\{ \frac{\sqrt{\pi}(\bar{u} - u_{10})}{\delta} \right\} \right]^{-1} \quad (4.6a)$$

Where

$$\bar{u} = 11.2 + 0.365T + 0.00706T^2 + 0.9 \ln(A) \quad (4.6b)$$

And

$$\delta = 4.3 + 0.145T + 0.00196T^2 \quad (4.6c)$$

In Equation 4.6b, A is the age of the snow on the ground in hours. Since this is very difficult to pin down, we will assume $A=24.0$. The blowing snow probability will be computed whenever the satellite is over a snow, sea ice or land ice surface. If the satellite is not over these surfaces, then the value should be set to invalid.

4.6 Apparent Surface Reflectance (ASR)

Apparent Surface Reflectance (ASR) is essentially a calculation of the received laser pulse energy from the surface divided by the transmitted laser energy multiplied by the two-way atmospheric transmission (T^2). In the case of a planetary body like the moon, which has no atmosphere, the ASR would be equal to the actual surface reflectance at the laser wavelength. On the earth however, the ASR is modified by the atmospheric transmission, which is in general not known. For a clear atmosphere, T^2 is about 0.81 at sea level (532 nm). Clouds and aerosols introduce further transmission loss ranging from a few tenths to a few orders of magnitude. This of course means that the ASR will always be less than the actual surface reflectance. For instance, if snow has a reflectance of 0.9 at 532 nm, then the ASR measured through a clear atmosphere at sea level will be 0.73 (0.81 x 0.9). If the surface reflectance is known well enough, the ratio of the apparent surface reflectance to the actual surface reflectance can be used as a relative measure of T^2 and thus as an indicator of the likely presence of clouds. This will be discussed further in section 4.6.1.

For ATLAS, ASR can be calculated as (following Yang et al., 2013):

$$\rho_{app} = \frac{\pi N_p r^2 D_c F}{NE A_t S_{ret}} \quad (4.7)$$

where N_p is the number of photons received from the surface, r is the distance between the satellite and the surface, D_c is the detector dead time correction factor, F is a calibration factor, analogous to but not the same as α in equation 2.11, E is the laser pulse energy, A_t is area of the

telescope, and S_{ret} is the product of the transmittance of the optics and the quantum efficiency of the detector, and N is the number of laser pulse summed (400). **Note that S_{ret} is known as the receiver return sensitivity and will be periodically updated and obtained from ATL03.** The calibration factor F is required since we do not know the optical throughput of the system perfectly and it may change with time. It should be possible to calculate F by using data over the high Antarctic plateau where the surface reflectivity is fairly well known and the atmosphere is clear. In this region, ρ_{app} should have a value of approximately 0.95 times the two way transmission to the Antarctic plateau which can be calculated (approximately 0.88). We plan to do this using the first data acquired by ATLAS and then periodically re-evaluate its magnitude as the mission progresses. F will be an algorithm adjustable parameter that is read in by the SIPS software (the final codes used to produce data products. SIPS is the Science Investigator Processing System). We will assume initially that $F = 1$. Note also that the above equation also assumes a lambertian surface reflectance.

Equation 4.7 was used to compute the ATLAS apparent surface reflectance as a function of received surface photons (N_p) (see Figure 4.6.1). For this computation, the following values were used: $r = 496$ km; $D_c = 1.1$; $F = 1.0$; $E = 160$ μ J; $A_t = 0.43$ m²; $S_{ret} = 3.79e17$, $N=400$. Note that A_{teles} assumes a telescope diameter 80 cm with a central obscuration of 30 cm.

In practice, the accuracy of the ASR calculation relies on the accuracy of surface detection; only if all photons from surface are detected, will we be able to determine the ASR accurately. In practice, this should be possible. The surface return will often come back in one atmospheric bin (30 m width), or at most 2-3 bins over very rough or highly sloping terrain.

We have two options for calculating N_p in Equation 4.7. The first is simply to use the *Surface Sig* parameter calculated and stored on ATL04 and read in by the ATL09 algorithm. The second way is to define N_p is using the ATL03 parameters *sig_count_high*, *sig_count_med* and *sig_count_low*. These parameters reside on the ATL04 product. We define a new control parameter called *Surface_Signal_Source* to select which surface signal to use for N_p in equation 4.8. *Surface_Signal_Source=1* will mean to use the surface signal computed from the atmospheric histograms (parameter *Surface_Sig*). If *Surface_Signal_Source=2*, then use the sum of *sig_count_high* and *sig_count_med* to define N_p . NOTE that this sum will need to be dead time corrected (see section 2.1).

The transmitted laser energy for each beam, E should be known to within 5% and should be available at 25 Hz.

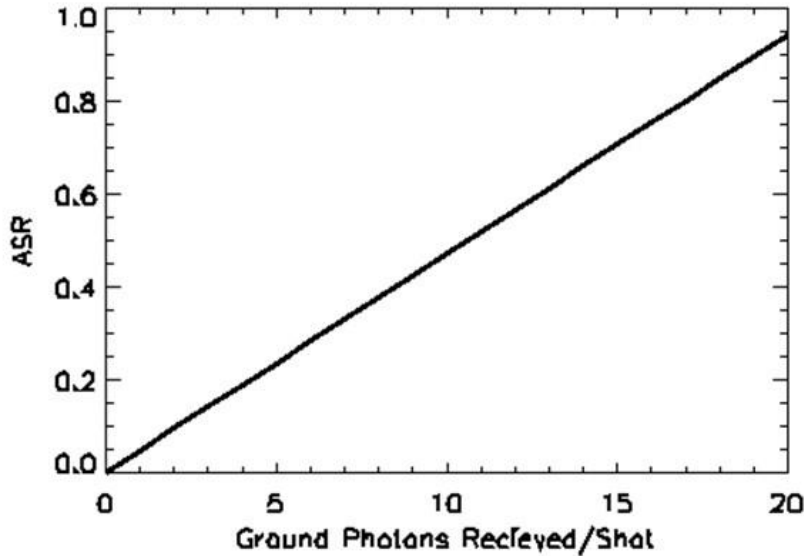


Figure 4.6.1 The apparent surface reflectance as computed from Equation 4.7 as a function of the number of surface return photons received per laser pulse. In practice, the ATLAS atmospheric data will be the sum of 400 laser pulses, and thus the photons received 400 times larger.

4.6.1 Cloud Detection using ASR

For a given surface and laser system, clouds lower the returning energy that is reflected by the surface (evidenced by a lower N_p) and hence lowers the ASR. Obviously, when clouds are present, ASR is a function of cloud optical depth (COD), but it is also a lesser function of cloud height and cloud microphysical properties. Figure 4.6.2 illustrates how cloud properties affect ASR. The black and gray curves are results of radiative transfer calculations with a 3D Monte Carlo model. Normalized by the clear-sky ASR, the results shown represent the two-way transmittance of the atmosphere. For example, a cloud with COD = 0.1 decreases the surface return by about 8% to 17%; while a cloud with COD = 1.0 decreases the surface return by 57% to 85%. The variability in surface return for a given COD is due to the variability in cloud altitude and microphysics. Fig. 3.6.2a shows that the lower the cloud, the higher the ASR. This is due to the fact that for lower clouds, photons that experienced multiple scattering have a larger probability of staying in the telescope field of view (Yang et al, 2010, 2011). Similarly, as shown in Figure 4.6.2b, everything else being equal, the larger the particle size, the higher is the ASR. This is because of larger particles' larger forward scattering probabilities; hence more photons tend to stay in the FOV.

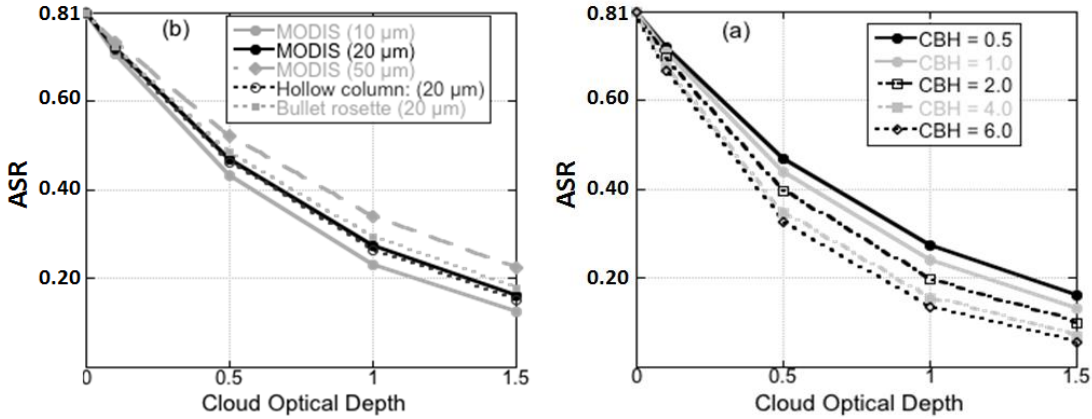


Figure 4.6.2. The effect of cloud properties on ICESat-2 ASR. Results are from Monte Carlo simulations over a surface of reflectivity 1. Telescope of field of view (FOV) is 40 m in diameter. (a) ASR changes as a function of COD for different cloud base heights (CBH) (in km). Cloud thickness is assumed to be 0.5 km; MODIS ice phase function for particle effective radius $r_e=20 \mu\text{m}$ is used. (b) Same as (a) but for different cloud particle sizes and shapes. The numbers in the *parentheses* in the legend are the effective radii. Clouds are assumed to be located at 0.5 - 1.0 km.

Overall, Figure 4.6.2 shows that clouds provide a strong signal in ASR that can be used for cloud detection. It is worth noticing that the cloud detection method presented here relies on the relative change of the ASR; hence absolute calibration of the instrument is not as important an issue, but the instrument stability can certainly affect the accuracy of the cloud detection results.

Since clouds can significantly reduce the ASR measured by the ICESat-2 detectors, it is possible to set a threshold to separate cloudy and clear conditions. However, if surface reflectivity varies significantly from location to location, cloud detectability will be lower compared to an otherwise uniform surface. To show this, we first examine how the ASR varies under clear sky conditions over the ice sheets. Figure 4.6.3a gives the results over Greenland, East and West Antarctica. Data are from the GLAS L2A campaign that began on 25 September and lasted until 19 November, 2003. All data for which clouds were detected have been removed.

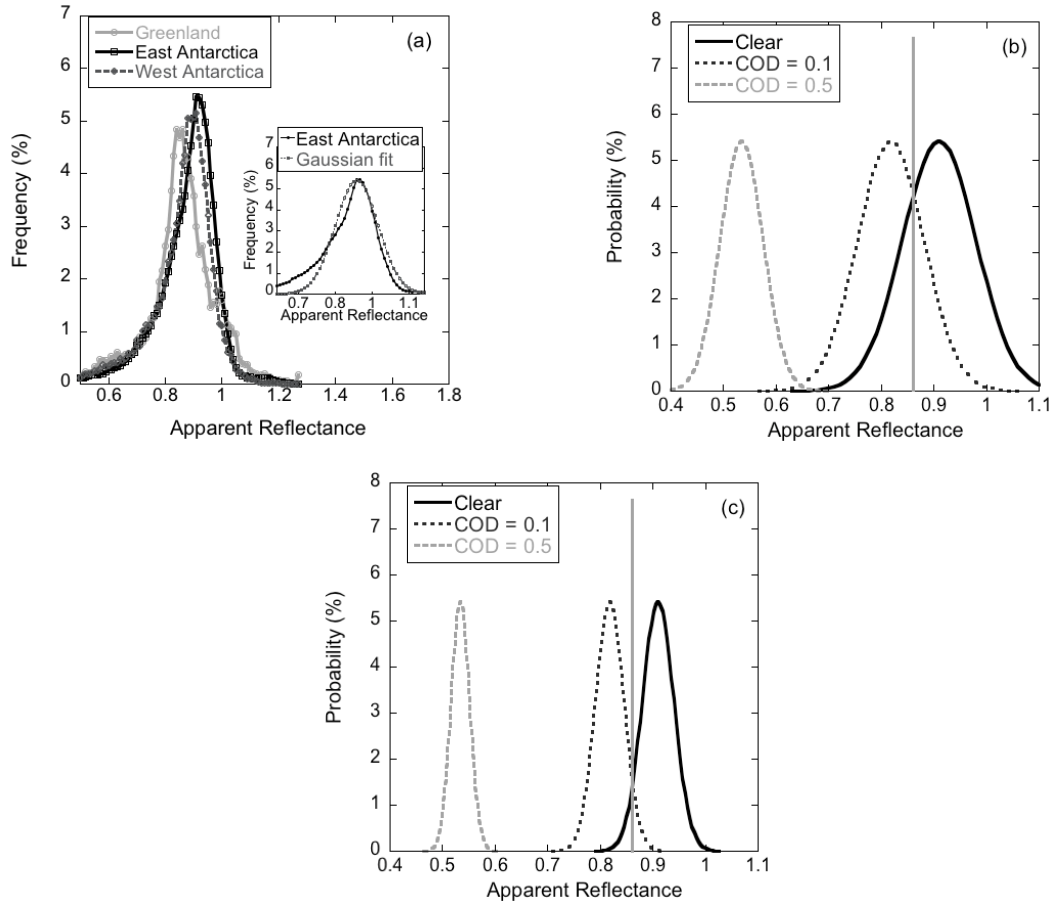


Figure 4.6.3 (a) Distribution of 1064 nm channel clear sky ASR. The inset is the Gaussian fit for the distribution over the East Antarctica. Data are from the GLAS L2A campaign. (b) Idealized ASR (Gaussian) for clear sky (mean = 0.91; standard deviation = 0.07) (solid black line), and the corresponding distributions for COD = 0.1 (dashed black line) and COD = 0.5 (dashed grey line). Also shown is an example threshold (solid gray line). (c) Same as (b), but for a Gaussian distribution with mean = 0.91 and standard deviation = 0.03.

The L2A campaign was selected because during this period GLAS had a fully functional atmosphere channel and the best cloud detection ability. Since the GLAS 532 nm channel is generally saturated by the surface signal, the ASR was derived from the 1064 nm channel measurements. It can be seen from the figure that the mode of the distribution from the Greenland ice sheet is lower than that of the Antarctica regions, with the highest from the East Antarctica.

The distributions shown in Figure 4.6.3a resemble a bell shape (Gaussian). To better illustrate the impact of surface reflectance variability on cloud detection, the clear sky distributions are fitted with Gaussian functions. The best fit for the distributions of Greenland, East and West Antarctica regions have means of 0.87, 0.91 and 0.89 and standard deviations of 0.07, 0.07 and 0.06, respectively. Figure 4.6.3b uses the Gaussian fit to the East Antarctica distribution (solid

black line) as an idealized ASR of snow cover under clear sky conditions. When clouds are present, the ASR will be smaller. For a plane parallel cloud, the shape of the distribution will stay Gaussian, only with a smaller mean and a smaller standard deviation. The change is a function of the cloud properties. For example, based on the radiative transfer simulations, for a cloud at 0.5 to 1.0 km with MODIS ice phase function for $r_e = 20 \mu\text{m}$, the ASR would decrease by 10% for COD = 0.1 and 41% for COD = 0.5. This example is plotted in Figure 4.6.3b with the dashed lines.

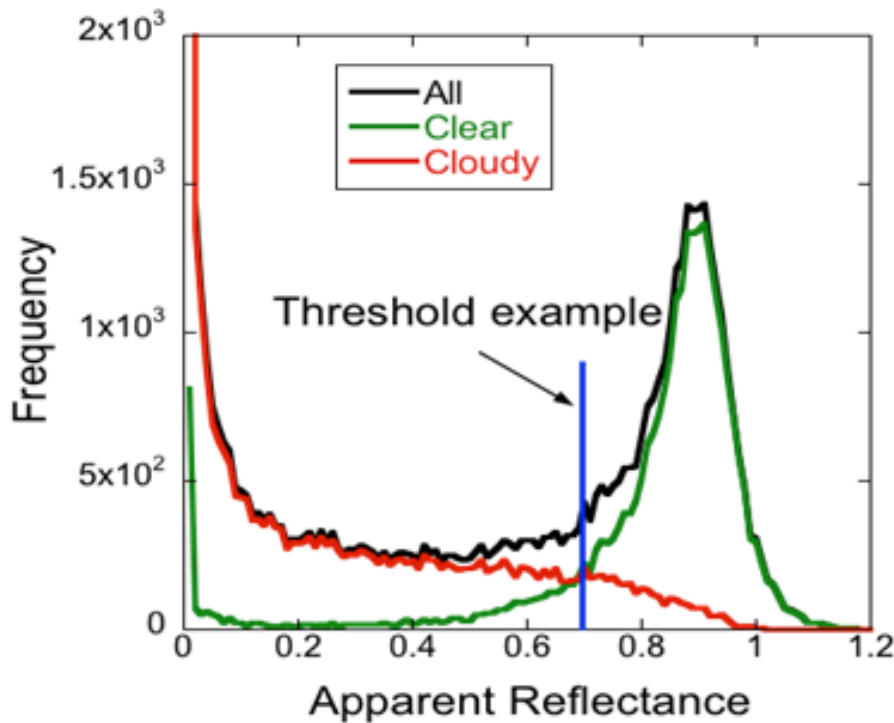


Figure 4.6.4. ASR distributions for clear (green), cloudy (red) and total (black) sky conditions over the West Antarctica ice sheet. Data are from the GLAS L2A campaign.

As can be seen in Figure 4.6.3b, there is an overlap between the ASR for clear sky and for cloudy sky (e.g. the curve for COD = 0.1). Hence it is no longer possible to completely separate clear and cloudy pixels with a single threshold: no matter where the threshold is set, some of the pixels will be misclassified. Generally, a smaller standard deviation in the ASR would indicate less overlap between the distributions under clear and cloudy sky conditions; hence allowing better cloud detection. Figure 4.6.3b and c demonstrate this point. The Gaussian distributions for clear sky in both panels have the same mean (0.91), yet their standard deviations are different, one is 0.07 (Figure 4.6.3b) and the other 0.03 (Figure 4.6.3c). As can be seen, the case with smaller standard deviation (Figure. 4.6.3c) corresponds to a smaller overlap, thus better cloud

detection. Obviously, for a given distribution of ASR, the misclassification rate is a function of the threshold and cloud optical depth and height.

Figure 4.6.4 shows an experiment of applying the ASR based cloud detection method to ICESat data. Again, the 1064 nm channel data from the GLAS L2A campaign is used. For this campaign, accurate cloud detection was achieved from the atmospheric channel (Palm et al 2002); hence the “truth” of which pixel is clear and which one is cloudy is known. The ASR distributions under clear and cloudy sky conditions are built from all the clear and cloudy pixels, respectively. As shown in the figure, an overlap exists between the distributions for clear and cloudy sky conditions; hence no threshold could separate all the clear pixels from the cloudy ones. The bimodal distribution shown in Figure 4.6.4 indicates that the ASR is a good test for cloud detection because misclassification can be minimized by putting the threshold in the valley region of the histogram. A sample threshold of 0.7 is marked on Figure 4.6.4. With this threshold, 15% of the clear pixels are misclassified as cloudy and 8% of the cloudy misclassified as clear. Certainly the threshold can be adjusted to make the results either more cloud or clear conservative. As shown in Yang et al. (2013), the variability of the ASR at 532 nm is much smaller than that at the 1064 nm channel; hence cloud detectability will be strongly enhanced for the ATAS data.

4.6.2 ASR Cloud Detection Algorithm Implementation

The basic problem with the creation of an algorithm for cloud detection using ASR is the fact that for any given ATLAS observation the true surface reflectance (SR) is not well known. In order to detect the presence of cloud, we need to know the true surface reflectance (R_{true}) to within a certain tolerance. The accuracy with which we know the SR will determine the smallest cloud optical depth that can be detected. Based on model results, we feel the detection limit for this method will be optical depths in the range 0.2 to 0.4. Initially we will use the best available data sets on the global surface reflectivity at 532 nm as a measure of R_{true} (for instance from GOME, Koelemeijer et al., 2003). This global data set provides the average surface reflectivity at a resolution of 1x1 degree for each month of the year. We will use this data set to produce an ancillary file for use in the SIPS processing as described in the next section. We call this file the initial clear sky ASR climatology.

4.6.2.1 Initial Clear Sky ASR Climatology

The clear sky ASR is a product of the true surface reflectance and two-way clear sky transmittance. Clear sky is defined as a molecular-only atmosphere. Ozone attenuation is not included in the computation. The initial values of clear sky ASR will serve as the first guess of the actual values. This dataset will be provided by the ATBD authors. It is generated based on the Global Ozone Monitoring Experiment (GOME) monthly surface albedo (over land and snow/ice surfaces only; see Figure 4.6.5) [Koelemeijer et al., 2003] and the Cox-Munk model results (over water) following the procedure below (and graphically shown in Figure 4.6.6):

1. Read in the GOME monthly surface reflectivity climatology, which is in $0.25^\circ \times 0.25^\circ$ resolution. Duplicate the data into $1/25 \times 1/25$ degree resolution. Call this reflectance R_{land} (land reflectance)
2. Read in the 5 min global height data (DEM) and calculate the two-way molecular transmittance (to the local surface height) at 532 nm for each grid point and call it T^2 .
3. Read in the surface type data.
4. Assign an empirical value for ephemeral snow surface: $R_{\text{snow}} = 0.8$.
5. For each point in the $1/25$ degree resolution GOME-based dataset, check if it is over water; if yes, then do step (7). If no, then do step (6).
6. Record two values for this point: $A_L = R_{\text{land}} * T^2$, and $A_S = R_{\text{snow}} * T^2$. Where A_L is the clear sky land reflectance and A_S the clear sky snow reflectance.
7. Do nothing.

To calculate the latitude and longitude of the grid:

```

nlat=4500
nlon=9000
lat = fltarr(nlat,nlon)
lon = fltarr(nlat,nlon)
res_new = 1.0 / 25.0
for i = 0, nlat-1 do begin
    lat[i, *] = -90.0 + (0.5+float(i))*res_new
endfor
for j = 0, nlon-1 do begin
    lon[*, j] = -180.0 + (0.5+float(j))*res_new
endfor

```

The result will be a global data (over land/ice/snow only) set at $1/25$ degree resolution with the 2 values defined by step (6) above for each month of the year. In the implementation of the SIPS code, these data sets will be used in conjunction with daily global snow cover data sets from NOAA (this is further defined in Figure 4.6.8) and the surface type data set to obtain the value of clear sky ASR to use for cloud detection. This is discussed in detail in section 4.6.2.2. The process for generating the initial clear sky ASR data set is shown schematically in Figure 4.6.6. The ATBD authors will produce this data set for each month of the year and will give it to the SIPS for the real-time processing. We do not anticipate the need for re-generating these grids each year, but that is TBD.

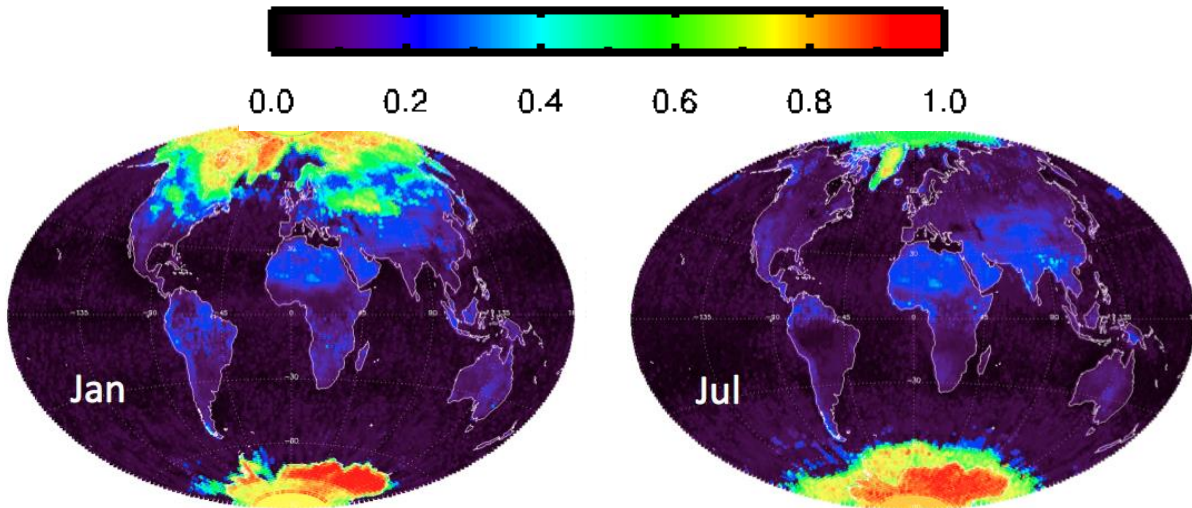


Figure 4.6.5. The monthly surface reflectivity climatology derived from the GOME data [Koelemeijer et al., 2003] for January and July. Data available at http://www.temis.nl/surface/gome2_ler.html

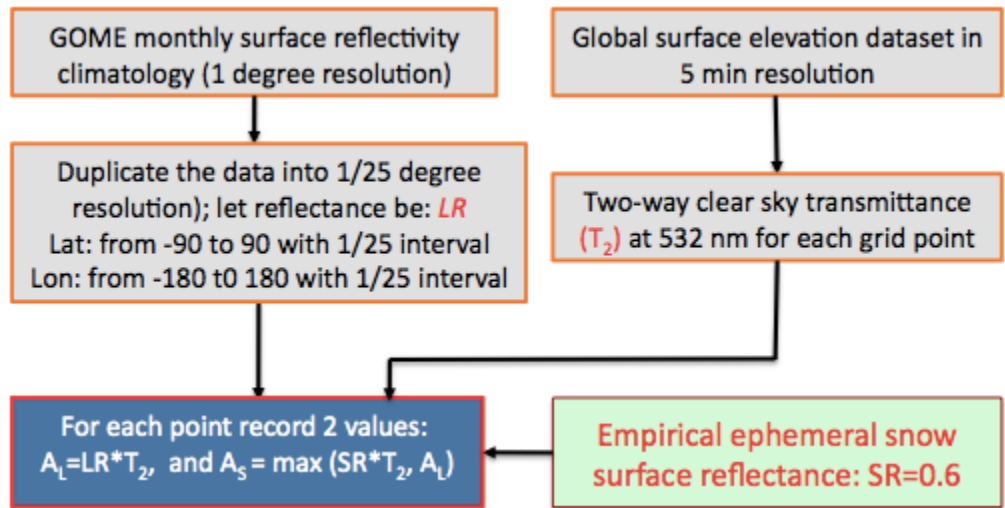


Figure 4.6.6. Flow chart for generating the initial clear sky ASR dataset. There will be one such dataset for each month of the year. Data set does not change from year to year.

4.6.2.2 Final Clear Sky ASR Determination

In order to detect the presence of cloud from the ATLAS ASR observations, we need to first know the clear sky ASR. A method for estimating a first guess (initial clear sky ASR) value for this quantity over land was given in section 4.6.2.1 above. However, we believe that by using ATLAS data itself, we can improve upon this initial guess at least in some cases. Obtaining the best possible value for the clear sky ASR is extremely important as the accuracy with which we

know this value will determine the smallest cloud optical depth that can be detected. The ATLAS measured ASR (ASR') is used as a check on the initial values derived in section 4.6.2.1. If the ATLAS measured ASR is deemed accurate, then it will be used instead of the initial clear sky values obtained from the GOME-based climatology. Figure 4.6.7 illustrates the steps of calculating the final clear sky ASR value (ACLR_{tru}).

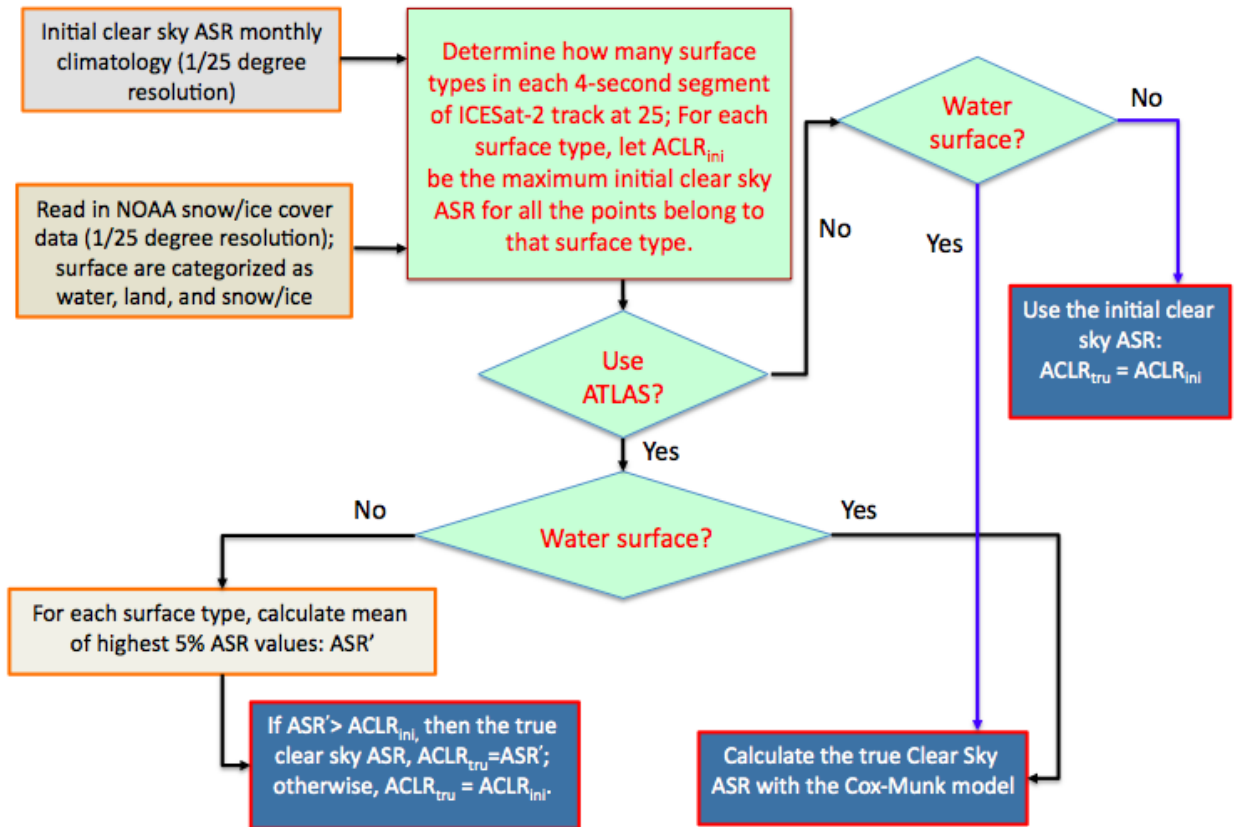


Figure 4.6.7. Flow chart for the clear sky ASR determination for every four seconds of data.

Detailed procedures can be described as follows:

1. Read in the initial clear sky ASR climatology (GOME) for the current month, which has a spatial resolution of 1/25 degree. As described in Section 4.6.2.1, each grid point over land has two ASR values (AL, and AS) recorded, corresponding to land and snow/ice surface types respectively.
2. Read in the NOAA snow/ice cover data set for the current day.
3. Determine the initial clear sky ASR values (ACLR_{clim}) for each 4 second segment of the ICESat-2 track at 25 Hz (100 points in total). First classify the surface type of each point into land, water and snow/ice according to the NOAA daily snow/ice cover (see Figure 4.6.8.). Based on the surface type of each point, determine its initial clear sky ASR value

(ACLRclim) using the nearest neighbor technique (from the ASR climatology data set defined in section 4.6.2.1 or calculated from Cox-Munk if over water).

4. Check how many surface types there are in total for the 100 points (maximum 3 types). If a surface type has less than 20 points, then do not count it as a separate surface type and mark those points as “undetermined”.
5. For all the points belonging to each valid surface type, determine a single clear sky ASR initial value by picking the maximum ACLRclim, call this value(s) ACLRini.
6. For surface type of water, set ACLRtru according to the Cox-Munk reflectivity – wind speed relationship (equation 3.7 below).
7. For surface types that are not water, if “Use_ATLAS” is false, go to step 9, otherwise compute ASR for the 4 seconds of ATLAS data at 25 Hz. For each surface type, calculate mean of highest 5% of the ATLAS ASR values: ASR’. If $ASR' > ACLRini$ then $ACLRtru = ASR'$; otherwise, $ACLRtru = ACLRini$.
8. Now we have the ACLRtru for each valid surface type for the four seconds of data. If there are data points with surface type “undertermined”, assign them the surface type with the most number of points. The values of ASR’ used in step 6 have to pass a quality control procedure TBD.
9. If “Use_ATLAS” is false and it is not over water, set ACLRtru to ACLRini.

In the implementation of the above procedure there will be a control parameter, Use_ATLAS (see Table 4.2) read in by the SIPS processing system that will determine whether or not the ATLAS measured values of ASR (ASR’) are used in the computation of ACLRtru. If Use_ATLAS is false, then the initial clear sky reflectance, $ACLR_{ini}$, is used as the true surface reflectance ($ACLR_{tru}$). The value of $ACLR_{tru}$ is stored on the ATL09 product as parameter *Surf_Refl_True*.

Note: To obtain the latitude and longitude of each grid cell of the initial clear sky ASR climatology:

```
res = 1.0/25.0
```

```
nlat = long(180.0/res)
```

```
nlon = long(360.0/res)
```

```
lat = fltarr(nlat, nlon)
```

```
lon = fltarr(nlat, nlon)
```

```
for i = 0, nlat-1 do begin
```

```
  lat[i, *]= -90.0+(0.5+float(i))*res
```

```
endfor
```

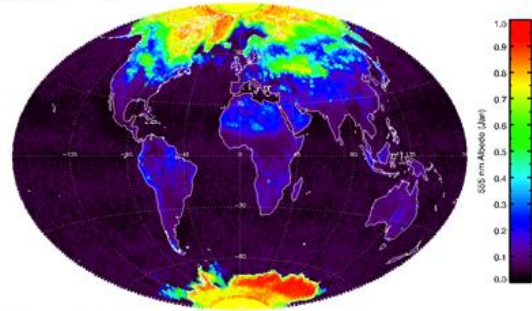
```
for j = 0, nlon-1 do begin
```

```
  lon[* , j]= -180.0+(0.5+float(j))*res
```

```
endfor
```

GOME: <http://www.temis.nl/data/1er.html>

Global Snow and Ice Cover Map is derived from combined observations of METOP AVHRR, MSG SEVIRI, GOES Imager and DMSP SSMIS 4 km resolution. Also includes land/water mask.



http://www.star.nesdis.noaa.gov/smcd/emb/snow/HTML/multisensor_global_snow_ice.html

Global Multisensor Snow/Ice Cover Map

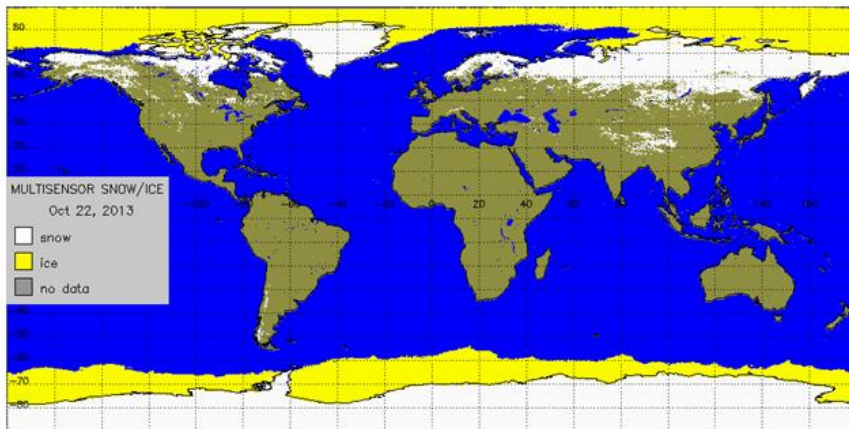


Figure 4.6.8. Examples of ancillary data sets that will be used in selecting a value of the true surface reflectance (R_{true})

The snow and ice data can be obtained from:

http://satepsanone.nesdis.noaa.gov/northern_hemisphere_multisensor.html

also an IDL program can be found there to read the data.

4.6.2.3 Cloud Detection Using Apparent Surface Reflectance

Once we have the clear sky ASR, ACL_{true} , for the 4 seconds of observations, cloud detection is straightforward. Figure 4.6.9 gives the flow chart of the procedure. The details of each step are as follows:

- 1 Set ASR Cloud Threshold $T = ACL_{true} * \phi$, where ϕ is a factor for correcting the potential clear sky ASR biases. At the initial stage ϕ is set to be 0.9 over land and 1.0 over ocean.
- 2 For each of the 100 ASR values, Compute the probability (P) of cloud occurrence as defined in Figure 4.6.9. If $P \leq 40\%$, then label the point clear. If $P > 40\%$, label the point cloudy.

- 3 As shown in Table 4.5, assign a confidence flag to each of the cloud detection results.

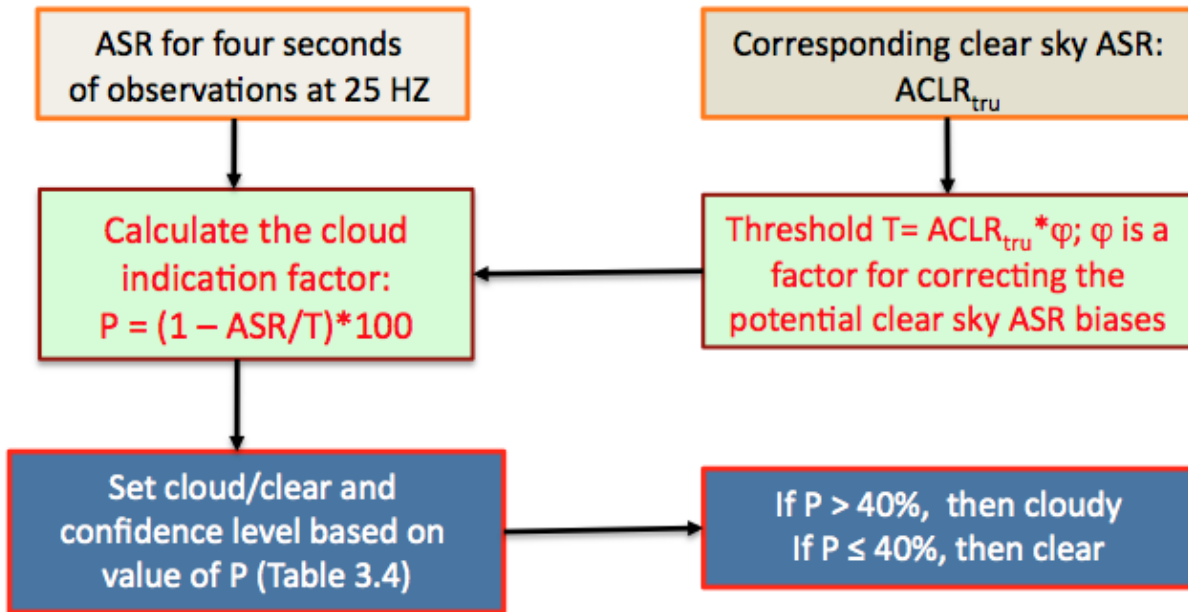


Figure 4.6.9. Flow chart for cloud determination for four seconds of data after the clear sky ASR is determined.

Using this procedure, if the measured ASR is less than $0.6 * T$ then the observation is defined as cloudy. The cloud probability will not be reported verbatim on the ATL09 product, but rather will be used to compute a 6 level flag as shown in Table 4.6. Figure 4.6.10 shows the viability of doing so with actual MABEL data.

Table 4.6. Cloud confidence flag (parameter *Cloud_Flag_ASR*).

$P = (1 - ASR/T) * 100$	Product Flag	Flag Meaning
80 – 100%	5	Cloudy with high confidence
60 – 80%	4	Cloudy with medium confidence
40 – 60%	3	Cloudy with low confidence
20 – 40%	2	Clear with low confidence
0 – 20%	1	Clear with medium confidence
$P < 0$	0	Clear with high confidence

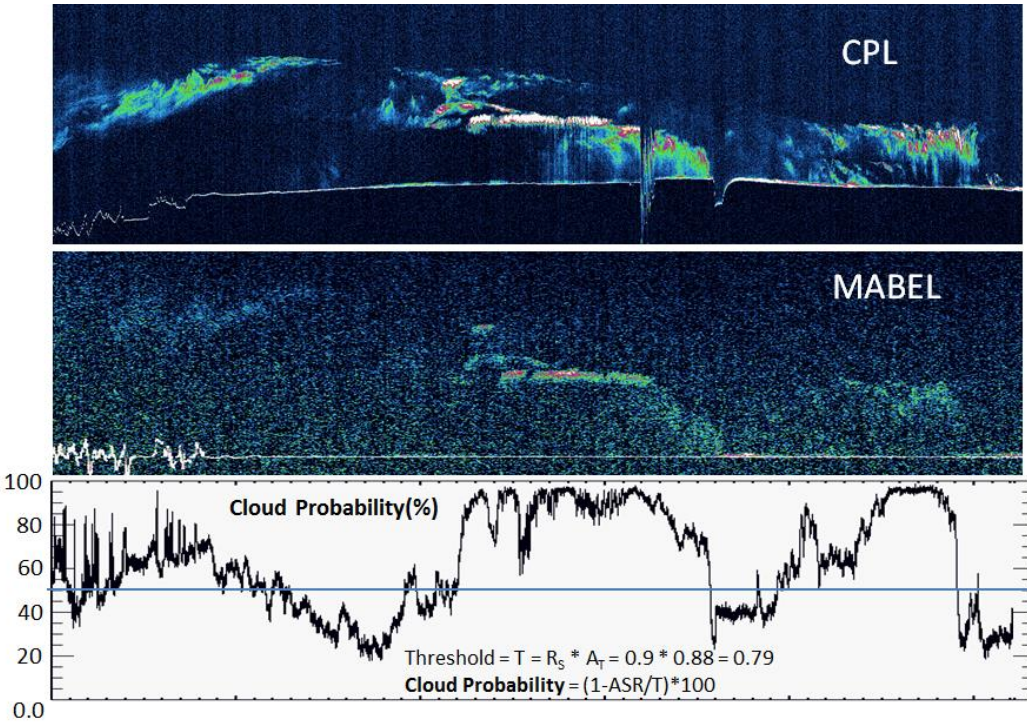


Figure 4.6.10 CPL (top) and MABEL (middle) for a scene over Greenland during the day. Example of cloud probability as computed from the MABEL measured apparent surface reflectivity and an assumed surface reflectivity of 0.90.

4.7 Ocean (or Open Water) Surface Reflectivity

Over water we can use the method of Lancaster et al. (2005) to compute the surface reflectance from surface wind speed (see Figure 4.7.1). Following Lancaster et al. (2005) the reflectance (R) of the ocean's surface is described by:

$$R = (1 - W)R_s + WR_f \quad (4.9)$$

Where R_s is the Fresnel reflectance from the surface, R_f is the reflection due to whitecaps and W is the fraction of the surface covered by whitecaps. Here we use $R_f = 0.22$ as the Lambertian reflectance of typical oceanic whitecaps at a wavelength of 532 nm (Koepke, 1984). Following Bufton et al. (1983), the Fresnel reflectance (R_s) is

$$R_s = \frac{\rho}{4\langle S^2 \rangle} \quad (4.10)$$

Where ρ is the Fresnel reflection coefficient and $\langle S^2 \rangle$ is the variance of the distribution of wave slopes. The Fresnel reflection coefficient is a function of wavelength and is computed as $\rho =$

0.0205 at 532 nm, from the tabulations of Hale and Querry [1973]. Cox and Munk (1954) provide an empirical description of $\langle S^2 \rangle$ as a function of wind speed:

$$\langle S^2 \rangle = 0.003 + 5.12 \times 10^{-3} U_{12.4} \quad (4.11)$$

Where $U_{12.4}$ is the wind speed at 12.4 m above the ocean surface. Numerical weather prediction models generally output wind speed at the 10 m height which can be adjusted to the 12.4 m level using equation 3.12 and assuming neutral atmospheric stability.

$$U_{12.4} = U_{10} \left(\frac{12.4}{10.0} \right)^{0.143} \quad (4.12)$$

Which assumes neutral stability. In computing the ocean lidar return from whitecaps the relative area of the ocean surface that they cover is estimated from the relation from Monahan and O’Muircheartaigh (1980):

$$W = 2.95 \times 10^{-6} U_{10}^{3.52} \quad (4.13)$$

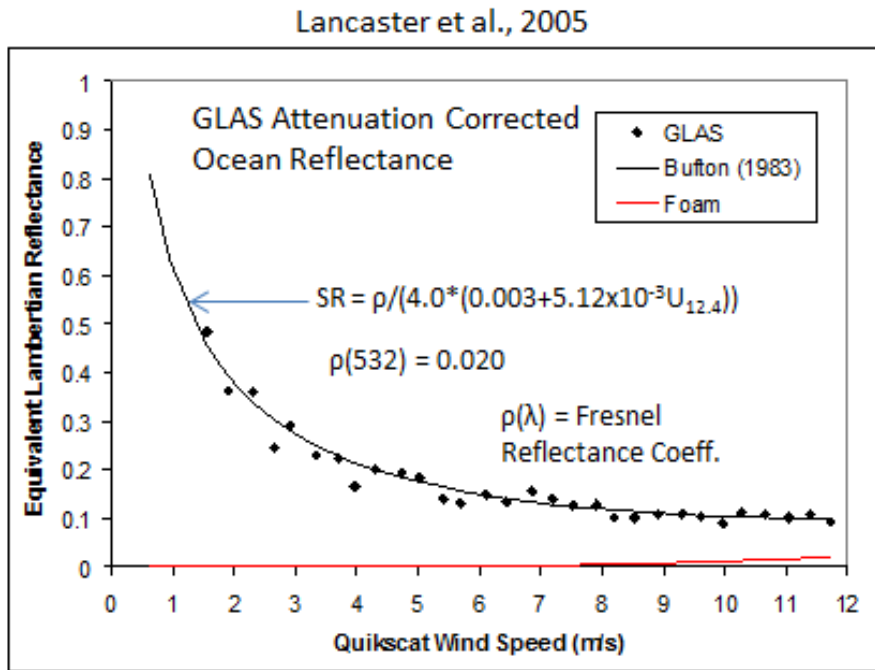


Figure 4.7.1. The theoretical ocean surface reflectivity curve (SR) for 1064 nm as a function of surface wind speed (solid black curve) and GLAS measured surface reflectivity (1064 nm) in areas known to be totally clear.

When the surface type flag indicates ocean or inland lakes, the above equations are used to compute the true surface reflectivity instead of the GOME-based climatological surface reflectivity data set.

Also (when over water), the computation of equation 3.9 shall be stored on the product as ATL09 parameter *Ocean_Surf_Reflec*.

4.8 Total Column Optical Depth Using ASR

The total atmosphere column particulate (not including molecular) optical depth can be computed from the apparent surface reflectance if the actual surface reflectance is well known. This condition holds over ocean where the surface reflectance can be computed from wind speed and over known surfaces like Antarctica and the interior of Greenland. Of course, for this method to be applicable, the surface return cannot be totally attenuated (zero). Thus, this technique is limited to cases where the overlying cloud and aerosol have a combined optical depth of less than about 3. Above that limit, the surface signal will be too small or totally attenuated (zero).

After computing R_{app} - the apparent surface reflectivity (at 25 Hz for all 3 beams) using equation 4.7, the true surface reflectance is computed as discussed in section 4.7 (if over water) or obtained from the GOME-based climatology of surface reflectance for the given surface type. Let the former be called R_{app} and the latter R_{true} . R_{app} must be corrected for molecular attenuation and the angle with which the laser beam makes with nadir (Θ):

$$R_{cor} = (R_{app}) / (\cos(\theta) \bar{T}_m^2) \quad (4.14)$$

where R_{cor} is the resultant corrected reflectance, Θ is the tilt angle of the lidar with respect to nadir viewing (normally 0.1 but can reach 5.0 and may vary with laser beam), and \bar{T}_m^2 is the mean molecular two-way transmission for the entire atmospheric column at 532 nm (~0.81 at sea level). The correction for the tilt angle is usually very minor. The relationship between the corrected observed ATLAS reflectance (R_{cor}) and the true (or modeled) surface reflectance (R_{true}) is described below:

$$R_{cor} = R_{true} e^{-2\tau} \quad (4.15)$$

where τ is the optical depth of the particulates (cloud plus aerosol) in the atmospheric column. Solving for τ results in the equation:

$$\tau = -\frac{1}{2} \ln(R_{cor} / R_{true}) \quad (4.16)$$

which will be valid for all conditions where the ATLAS surface return is not saturated and where a surface signal is not totally extinguished by overlying clouds or aerosol. If the result of equation 4.16 is negative ($R_{cor} > R_{true}$), then set the resulting optical depth to 0.0. The result of equation 4.16 will be the ATL09 parameter *Column_OD_ASR*.

A quality flag for the total column optical depth (parameter name: *Column_OD_ASR_QF*) shall be produced which will be a function of the surface type. The highest quality value is given for those optical depths produced over ocean and ice sheets. The complete summary of this flag is shown in Table 4.7.

Table 4.7. Total Column Optical Depth from ASR Quality Flag (output parameter *Column_OD_ASR_QF*)

Surface Type	<i>Column_OD_ASR_QF</i>
No Surface Signal	0
Land	1
Sea Ice	2
Land Ice (Antarctica, Greenland)	3
Water	4

The *Column_OD_ASR_QF* will be computed using the NOAA flag and the IGBP flag.

5.0 Consolidated Cloud Flag

This section is added for Version 7.2. Here we aim to combine the various flags (*cloud_flag_atm*, *cloud_flag_ASR* and *bsnow_con*) into one flag. This is done to make it easier for the user to ascertain if clouds or blowing snow are present. The new ATL09 parameter will be called *layer_flag*. The overall logic for the flag values is shown in figure 5.1. For nighttime data, *cloud_flag_atm* will be of high quality. Thus if it is > 0 , (meaning at least one cloud layer was detected from the backscatter profiles), then *layer_flag* is set to 1. If no layers were found from the backscatter profiles, but blowing snow was found and its confidence level (*bsnow_con*) is greater than 2, then *layer_flag* is set to 1, otherwise *layer_flag* = 0.

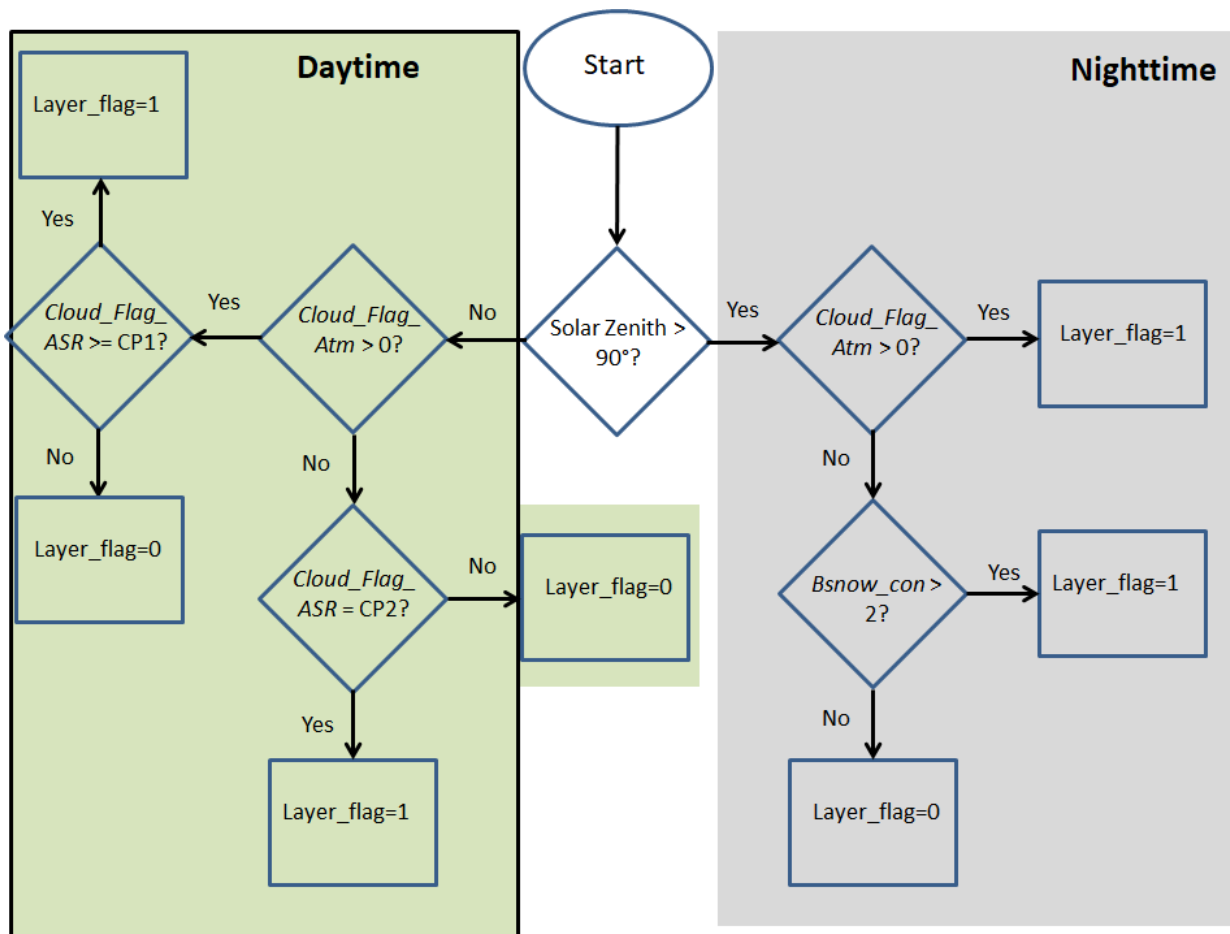


Figure 5.1 Logic flowchart for setting the ATL09 parameter *layer_flag*..

For daytime data, we again check *cloud_flag_atm*, and if it is > 0 we now check *cloud_flag_ASR* which is based on cloud detection from the apparent surface reflectivity. If its value is $\geq CP1$ (nominal value of 4), then we set *layer_flag* to 1, otherwise it is set to 0. If *cloud_flag_atm* = 0, but *cloud_flag_ASR* = CP2 (nominal value of 5), then *layer_flag* = 1, otherwise it is 0. The factors CP1 and CP2 should be adjustable parameters read in from an ancillary file.

6.0 Quality Assessment

This section discusses the types of plots and images that can be made from each of the atmosphere products (ATL04 and ATL09) to help in the assessment of their quality. It is assumed that they will be created by the SCF team and viewed in the visualizer.

6.1 Calibration

To assess the accuracy and stability of calibration, a time series of the calculated calibration constants should be plotted daily and weekly. The plot should consist of the calculated constants from ATL04 and the time interpolated constants on ATL09 (produced from Equation 3.3) for each of the strong beams. Further, a plot of the average calibrated attenuated backscatter (as a function of height) for three latitude bands (poleward of 60 degrees north and south and from 60S to 60N) is to be plotted on the same graph as the average attenuated molecular backscatter for that latitude band. In the calculation of the average

calibrated attenuated backscatter, profiles with clouds should be eliminated. These four plots should be done for each orbit. Note that the set of 4 plots should be made for each of the strong beams.

6.2 Background

The background is computed from the atmospheric profiles using two methods and reported on ATL04. Also on ATL04 is the 50 shot background computed onboard the instrument. Plots of background versus time or lat/lon should be generated for each orbit for all three methods plotted on the same plot. The solar zenith angle should also be plotted.

6.3 Surface Signal

A plot of the value of the surface signal should be made for each orbit. The surface signal (in photon counts) will be plotted as a function of latitude/longitude and show the percentage of time the surface was detected.

6.4 Calibrated Attenuated Backscatter

Images of scattering ratio should be generated. The scattering ratio is defined as the calibrated attenuated backscatter divided by the molecular backscatter. There should be two images for each orbit – one day (solar zenith angles less than 95 degrees) and one night (solar zenith angles greater than 95 degrees). The y axis will be height from -1 km to 20 km, and the x axis labeled with latitude and longitude. A map of the orbit track should also be provided. In the construction of the images, about 100 profiles (4 seconds) of data should be averaged to produce 1 image line.

6.5 Layer Heights

An image of calibrated attenuated backscatter should be made (of length $\frac{1}{4}$ orbit) and the layer heights superimposed on the image. Statistics on the percent cloudiness and the average number of layers found per orbit should be written on the plot.

6.6 Apparent Surface Reflectance

A plot of Apparent Surface Reflectance (ASR) as a function of lat/lon with a map of the orbit track shown on the same plot. Also images of calibrated backscatter with the ASR cloud probability flag (Table 3.4, parameter *Cloud_Flag_ASR*) indicated on the image should be generated. Each image should span roughly $\frac{1}{4}$ of an orbit. This cloud flag could also be plotted on the layer height image (5.5 above) if feasible.

6.7 Ocean Surface Reflectance

A plot of the ocean surface reflectance (ATL09 parameter *Ocean_Surf_Reflec*) as a function of the 10 m wind speed should be made. Note that this parameter is only computed over water and will be invalid over land.

6.8 Total Column Optical Depth

The total column optical depth as computed from ASR (Equation 3.16, ATL09 parameter *Column_OD_ASR*) should be plotted for each orbit.

6.9 Multiple Scattering Warning Flag

The multiple scattering warning flag (parameter *msw_flag*) should be plotted for each orbit

7 Product Quality Parameters

The following are parameters that can be computed from the data that can aid in assessing the overall quality of the atmosphere products. Their magnitudes can be compared with a TBD range of values to assign a pass/fail type of grade to a given granule.

ATL04: 1) The number of calibration values and their average and standard deviation. 2) Average and standard deviation of the laser energy. 3) Average, min and max surface signal and the average of the retrieved surface height minus the DEM height. 4) Percent of time surface was detected. 5) Average, min and max background value computed from the 3 methods.

ATL09: 1) The average and standard deviation of the ratio of calibrated backscatter to molecular backscatter between 11 and 13.5 km (or top of profile) for all data poleward of 60 degrees north and south. 2) The min, max and average number of cloud layers detected from the DDA algorithm. 3) Percent clouds as detected by the DDA algorithm and from the Apparent Surface Reflectivity (ASR) method. 4) Min, max, average and standard deviation of ASR (parameter *apparent_surf_reflec*). Min, max and average of the ocean surface reflectance (parameter *ocean_surf_reflec*) and the total column optical depth (parameter *column_od_asr*). 5) Percent of time ground was detected.

Appendix A.

pro pint2

```
; Program to interpolate pressure to lidar bin resolution from radiosonde data
; Note: Can be used with model data as well
; Inputs: p - pressure at radiosonde (model) levels (millibars)
;         t = temperature at radiosonde (model) levels (degrees Celsius).
;         z - height in meters of the p,t observation
; Output: pressure in millibars at the lidar bin resolution (delz, here = 30m)
; SPP 28Sep14
```

```
nlevs = 0
openr,1,'F:\Sondes\bermuda_sonde2' ; this is radiosonde data from Bermuda 09/22/14 12Z
readf,1,nlevs
p = fltarr(nlevs)
t = fltarr(nlevs)
z = fltarr(nlevs)
for i=0,nlevs-1 do begin
  readf,1,a,b,c
  p(i) = float(b) ; pressure in mb
  z(i) = float(a) * 1000.0 ; height in m
```

```

    t(i) = float(c)      ; temperature in degrees Celsius
endfor
close,1

print,' nlevs = ', nlevs
t = t + 273.15          ; convert temperature to Kelvin
delz = 30.0d0          ; bin size (30 m)
top = z(nlevs-1)
bot = z(0)
print,'bot, top = ', bot, top
np = fix(top/delz) + 1
press = dblarr(np)
temp = dblarr(np)
height = fltarr(np)
ht = bot
layer = 1
bin = 1
press(0) = p(0)

layer_thickness = z(layer) - z(layer-1)
layer_bins = layer_thickness / delz
temp_delta = (t(layer) - t(layer-1)) / layer_bins
temp(0) = t(0)

x = double((z(1) - z(0)) / alog(p(0)/p(1))) ; this is the chi factor in ATBD eqn 2.4

while (ht lt top) do begin
    if (ht gt z(layer)) then begin
        layer++
        print,'layer = ',layer
        x = double((z(layer) - z(layer-1)) / alog(p(layer-1)/p(layer))) ; this is the chi factor in ATBD
    eqn 2.4
        layer_thickness = z(layer) - z(layer-1)
        layer_bins = layer_thickness / delz
        temp_delta = (t(layer) - t(layer-1)) / layer_bins
    endif

    press(bin) = press(bin-1) * exp(-delz/x)
    temp(bin) = temp(bin-1) + temp_delta
    height(bin) = ht/1000.0

```

```

ht = ht + delz
bin++
endwhile

print, 'Number of', delz, 'm bins created: ',bin-1
;print,press

loadct,38,file='c:\Cpl\Config\colors.palm.tbl'

window,1
plot,press,height,background=255,color=0, xtitle='Pressure (mb)', ytitle='Height (km)'

oplot,temp,height, color=50
oplot,p,z/1000.0,psym=1,color=0,symsize=1
oplot,t,z/1000.0,psym=1,color=0,symsize=1

r = fltarr(256)
g = r
b = r
tvlct,r,g,b,/get
tvimage = tvrd()
help,tvimage
write_gif, 'F:\Sondes\pressure.jpg', tvimage, r,g,b

number_density = press * 1000.0 / (1.3806488e-16 * temp)
bmol = 5.450d0 * number_density * (550.0d0/532.0d0)^4 * 1.0d-26

window,3
plot,bmol,height,background=255,color=0, xtitle='532 nm Molecular Backscatter',ytitle='Height
(km)'

tvimage = tvrd()
help,tvimage
write_gif, 'F:\Sondes\molecular.jpg', tvimage, r,g,b

end

```

Appendix B.

Relation between geopotential height and geometric height

$$z = \frac{H}{G} \left(\frac{a}{a - \frac{H}{G}} \right)$$

Where:

z is the geometric height

H is the geopotential height

$a = 6378137.0$ m earth semi-major axis

$$G = \frac{\gamma(\phi)}{g_0}$$

$$g_0 = 9.81 \text{ ms}^{-2}$$

$$\gamma(\phi) = \gamma_e \frac{1 + k \sin^2 \phi}{\sqrt{1 - e^2 \sin^2 \phi}}$$

$$\gamma_e = 9.8321849378 \text{ ms}^{-2}$$

$$k = 0.00193185265241$$

$$e^2 = 6.69437999014 \times 10^{-3}$$

ϕ = latitude

Reference: Lambert et al., 1999

And

<http://www.ofcm.gov/fmh3/pdf/12-app-d.pdf>

References

- Bodhaine B. A., N. B. Wood, E. G. Dutton, and J. R. Slusser: "On Rayleigh optical depth calculations", *J. Atmos. Ocean Technol.*, 16, 1854-1861 (1999) and/or the CALIPSO level 1 ATBD
- Essery, R., L. Long and J. Pomeroy, 1999, A distributed model of blowing snow over complex terrain. *Hydrol. Process.* 13, 2423±2438 (1999)
- Iqbal, M., *An Introduction to Solar Radiation*, Academic Press, New York, NY, 1983.
- Ismail, S. and E. Browell, 1989: Airborne and spaceborne lidar measurements of water vapor profiles: a sensitivity analysis. *Appl. Opt.*, 28, 3603-3615
- Lambert, A., P.L. Bailey, D.P. Edwards, J.C. Gille, C.M. Halvorson, B.R. Johnson, S.T. Massie and K.A. Stone, 1999, High Resolution Dynamics Limb Sounder Level-2 Algorithm Theoretical Basis Document. http://disc.sci.gsfc.nasa.gov/repository/Mission/HIRDLS/3.3_Product_Documentation/3.3.4_Product_Gen_Algorithms/sw-hir-339.pdf
- <http://www.ofcm.gov/fmh3/pdf/12-app-d.pdf>
- She, C., 2001: Spectral structure of laser light scattering revisited: Bandwidths of nonresonant scattering lidars. *Appl. Opt.*, 40, 4875–4884.
- Vigroux, E., Contribution a l'etude experimentale de l'absorption de l'ozone, *Ann. Phys.*, 8, 709-761, 1953.